Functional analysis of novel protein-protein interactions involving ROP GTPases in *Arabidopsis thaliana* and *Populus trichocarpa*

Xiaoyan Jia

Dissertation submitted to the faculty of the Virginia Polytechnic Institute and State University in partial fulfillment of the requirements for the degree of

Doctor of Philosophy

In

Forestry

Amy M. Brunner, Co-Chair

Eric P. Beers, Co-Chair

Jason A. Holliday

Bingyu Zhao

July 15th, 2013

Blacksburg, Virginia, United States

Keywords: protein-protein interaction, yeast two-hybrid, ROP GTPase, ROP11, CSN5, *Arabidopsis thaliana*, *Populus trichocarpa*

Functional analysis of novel protein-protein interactions involving ROP GTPases in *Arabidopsis thaliana* and *Populus trichocarpa*

Xiaoyan Jia

ABSTRACT

We are using the yeast two-hybrid (Y2H) system to identify novel protein-protein interactions (PPI) relevant to wood formation. Bait proteins for Y2H binary assays and screening against a xylem cDNA prey library were selected from approximately 400 *Populus trichocarpa* genes that are at least 8-fold more highly expressed in differentiating secondary xylem versus phloem-cambium, and designated here as poplar biomass (PB) genes. Here we report some of the interactions involving selected PB proteins and efforts to characterize their functions in *Populus* and *Arabidopsis*.

Members of the ROP GTPase family, PB15 in poplar and ROP11 in Arabidopsis, interact with the domain of unknown function (DUF) 620 (DUF620) proteins (e.g., PB129 in poplar). Ectopic co-expression of PB15 and PB129 in Arabidopsis caused outgrowths at the base of flower pedicels and altered leaf morphology. Interestingly, the co-expression phenotype could not be observed in transgenic plants that are only expressing either one of the interacting partners separately. Transgenics altered in expression of *PB15* and/or *PB129* were prepared in *Populus* and characterization of transgenic trees will be performed in greenhouse and field.

In addition to DUF620 family proteins, ROP11 also interacts with the COP9 subunit CSN5A in Arabidopsis. We confirmed the interaction of ROP11 and CSN5A in Y2H and employed available mutants for *ROP11* and *CSN5A* in Arabidopsis to genetically characterize this interaction. Surprisingly, loss of *ROP11* was found to rescue the *csn5a-2* pleiotropic phenotype. Ectopic expression of a *ROP11* dominant negative mutant in the *csn5a-2* background also complemented the stunted growth phenotype. Transcript analysis and gel blot assays showed that *CSN5A* transcript levels remained unchanged in all rescue lines, whereas CSN5A protein levels increased relative to WT. Taken together, we concluded that ROP11 negatively regulate CSN5A protein level in plant by some as yet unknown mechanism.

Acknowledgements

I would like to use this opportunity to express my gratitude to all the individuals who provided assistance during my PhD program at Virginia Tech.

First and foremost, I would like to express my very great appreciation to my advisors, Dr. Eric Beers and Dr. Amy Brunner, for their invaluable scholastic guidance, generous support and kind encouragement during the entire course of my doctorate research.

Advice given by my committee members, Dr. Bingyu Zhao and Dr. Jason Holliday, has been constructive and of great help during my professional development.

I'm highly indebted to many people I worked with for their help in my research and in writing this dissertation. I am particularly grateful for the assistance given by Dr. Chengsong Zhao; whenever I encountered problems with my experiments, he was there to help. I would like to offer my special thanks to Earl Petzold, who is a good lab manager and fun person to work with.

I would like to thank Dr. Mingzhe Zhao for his contribution to the PB15-PB129 characterization and Dr. Takeshi Fujino for fixation, sectioning and photomicroscopy of PB15-PB129 overexpressors described in Chapter 2. I would like to thank Xiaoyan Sheng, for her assistance and various contributions on poplar transformations, RT-qPCR and transgenic tree field trial data. Thanks to Dr. Bidisha Chanda for her contributions related to PB504-CesA interaction and characterizations.

I would like to thank Molecular Plant Sciences program class of 2008: Nan, Fang, Shelley, Megan, Dev and Will, for help and for friendship. I also want to thank the coordinator of 2008 MPS program, Dr. Glenda Gillaspy, for assistance during my admission to Virginia Tech, first year of grad school and advice on ROP11-CSN5A research.

Thanks to Sue Snow for her excellent service at department of Forest Resources and Environmental Conservation.

Table of contents

List of Figures

List of Tables

Chapter 1

Literature review

1.1 Wood formation and *Populus trichocarpa* as a model species

Wood is the supportive and conductive tissue of trees. The annual cycle of wood formation is the basis for the increase in stem diameter in trees. Wood (secondary xylem) formation involves the succession of five developmental steps: 1) cell division from vascular cambium, 2) expansion of newly produced cells, 3) deposition of a variety of secondary cell wall materials, 4) programmed cell death, and 5) heartwood formation (Plomion et al., 2001; Dejardin et al., 2010). Major efforts to understand the genomic basis for wood formation began about 15 years ago with the sequencing of expressed sequence tags (ESTs) from *Populus trichocarpa* and hybrid poplar species (Sterky et al., 1998). Advances in transcriptomic analyses have facilitated the discovery of genes and gene networks that regulate secondary meristems, cell fate (xylem and phloem differentiation) and secondary cell wall deposition (Hertzberg et al., 2001; Moreau et al., 2005; Dharmawardhana et al., 2010). Discoveries of transcriptional networks regulating secondary wall biosynthesis in the herbaceous model plants *Arabidopsis thaliana* have greatly improved our understanding of transcriptional regulation in trees (Zhao et al., 2005; Demura and Fukuda, 2007; Mitsuda et al., 2007; Zhao et al., 2008; Zhong et al., 2010). Even though substantial progress has been made from genomic studies of wood formation in trees such as pine, spruce, eucalyptus and other model plants such as Arabidopsis and alfalfa, elucidation of the molecular mechanisms underlying wood formation still has a long way to go.

Trees of the genus *Populus* comprise about 30 species of poplars, cottonwoods, and aspens that are widely distributed over the northern hemisphere and planted in most parts of the world temperate zone. Poplars, because of their fast growth, their uses as sources of fuel, fiber, lumber and animal feed, have drawn the attention of many researchers worldwide. With the completion and release of the black cottonwood (*Populus trichocarpa*) full genome sequence by the US Department of Energy in 2006 (Tuskan et al., 2006), *Populus* has emerged as a model system to study plant biology, especially that which is relevant to forest trees and other woody perennials. This model system has advantages in studying wood formation, long-term perennial growth, and seasonality that cannot be matched by herbaceous model plants such as Arabidopsis (Jansson and Douglas, 2007).

1.2 Biomass proteins

Based on a comparison of transcript profiles from *Populus trichocarpa* xylem and cambium-phloem cells (Rodgers-Melnick et al., 2011). We were able to select approximately 400 genes that are at least 8-fold more highly expressed in differentiating xylem cells versus cambial zone cells and differentiating phloem cells. We have named this set of xylem tissue up-regulated genes the poplar biomass (PB) gene set. The biased expression of these genes in differentiating

xylem cells indicates that their protein products play important roles in xylem formation. This set of proteins includes those involved in lignin, cellulose, hemicellulose, and pectin biosynthesis, cell wall remodeling, signal transduction, transcriptional regulation, and many proteins of uncharacterized functions. Knowledge of interactions between these proteins and other proteins in differentiating xylem cells facilitates formation of new hypotheses about xylem formation in general and is an important starting point for studying specific protein functions in xylem formation.

1.3 Yeast two-hybrid system

The yeast two-hybrid (Y2H) system is so far the most popular and widely accepted genetic assay to identify and characterize novel protein-protein interactions (Lentze and Auerbach, 2008). The Y2H system was first introduced in 1989 (Fields and Song, 1989). The system utilizes the modularity of transcription factors with a separable DNA-binding (DB) domain and transcriptional activation domain (AD) that can be reconstituted to restore function upon physical interaction (Brent and Ptashne, 1981). The protein of interest (X), or bait, is fused to the DB of a transcription factor such as Gal4 or LexA. The potential interacting protein (Y), or prey, is fused to the corresponding AD. DB-X and AD-Y are then co-transformed into an appropriately engineered yeast strain. Reporter genes would be expressed in the engineered yeast if X interacts with Y resulting in both DB-X and AD-Y occupying the promoter region of yeast reporter genes and activating their transcription (Ratushny and Golemis, 2008).

We are using Y2H to identify protein-protein interactions (PPIs) among the PB proteins (http://xylome.vbi.vt.edu/index.html). For this dissertation I focus mainly on PPIs involving two small GTPases, PB15 in poplar and ROP11 in Arabidopsis. A novel interaction between PB15 and PB129 was discovered as a result Y2H experiments. PB15 (*Potri.011G061500*) is 15-fold more highly expressed in developing xylem relative to phloem-cambium cells. Based on sequence homology with other plant species, this 196 amino acids protein is a small guanosine triphosphatase (GTPase), most closely related to ROP (Rho-like GTPase of plant) family G proteins. The transcript level of PB129 (*Potri.010G174200*) is 12.3 times greater in xylem versus phloem-cambium. PB129 is annotated as a domain of unknown function 620 (DUF620) protein. Similar studies in Arabidopsis later confirmed the ability of some ROP GTPases (i.e., ROP10 and ROP11) to interact with DUF620 proteins (Arabidopsis Interactome Mapping, 2011).

1.4 Small GTPases

Small GTPases constitute a large superfamily of G proteins named after its founding member RAS (Takai et al., 2001). On the basis of sequence and functional similarities, the RAS superfamily of G proteins is divided into five major branches: Ras, Rho, Rab, Ran and Arf (Wennerberg et al., 2005). Viridiplantae (land plants and green algae) apparently lack members of the Ras subfamily; instead, plants contain a unique subfamily of Rho GTPases, called ROPs (Brembu et al., 2006). ROPs are sometimes referred to as RACs, because the best characterized

Arabidopsis ROPs are most similar to the mammalian Rac proteins with up to 61% amino acid identity with human Rac1, for example (Berken and Wittinghofer, 2008).

Ras superfamily GTPases have two interconvertible states, GTP-bound active and GDP-bound inactive (Vetter and Wittinghofer, 2001; Berken and Wittinghofer, 2008). The conversion from GTP bound form to GDP bound is catalyzed by their shared intrinsic GTPase activity, residing on evolutionarily preserved G-domains. There are mainly three groups of molecules that regulate Ras GTPases. GTPase activating proteins (GAPs) promote the GTPase activities of Ras and therefore favor the inactive state. On the other hand, guanine nucleotide exchange factors (GEFs) accelerate the otherwise slow spontaneous exchange of GDP for GTP and favor the active state. Guanine nucleotide dissociation inhibitors (GDIs) can prevent both GDP dissociation and GTP hydrolysis in addition to their role as modulators of the subcellular localization of the G proteins. All three kinds of GTPase regulators have been identified and characterized in Arabidopsis (Bischoff et al., 2000; Qiu et al., 2002; Hwang et al., 2008).

1.5 ROP GTPases in plants

There are 11 members of ROPs in *Arabidopsis thaliana* (Li et al., 1998). They share 70-98% amino acid identity (Berken and Wittinghofer, 2008). The 11 ROPs are classified into two groups based on their C-terminal hypervariable regions (HVR) and lipid modifications (Sorek et al., 2011). Type I Arabidopsis ROPs include ROP1 to ROP8, which are defined by their characteristic CaaX box motif at the C-terminus. The cysteine residue is usually the lipid modification site, often comprising geranylgeranylation or farnesylation catalyzed by geranylgeranyl transferase and farnesyl transferase, respectively. The last three amino acid residues are cleaved after covalent linkage of lipids. Type II ROPs (ROP9, ROP10 and ROP11) do not have a CaaX box motif. Rather, they have a GC-CG box in which two cysteine residues serve as palmitoylation (also called S-acylation) sites (Lavy et al., 2002; Lavy and Yalovsky, 2006; Sorek et al., 2011).

The function of ROPs is linked to cell polarization, polar growth and cell morphogenesis (Yang, 2008). Expression of a constitutively active mutant of ROP1 resulted in non-polarized pollen tube growth (Li et al., 1999). ROP2 and ROP4 are reported to promote epidermal pavement cell lobe formation (Fu et al., 2005). ROP2 and ROP6 are activated by auxin to regulate pavement cells lobe formation and indentation via actins and microtubules, respectively (Xu et al., 2010). Research also showed that ROPs mediate auxin-regulated gene expression, and directional auxin transport (Wu et al., 2011). However, due to the functional redundancy and relative lack of phenotypes resulting from loss-of-function alleles, our knowledge about this family of molecular switches is still limited and largely based on phenotypes associated with overexpression of constitutively active and dominant negative ROP proteins.

Populus trichocarpa has 12 ROP GTPases. They share 73 to 100% amino acid sequence similarity (Phytozome http://www.phytozome.net/). None of their molecular functions has been well characterized in poplar, especially, the role they play in xylem formation. However, ROPs from other species have been implicated in xylem development. For example, overexpression of a *Eucalyptus* vascular-expressed ROP small GTPase *EgROP1* in *Arabidopsis thaliana* has been shown to alter leaf pavement cell morphology, leaf trichome morphology, secondary xylem cell morphology, secondary xylem cell wall thickness, and lignin and xylan compositions (Foucart et al., 2009). More recent work in the Fukuda lab has demonstrated that Arabidopsis ROP11 is locally activated in xylem cells to recruit MIDD1 (microtubule depletion domain 1) and induce local disassembly of cortical microtubules yielding the pitted patterning of secondary cell walls (Oda and Fukuda, 2012).

1.6 References

Arabidopsis Interactome Mapping C (2011) Evidence for network evolution in an Arabidopsis interactome map. Science **333:** 601-607

Berken A, Wittinghofer A (2008) Structure and function of Rho-type molecular switches in plants. Plant Physiol Biochem **46:** 380-393

Bischoff F, Vahlkamp L, Molendijk A, Palme K (2000) Localization of AtROP4 and AtROP6 and interaction with the guanine nucleotide dissociation inhibitor AtRhoGDI1 from Arabidopsis. Plant Mol Biol **42:** 515-530

Brembu T, Winge P, Bones AM, Yang Z (2006) A RHOse by any other name: a comparative analysis of animal and plant Rho GTPases. Cell Res **16:** 435-445

Brent R, Ptashne M (1981) Mechanism of action of the lexA gene product. Proc Natl Acad Sci U S A **78:** 4204-4208

Dejardin A, Laurans F, Arnaud D, Breton C, Pilate G, Leple JC (2010) Wood formation in Angiosperms. C R Biol **333:** 325-334

Demura T, Fukuda H (2007) Transcriptional regulation in wood formation. Trends Plant Sci **12:** 64-70

Dharmawardhana P, Brunner AM, Strauss SH (2010) Genome-wide transcriptome analysis of the transition from primary to secondary stem development in Populus trichocarpa. BMC Genomics **11:** 150

Fields S, Song O (1989) A novel genetic system to detect protein-protein interactions. Nature **340:** 245-246

Foucart C, Jauneau A, Gion JM, Amelot N, Martinez Y, Panegos P, Grima-Pettenati J, Sivadon P (2009) Overexpression of EgROP1, a Eucalyptus vascular-expressed Rac-like small GTPase, affects secondary xylem formation in Arabidopsis thaliana. New Phytol **183:** 1014-1029

Fu Y, Gu Y, Zheng ZL, Wasteneys G, Yang ZB (2005) Arabidopsis interdigitating cell growth requires two antagonistic pathways with opposing action on cell morphogenesis. Cell **120:** 687-700

Hertzberg M, Aspeborg H, Schrader J, Andersson A, Erlandsson R, Blomqvist K, Bhalerao R, Uhlen M, Teeri TT, Lundeberg J, Sundberg B, Nilsson P, Sandberg G (2001) A transcriptional roadmap to wood formation. Proc Natl Acad Sci U S A **98:** 14732-14737

Hwang JU, Vernoud V, Szumlanski A, Nielsen E, Yang Z (2008) A tip-localized RhoGAP controls cell polarity by globally inhibiting Rho GTPase at the cell apex. Curr Biol **18:** 1907-1916

Jansson S, Douglas CJ (2007) Populus: a model system for plant biology. Annu Rev Plant Biol **58:** 435-458

Lavy M, Bracha-Drori K, Sternberg H, Yalovsky S (2002) A cell-specific, prenylation-independent mechanism regulates targeting of type II RACs. Plant Cell **14:** 2431-2450

Lavy M, Yalovsky S (2006) Association of Arabidopsis type-II ROPs with the plasma membrane requires a conserved C-terminal sequence motif and a proximal polybasic domain. Plant J **46:** 934-947

Lentze N, Auerbach D (2008) The yeast two-hybrid system and its role in drug discovery. Expert Opin Ther Targets **12:** 505-515

Li H, Lin YK, Heath RM, Zhu MX, Yang ZB (1999) Control of pollen tube tip growth by a pop GTPase-dependent pathway that leads to tip-localized calcium influx. Plant Cell **11:** 1731-1742

Li H, Wu G, Ware D, Davis KR, Yang Z (1998) Arabidopsis Rho-related GTPases: differential gene expression in pollen and polar localization in fission yeast. Plant Physiol **118:** 407-417

Mitsuda N, Iwase A, Yamamoto H, Yoshida M, Seki M, Shinozaki K, Ohme-Takagi M (2007) NAC transcription factors, NST1 and NST3, are key regulators of the formation of secondary walls in woody tissues of Arabidopsis. Plant Cell **19:** 270-280

Moreau C, Aksenov N, Lorenzo MG, Segerman B, Funk C, Nilsson P, Jansson S, Tuominen H (2005) A genomic approach to investigate developmental cell death in woody tissues of Populus trees. Genome Biol **6:** R34

Oda Y, Fukuda H (2012) Initiation of cell wall pattern by a Rho- and microtubule-driven symmetry breaking. Science **337:** 1333-1336

Plomion C, Leprovost G, Stokes A (2001) Wood formation in trees. Plant Physiol **127:** 1513-1523

Qiu JL, Jilk R, Marks MD, Szymanski DB (2002) The Arabidopsis SPIKE1 gene is required for normal cell shape control and tissue development. Plant Cell **14:** 101-118

Ratushny V, Golemis E (2008) Resolving the network of cell signaling pathways using the evolving yeast two-hybrid system. Biotechniques **44:** 655-662

Rodgers-Melnick E, Mane SP, Dharmawardhana P, Slavov GT, Crasta OR, Strauss SH, Brunner AM, Difazio S (2011) Contrasting patterns of evolution following whole genome versus tandem duplication events in Populus. Genome Res

Sorek N, Gutman O, Bar E, Abu-Abied M, Feng X, Running MP, Lewinsohn E, Ori N, Sadot E, Henis YI, Yalovsky S (2011) Differential effects of prenylation and s-acylation on type I and II ROPS membrane interaction and function. Plant Physiol **155:** 706-720

Sterky F, Regan S, Karlsson J, Hertzberg M, Rohde A, Holmberg A, Amini B, Bhalerao R, Larsson M, Villarroel R, Van Montagu M, Sandberg G, Olsson O, Teeri TT, Boerjan W, Gustafsson P, Uhlen M, Sundberg B, Lundeberg J (1998) Gene discovery in the wood-forming tissues of poplar: analysis of 5, 692 expressed sequence tags. Proc Natl Acad Sci U S A **95:** 13330-13335

Takai Y, Sasaki T, Matozaki T (2001) Small GTP-binding proteins. Physiol Rev **81:** 153-208

Tuskan GA, Difazio S, Jansson S, Bohlmann J, Grigoriev I, Hellsten U, Putnam N, Ralph S, Rombauts S, Salamov A, Schein J, Sterck L, Aerts A, Bhalerao RR, Bhalerao RP, Blaudez D, Boerjan W, Brun A, Brunner A, Busov V, Campbell M, Carlson J, Chalot M, Chapman J, Chen GL, Cooper D, Coutinho PM, Couturier J, Covert S, Cronk Q, Cunningham R, Davis J, Degroeve S, Dejardin A, Depamphilis C, Detter J, Dirks B, Dubchak I, Duplessis S, Ehlting J, Ellis B, Gendler K, Goodstein D, Gribskov M, Grimwood J, Groover A, Gunter L, Hamberger B, Heinze B, Helariutta Y, Henrissat B, Holligan D, Holt R, Huang W, Islam-Faridi N, Jones S, Jones-Rhoades M, Jorgensen R, Joshi C, Kangasjarvi J, Karlsson J, Kelleher C, Kirkpatrick R, Kirst M, Kohler A, Kalluri U, Larimer F, Leebens-Mack J, Leple JC, Locascio P, Lou Y, Lucas S, Martin F, Montanini B, Napoli C, Nelson DR, Nelson C, Nieminen K, Nilsson O, Pereda V, Peter G, Philippe R, Pilate G, Poliakov A, Razumovskaya J, Richardson P, Rinaldi C, Ritland K, Rouze P, Ryaboy D, Schmutz J, Schrader J, Segerman B, Shin H, Siddiqui A, Sterky F, Terry A, Tsai CJ, Uberbacher E, Unneberg P, Vahala J, Wall K, Wessler S, Yang G, Yin T, Douglas C, Marra M, Sandberg G, Van de Peer Y, Rokhsar D (2006) The genome of black cottonwood, Populus trichocarpa (Torr. & Gray). Science **313:** 1596-1604

Vetter IR, Wittinghofer A (2001) The guanine nucleotide-binding switch in three dimensions. Science **294:** 1299-1304

Wennerberg K, Rossman KL, Der CJ (2005) The Ras superfamily at a glance. J Cell Sci **118:** 843-846

Wu HM, Hazak O, Cheung AY, Yalovsky S (2011) RAC/ROP GTPases and auxin signaling. Plant Cell **23:** 1208-1218

Xu TD, Wen MZ, Nagawa S, Fu Y, Chen JG, Wu MJ, Perrot-Rechenmann C, Friml J, Jones AM, Yang ZB (2010) Cell Surface- and Rho GTPase-Based Auxin Signaling Controls Cellular Interdigitation in Arabidopsis. Cell **143:** 99-110

Yang ZB (2008) Cell Polarity Signaling in Arabidopsis. Annual Review of Cell and Developmental Biology **24:** 551-575

Zhao C, Avci U, Grant EH, Haigler CH, Beers EP (2008) XND1, a member of the NAC domain family in Arabidopsis thaliana, negatively regulates lignocellulose synthesis and programmed cell death in xylem. Plant J **53:** 425-436

Zhao C, Craig JC, Petzold HE, Dickerman AW, Beers EP (2005) The xylem and phloem transcriptomes from secondary tissues of the Arabidopsis root-hypocotyl. Plant Physiol **138:** 803-818

Chapter 2

Functional analysis of PB15 and PB129 in Arabidopsis

2.1 Introduction

Arabidopsis was the first established model plant for molecular genetics studies. As a member of the mustard (Brassicaceae) family, Arabidopsis is closely related to many economically important crop plants, for example, turnip, cabbage, broccoli and canola. But Arabidopsis itself is not of major agronomic significance (http://www.arabidopsis.org/index.jsp). However, this species offers advantages for basic research in genetics and molecular biology. Important features include a fast life cycle, prolific seed production through self-pollination, small genome size and good representation of the complexity of a flowering plant (Koornneef and Meinke, 2010). Loss-of-function and gain-of-function studies in Arabidopsis are classic approaches to study plant gene functions. Phenotypes of the mutant plants may provide information about the pathways in which these genes play a role. By manipulating two interacting proteins simultaneously in one plant, it may be possible to reveal more clues about specific pathways than would be discovered by overexpressing or knocking out only one member of an interacting pair. This is especially ture for signaling proteins like GTPases, which can be active in multiple pathways and comprise multigene families where partial redundancy confounds single gene loss-of-function analyses.

PB15 shares the highest sequence similarity with ROP7 (*At5g45970*) among all the 11 Arabidopsis ROPs. *ROP7* was found to be exclusively expressed in vascular tissue, and specifically in developing primary xylem elements (Brembu et al., 2005). The *rop7* null mutant appeared to exhibit no abnormal phenotype in terms of overall morphology or in composition and appearance of the vascular tissue. However, ectopic expression of constitutively active ROP7 (*CA-ROP7*) caused reduced lobe length of pavement cells in the epidermis, although no consistent effects on xylem cells were observed (Brembu et al., 2005). Phylogenetic analysis suggested that PB15 and ROP7 are orthologs, and both are preferentially expressed in xylem, suggesting they could perform similar functions.

Through the poplar biomass interactome project, we discovered that PB15 and PB129 (a domain of unknown function 620 protein; DUF620) interacted. We hypothesized that the interaction of PB15 and PB129 in *Populus trichocarpa* was conserved in Arabidopsis. However, the Arabidopsis interactome project showed that ROP11 (*At5G62880*) but not ROP7 (the PB15 ortholog) interacted with a AtDUF620 protein (*At1G79420*) in the Y2H system (Arabidopsis Interactome Mapping, 2011). Nonetheless, we reasoned that the availability of molecular genetic tools in Arabidopsis could facilitate more rapid analysis of the ROP-DUF620 interaction involving ROP11 and AtDUF620, while we prepared transgenic poplar trees for specific analysis

of PB15 and PB129 functions. Therefore, studies of *rop11* and *duf620* mutants in Arabidopsis were conducted.

The cauliflower mosaic virus (CaMV) *35S* promoter sequence is commonly used for strong and universal (i.e., constitutive) expression of foreign or endogenous genes in higher plants (Franck et al., 1980; Kay et al., 1987). This virus promoter ensures that any downstream coding sequence will be removed from plant regulatory control, resulting in high-level accumulation of gene transcripts. Although gene expression increases caused by the *35S* promoter can result in hypermorphic phenotypes that accurately reveal gene function, phenotypes caused by *35S*-driven expression may also be misleading (e.g., neomorphs) due to disruption or masking of tissue or organ specific functions of native genes (Yoo et al., 2005). Native promoters or tissue-specific promoters can be useful alternatives to the constitutive *35S* promoter. For PB15 and PB129, it was hypothesized that vascular tissue-specific expression in Arabidopsis would reveal their functions in wood formation in poplar. From previous work in our lab, the treachery element (TE)-specific protease XYLEM CYSTEINE PROTEASE2 (XCP2) promoter is known to drive xylem-specific expression of downstream genes (Zhao et al., 2005; Avci et al., 2008). For phloem-specific expression, the *SUC2* promoter has been used by many investigators (Truernit and Sauer, 1995).

Here we use three different promoters, *35S*, *XCP2* and *SUC2*, to manipulate the expression of *PB15* and/or *PB129* in Arabidopsis. For all three promoters, single-gene transgenic lines did not exhibit any observable phenotype, with the exception of the *SUC2::PB129* expressor line where flowering time and fiber development were altered. Overexpression of *PB15* and *PB129* in the same Arabidopsis plants caused outgrowths at the base of flower pedicels and other changes in plant morphology. These phenotypes were apparently not stable and work with these lines was discontinued after significant effort was made to obtain reproducible sustainable phenotypes.

2.2 Materials and methods

2.2.1 Plant materials and growth conditions

Ecotype Columbia-0 was used as Arabidopsis wild-type control in this study. The *rop7* mutant was described previously (Brembu et al., 2005). T-DNA insertion lines of SALK_013327 (*rop11-1*) and SALK_148089 (*duf620-1*) were identified from the Arabidopsis Biological Resource Center (ABRC) at the Ohio State University (Alonso et al., 2003). T-DNA insertion line GABI_705G02 (*duf620-2*) was purchased from Nottingham Arabidopsis Stock Centre (NASC) and genotyped in the lab. Arabidopsis plants were grown under long-day conditions (16 h of light/8 h of dark) in growth chamber at 22 °C unless otherwise specified.

2.2.2 Constructs

35S::PB15

PB15 coding sequence was amplified from *Populus trichocarpa* cDNA with forward primer ATGAGTACAGCAAGATTTAT and reverse primer CCCGGGCTAGAGGAAAGCACATGTTC (with *Xma*I restriction site added). PCR product was cloned into pGEM-T Easy (Promega Corp. Madison, WI) vector as shuttle vector. Then fragment containing *PB15* cDNA was digested with *Nco*I and *Xma*I restriction enzymes and subcloned into pFGC5941 binary vector.

35S::PB129

PB129 coding sequence was amplified from *Populus trichocarpa* cDNA with forward primer CTCGAGATGGGCTCAAGAGCAAGAAG (with *Xho*I site adapter) and reverse primer CCCGGGTCATGGAGAAGCATCATAGA (with *Xma*I site adapter). PCR product was cloned into pGEM-T easy vector and then digested with *Xho*I and *Xma*I restriction enzymes and subcloned into pFGC5941 binary vector (Figure 2.1).

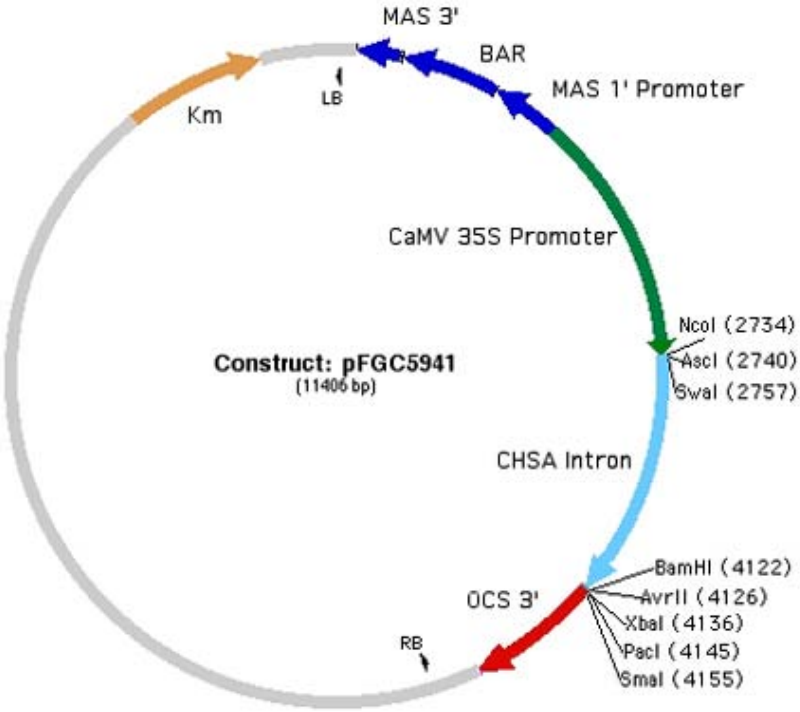

Figure 2.1. pFGC5941 vector map

SUC2::PB15

SUC2 promoter sequence was amplified from Arabidopsis genomic DNA with forward primer GCATGCAAAATAGCACACCA and reverse primer GGATCCTTTGACAAACCAAGAAAGTA (with *Bam*HI site adapter). *PB15* coding sequence was amplified from *Populus trichocarpa* cDNA with forward primer GGATCCATGAGTACAGCAAGATTTAT (with *Bam*HI site adapter) and reverse primer CTAGAGGAAAGCACATGTTC. *SUC2* promoter and *PB15* were then cloned into pGEM-T easy vector. *SUC2* promoter was cleaved by *Bam*HI and *Eco*RI and subcloned into pFGC5941 binary vector and *PB15* was ligated downstream of *SUC2* promoter through double digestion with *Bam*H1 and *Spe*I.

SUC2::PB129
SUC2 promoter sequence was amplified from Arabidopsis genomic DNA with forward primer AAGCTTGCATGCAAAATAGCACACCA (with *Hind*III site adapter) and reverse primer TCTAGATTTGACAAACCAAGAAAGTA (with *Xba*I site adapter). *PB129* coding sequence was amplified from *Populus trichocarpa* cDNA with forward primer TCTAGAATGGGCTCAAGAGCAAGAAG (with *Xba*I site adapter) and reverse primer GAGCTCTCATGGAGAAGCATCATAGA (with *Sac*I site adapter). Then *SUC2* promoter and *PB129* coding region were cloned into pGEM-T easy vector. *SUC2* promoter and *PB129* were transfered into binary vector pBI121 (Jefferson et al., 1987) to replace CaMV *35S* promoter and β-glucuronidase gene, respectively.

XCP2::PB15
XCP2 promoter region was amplified from Arabidopsis genomic DNA with forward primer GCCGCAAATCCATGATTTGTA and reverse primer CTCGAGAAAGAGCCGTTTGAG (with *Xho*I site adapter). PCR product was cloned into pGEM-T easy vector. After digestion with *Eco*RI and *Xho*I, *XCP2* promoter was used to replace *35S* promoter in pFGC5941 vector. *PB15* coding sequence was amplified from *Populus trichocarpa* cDNA with forward primer CTCGAGATGAGTACAGCAAGATTTAT (with *Xho*I site adapter) and reverse primer CCCGGGCTAGAGGAAAGCACATGTTC (with *Xma*I site adapter) and cloned into pGEM-T easy vector. *PB15* was then cloned into the pFGC5941 vector carrying *XCP2* promoter through double digetion with *Xho*I and *Xma*I.

XCP2::PB129
XCP2::PB129 was created by replacing *35S* promoter of the *35S::PB129* construct with *XCP2* promoter through *Eco*RI and *Xho*I sites.

2.2.3 Arabidopsis Transformation

Arabidopsis transformation was accomplished using a modified version of the floral dip method (Clough and Bent, 1998). *Agrobacterium tumefaciens* strain GV3101 (pMP90) carrying the relevant binary plasmid was inoculated into 2 ml liquid 2XTY medium (16 g Bacto-tryptone, 10

g Bacto-yeast extract, 5 g NaCl per liter) with appropriate antibiotics. After overnight growth at 28 °C with shaking (200rpm), 200 µl bacteria media were inoculated into 125 ml 2XTY and continued growing for 18-24 h. The overnight culture was pelleted and resuspended in infiltration buffer (5% sucrose, 0.03% Silwet L-77), resulting in an OD600 reading of 0.8. Plant inflorescences were dipped into infiltration media for 10 minutes. Transformants were selected using antibiotic or herbicide selectable marker.

2.2.4 Genotyping

Genotypes of mutant and transgenic Arabidopsis plants were confirmed by PCR based genotyping.

In the T-DNA insertion line SALK_013327 (*rop11-1*), the presence of *ROP11* was detected using *ROP11_For1* TCGATTCGTAACGCCATACT and *ROP11_Rev2* TTGACAGTGGTGCCTTCAAC. The presence of T-DNA insertion was confirmed using *ROP11_For1* and SALK left border primer *SALK_LB* GCGTGGACCGCTTGCTGCAACT.
In the T-DNA insertion line SALK_148089 (*duf620-1*), the presence of *DUF620-1* was detected using *Duf_UP* ATGAGCAACTCAAAGTCATA and *Duf_Down* CTGGATTAGACGACGAAGTG. The presence of T-DNA insertion was confirmed using *Duf_UP* and *SALK_LB*.
In the T-DNA insertion line GABI_705G02 (*duf620-2*), the presence of *DUF620-2* was detected using *Duf2For1* GATGGGGAAGCTCAAGATGA and *Duf2Rev1* GCAGACAATGCGAGTGTGTT. The presence of T-DNA insertion was confirmed using *Duf2For1* and *GABI_LB* CCCATTTGGACGTGAATGTAG.

2.3 Results

2.3.1 Ectopic co-expression of *PB15* and *PB129* in Arabidopsis caused outgrowths at the base of flower pedicels and altered leaf morphology

Creation of transgenic poplar trees may take months in the lab and years if one wish to study the transgenic plants in the field (Leple et al., 2007). Consequently, to coincide with our poplar transgenics studies (see chapter 3), we attempted to perform functional analyses of PB15 and PB129 in Arabidopsis where introduction of stable, heritable transgenes is relatively rapid. Transgenic plants that expressed *35S::PB15* or *35S::PB129* individually did not exhibit any visible phenotype relative to WT. However, transgenic plants expressing high levels of both PB15 and PB129 displayed vascular tissue-related and leaf morphology phenotypes. As shown in Figure 2.2, A and B, compard to WT plants, three-week-old T3 transgenic plants displayed unusual leaf morphologies including narrow serrated or rounded leaf blades with short petioles. Interestingly, despite their distinct leaf morphologies, both plants are progeny of self-fertilization of the same T2 parental line.

An older co-overexpressor line with a mature inflorescence stem showed unusual outgrowths at the base of flower pedicels in the inflorescence stem (Fig. 2.2, C). Sectioning revealed that the outgrowth regions are expanded interfascicular regions and fiber cells within these outgrowths are much larger compared to cells in normal interfascicular regions.

Our transgenic studies of PB15 and PB129 tentatively indicated that PB15 and PB129 interacted genetically in Arabidopsis and could affect multiple aspects of plant growth and morphology. The results also confirmed that by manipulating two interacting protein it is sometimes possible to reveal roles of interacting proteins that were not detectable following alteration of each protein separately.

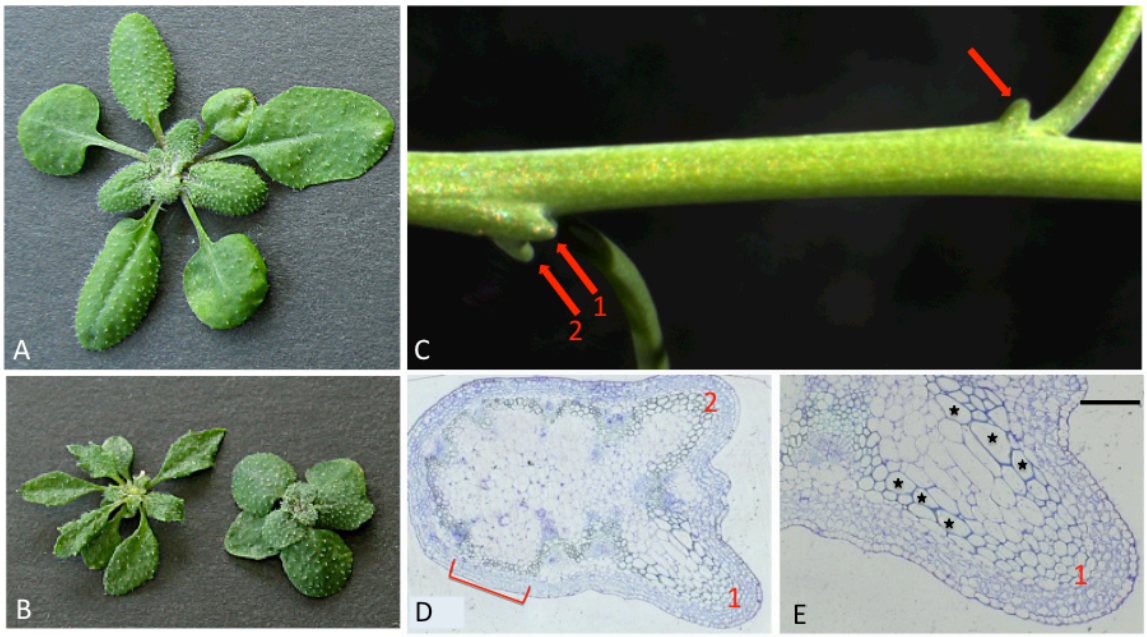

Figure 2.2. Co-overexpression of interactors PB15 and PB129 alters fiber size and morphology in Arabidopsis.

(A, B) Three-week-old wild type (A) and representative T3 plants (B) from a single T2 *35S::PB15*; *35S::PB129* parent illustrate diverse effects on leaf morphology: narrow serrated leaf (plant on left) and rounded leaf blade with short petiole (plant on right).

(C) The inflorescence stem of a *35S::PB15*; *35S::PB129* plant shows unusual outgrowths at the base of flower pedicels (red arrows).

(D) Sectioning through outgrowths 1 and 2 reveals the presence of expanded interfascicular regions containing enlarged fibers compared to fibers in normal interfascicular regions (bracket). (E) A higher magnification of outgrowth 1. Several enlarged fibers are marked (★) Bars in (E) = 100 μm.

2.3.2 Phloem specific expression of *PB129* driven by *SUC2* promoter altered phloem fibers and delayed flowering

Gene expression is strictly regulated, both temporally and spatially. Both *PB15* and *PB129* are highly expressed in vascular tissue, particularly, in differentiating xylem cells. Thus, targeted expression of *PB15* and *PB129* in Arabidopsis xylem tissue may reveal functions, via hypermorphy, regarding secondary xylem formation. The *XCP2* promoter was used to specifically increase PB15 and PB129 production in Arabidopsis xylem. Unfortunately, neither *XCP2::PB15* nor *XCP2::PB129* transgenics exhibited any deviation from a WT in appearance.

Ectopic gene expression can also provide clues about gene function. Specifically, we reasoned that by expression of normally xylem-biased genes in the phloem, we might reprogram differentiating phloem to be more xylem-like because both xylem and phloem are differentiated from the vascular cambium. For this purpose we employed the widely used *SUC2* promoter to direct *PB15* and *PB129* expression in phloem (Truernit and Sauer, 1995). *SUC2::PB15* transgenic plants were not morphorlogically different from WT throughout their life cycle. However, phloem-specific expression of *PB129* yielded a vascular tissue-associated phenotype in a small number of plants and flowering was delayed for *SUC2::PB129* stable transgenic lines (Fig. 2.3, A). Most interestingly, altered fiber bundle size in the hypocotyl region was associated with elevated expression of *PB129* in phloem of three plants from the same transgenic event (Fig. 2.3, B to G). Thus phloem-specific expression of *PB129* suggested that PB129 (DUF620 proteins) play a role in the differentiation of xylem and phloem. However, because this phenotype was observed only for one transgenic event, additional investigation is needed to determine whether the phenotype is linked with PB129.

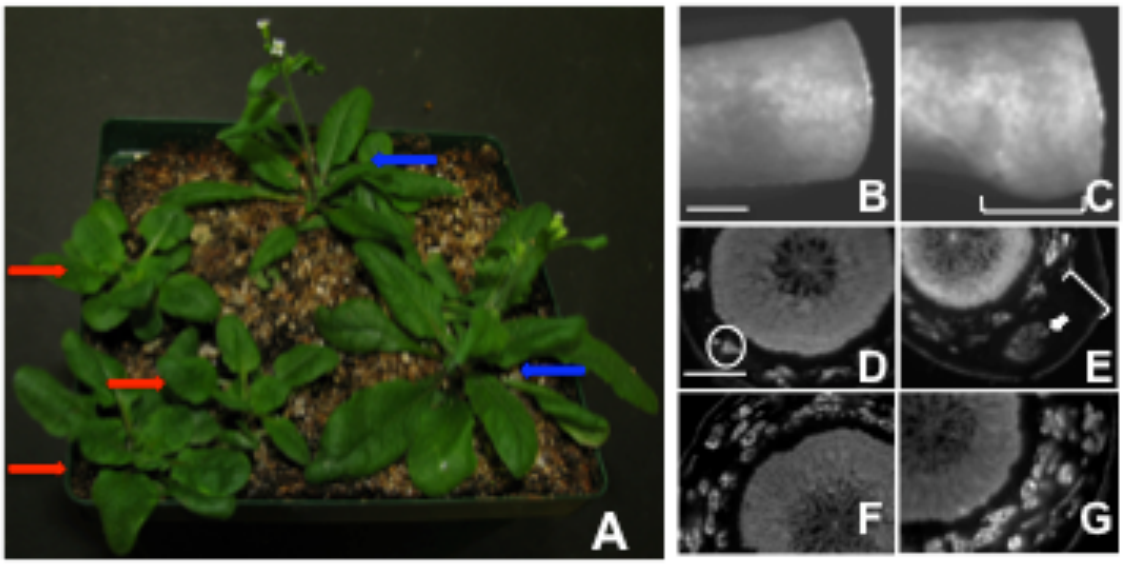

Figure 2.3. Plants of phloem-localized expression of *PB129*

(A) 5 weeks old Arabidopsis plants expressing *PB129* driven by *SUC2* promoter. Red arrows indicate phenotype-positive plants with wavy, crinkled leaves. Blue arrows, WT-like transgenic plants as control.

(B, C) Wild type hypocotyl exhibits uniform outline (B) compared to *SUC2::PB129* transgenic with bulge (C, bracket).

(D) Autofluorescence microscopy shows that phloem fibers in the wild type hypocotyl form in evenly-spaced bundles (circle).

(E-G) Ectopic phloem fiber production, including an unusually large bundle (E, arrow) in hypocotyl bulge (E, bracket) is associated with elevated expression of *PB129* in phloem of three plants from the same transgenic event.

Bar in (B) = 1 mm. Bar in (D for E-G) = 500 μm.

2.3.3 Loss-of-function studies with Arabidopsis interacting proteins, ROP11 and DUF620

Mutants of single ROP GTPase were identified and analyzed as starting point to study loss-of-functions of putative Arabidopsis homologs of PB15. Neither loss of *ROP7* (*rop7,* GABI-212D04) nor loss of *ROP11* (*rop11-1,* SALK_013327) yielded visible morphological phenotypes. Absence of phenotypes for *rop11* or *rop7* was not surprising because all 11 members of ROP GTPases from Arabidopsis are closely related (Berken and Wittinghofer, 2008), suggesting that redundancy can mask loss-of-function phenotypes. In fact, as ROP10 and ROP11 share over 90% amino acid sequence identity, it seems likely that when ROP11 is silenced, ROP10 (and/or other GTPases) can at least partially compensate ROP11 function.

One possible way to overcome genetic redundancy between ROP family members and study discrete ROP function is by eliminating its interacting partners. For the PB15 homolog (ROP11), we reasoned that if orthologs of PB129 (DUF620 proteins that interacted with ROP11) were silenced, some or all of ROP11 functions dependent on interaction with DUF620 proteins may be abolished and result in a phenotype.

The double loss-of-function line *rop7 duf620-1* was generated by crossing *rop7* and T-DNA insertion line SALK_148089 (*duf620-1*). *rop11 duf620-1* was generated by crossing *rop11-1* and *duf620-1*. *duf620-1 duf620-2* was generated by crossing *duf620-1* and GABI_705G02 (*duf620-2*). Unfortunately, none of the double mutants displayed unusual developmental or morphological phenotype. *rop11 duf620-1 duf620-2* triple mutants were also created but exhibited no phenotypic deviation relative to WT.

2.4 Discussion

2.4.1 Altering expression of two interacting proteins simultaneously

Our finding that transgenic plants expressing either *PB15* or *PB129* alone did not exhibit noticeable phenotypes, while co-expression lines showed interesting morphological changes suggests that simultaneously altering expression of two interacting proteins can provide novel information about gene functions. This research demonstrates the importance of studying PPIs via Y2H as a tool that can lead to fruitful studies of gene function in *planta*.

Although PB15 also interacts with Arabidopsis homologs of PB129 (data not shown), *PB15* over-expression individually in Arabidopsis was not sufficient to yield a phenotype. One potential explanation for this lack of phenotype from *PB15* overexpression is that although Arabidopsis presumably has some level of DUF620 proteins available for interaction with PB15, DUF620 proteins are quantitatively limiting factors for the formation of PB15-DUF620 interacting complexes. It this case, only when PB129 is also strongly expressed in the plant can the state of DUF620 protein scarcity be relieved and the formation of sufficient PB15-DUF620 interactions lead to the phenotype.

2.4.2 The pleiotropic roles for ROP GTPases in Arabidopsis

The ROP GTPases in plants are molecular switches that regulate a wide variety of cellular processes including cell division, polarization, morphogenesis, and directionality (Craddock et al., 2012). It is the very nature of ROPs as signaling switches, that affect so many aspects of cellular function, that makes the manipulation of ROPs expression hard to interpret because alteration of ROPs regulation and activity could potentially cause pleiotropic effects in plants.

As was observed in the T3 transgenic lines of *PB15* and *PB129* co-overexpressors, plants derived from the same parent line, display a diversity of leaf morphologies (Fig 2.2). Such variation from a single transgenic parent could be due to independent segregation of independent insertions for one or both of the *PB15* and *PB129* transgenes .

The phenotype of *PB15* and *PB129* overexpression plants suggested that these genes play roles in vascular tissue development and leaf morphology. Several reports have suggested that local auxin gradients function to activate ROPs and position them to the specific domain of cell membrane to initiate root hair formation (Duan et al., 2010; Xu et al., 2010). PIN protein directed auxin flow was affected by ROP effector ICR1 (Hazak et al., 2010). Outgrowth of interfascicular regions in Arabidopsis stem could be caused by auxin related mis-regulation of cell expansion and/or cell growth directionality.

2.4.3 Current status of this research

The co-overexpression *PB15* and *PB129* Arabidopsis plants described here constituted a small portion of the total transgenic population, where most transgenic individuals contained only one of the co-cultured transgenes. Subsequent generations resulting from self-fertilization of phenotype-positive lines contained both WT-like plants and a small number of phenotype-positive individuals. The protocol we used to generate co-overexpression lines was transforming WT Arabidopsis with co-cultured *PB15* and *PB129 Agrobacterium* media for floral dip. This method may not be effective for producing transformants with strong overexpression of both proteins. Consequently, an effort was made to generate double high expression lines through genetic crossing. WT plants were transformed with untagged (original experiments were conducted with YFP-tagged proteins) *35S::PB15* and *35S::PB129* separately. Transgenic lines that express *PB15* or *PB129* highly were selected and used for crossing and populations from following generation were screened for both *PB15* and *PB129* expression. However, double overexpressor lines failed to repeat the phenotype observed in the co-overexpression experiments for reasons that are currently unclear. It is worth noting, however, that the original construct of YFP-tagged *PB15* that yielded the aforementioned phenotype was tagged at the C-terminal end of PB15, which may have affected its localization or activity due to masking of the C-terminal CaaX domain required for proper plasma membrane localization (Lavy and Yalovsky, 2006).

2.5 References

Alonso JM, Stepanova AN, Leisse TJ, Kim CJ, Chen H, Shinn P, Stevenson DK, Zimmerman J, Barajas P, Cheuk R, Gadrinab C, Heller C, Jeske A, Koesema E, Meyers CC, Parker H, Prednis L, Ansari Y, Choy N, Deen H, Geralt M, Hazari N, Hom E, Karnes M, Mulholland C, Ndubaku R, Schmidt I, Guzman P, Aguilar-Henonin L, Schmid M, Weigel D, Carter DE, Marchand T, Risseeuw E, Brogden D, Zeko A, Crosby WL, Berry CC, Ecker JR (2003) Genome-wide insertional mutagenesis of Arabidopsis thaliana. Science **301:** 653-657

Arabidopsis Interactome Mapping C (2011) Evidence for network evolution in an Arabidopsis interactome map. Science **333:** 601-607

Avci U, Petzold HE, Ismail IO, Beers EP, Haigler CH (2008) Cysteine proteases XCP1 and XCP2 aid micro-autolysis within the intact central vacuole during xylogenesis in Arabidopsis roots. Plant J **56:** 303-315

Berken A, Wittinghofer A (2008) Structure and function of Rho-type molecular switches in plants. Plant Physiol Biochem **46:** 380-393

Brembu T, Winge P, Bones AM (2005) The small GTPase AtRAC2/ROP7 is specifically expressed during late stages of xylem differentiation in Arabidopsis. J Exp Bot **56:** 2465-2476

Clough SJ, Bent AF (1998) Floral dip: a simplified method for Agrobacterium-mediated transformation of Arabidopsis thaliana. Plant J **16:** 735-743

Craddock C, Lavagi I, Yang Z (2012) New insights into Rho signaling from plant ROP/Rac GTPases. Trends Cell Biol **22:** 492-501

Duan Q, Kita D, Li C, Cheung AY, Wu HM (2010) FERONIA receptor-like kinase regulates RHO GTPase signaling of root hair development. Proc Natl Acad Sci U S A **107:** 17821-17826

Franck A, Guilley H, Jonard G, Richards K, Hirth L (1980) Nucleotide sequence of cauliflower mosaic virus DNA. Cell **21:** 285-294

Hazak O, Bloch D, Poraty L, Sternberg H, Zhang J, Friml J, Yalovsky S (2010) A rho scaffold integrates the secretory system with feedback mechanisms in regulation of auxin distribution. PLoS Biol **8:** e1000282

Jefferson RA, Kavanagh TA, Bevan MW (1987) GUS fusions: beta-glucuronidase as a sensitive and versatile gene fusion marker in higher plants. EMBO J **6:** 3901-3907

Kay R, Chan A, Daly M, McPherson J (1987) Duplication of CaMV 35S Promoter Sequences Creates a Strong Enhancer for Plant Genes. Science **236:** 1299-1302

Koornneef M, Meinke D (2010) The development of Arabidopsis as a model plant. Plant J **61:** 909-921

Lavy M, Yalovsky S (2006) Association of Arabidopsis type-II ROPs with the plasma membrane requires a conserved C-terminal sequence motif and a proximal polybasic domain. Plant J **46:** 934-947

Leple JC, Dauwe R, Morreel K, Storme V, Lapierre C, Pollet B, Naumann A, Kang KY, Kim H, Ruel K, Lefebvre A, Joseleau JP, Grima-Pettenati J, De Rycke R, Andersson-Gunneras S, Erban A, Fehrle I, Petit-Conil M, Kopka J, Polle A, Messens E, Sundberg B, Mansfield SD, Ralph J, Pilate G, Boerjan W (2007) Downregulation of cinnamoyl-coenzyme A reductase in poplar: multiple-level phenotyping reveals effects on cell wall polymer metabolism and structure. Plant Cell **19:** 3669-3691

Truernit E, Sauer N (1995) The promoter of the Arabidopsis thaliana SUC2 sucrose-H+ symporter gene directs expression of beta-glucuronidase to the phloem: evidence for phloem loading and unloading by SUC2. Planta **196:** 564-570

Xu T, Wen M, Nagawa S, Fu Y, Chen JG, Wu MJ, Perrot-Rechenmann C, Friml J, Jones AM, Yang Z (2010) Cell surface- and rho GTPase-based auxin signaling controls cellular interdigitation in Arabidopsis. Cell **143:** 99-110

Yoo SY, Bomblies K, Yoo SK, Yang JW, Choi MS, Lee JS, Weigel D, Ahn JH (2005) The 35S promoter used in a selectable marker gene of a plant transformation vector affects the expression of the transgene. Planta **221:** 523-530

Zhao C, Craig JC, Petzold HE, Dickerman AW, Beers EP (2005) The xylem and phloem transcriptomes from secondary tissues of the Arabidopsis root-hypocotyl. Plant Physiol **138:** 803-818

Chapter 3

Functional analysis of PB15 and PB129 in *Populus*

3.1 Introduction

Forest trees have been proposed as candidate crops for the second-generation bioenergy production (Sims et al., 2010). But often, the increased demand for forest products is accompanied by rapid deforestation. The use of fast-growing, short-rotation forest trees has the potential to minimize or prevent deforestation that may accompany increased demand for energy production from forest trees. However, domestication of trees for such purposes using conventional cultivation and breeding techniques is not expected to meet future demands due to their time consuming, laborious protocols and the complex reproductive characteristics of trees (Harfouche et al., 2011). With the technological advancement of molecular biology and genetic transformation, genetically modified (GM) trees can provide additional or alternative solutions to problems facing foresters.

GM trees have been employed for various purposes. To date, over 30 forest tree species have been successfully transformed and regenerated (van Frankenhuyzen and Beardmore, 2004). Some of the targeted traits are commercially attractive, such as herbicide tolerance, the integration of delta-endotoxin genes (*cry*) from *Bacillus thuringiensis* (Bt) for insect resistance, and very importantly for bioenergy production, improved wood quality and quantity traits. Field trials have demonstrated the commercial feasibility of using lignin-modified trees for improved pulping efficiency. Leple et al. (2007) showed that downregulation of *Cinnamoyl-CoA reductase* (*CCR*) in transgenic poplar (*Populus tremula* × *Populus alba*) was associated with up to 47% reduced lignin content. Two lines of these GM poplars were more easily delignified at a lower alkali charge (16 versus 18%) (Leple et al., 2007). GM technology can also be used to help rescue tree species endangered by exotic diseases. For example, by 1950, most American chestnuts (*Castanea dentata*) had been invaded by a chestnut blight fungus, which was accidentally introduced into the United States around 1900. Integration of a chestnut blight-resistant gene into American chestnut could potentially restore the species to the forest (Merkle et al., 2007).

In the research described here, hybrid aspen INRA (Institut national de la recherche agronomique, France) clone 717-1B4 (*Populus tremula* × *Populus alba*) was selected for transformation because of the relative ease with which it can be transformed through *Agrobacterium tumefaciens* infection for the expression of transgenes (Brasileiro et al., 1991). While constitutive or ectopic expression (gain-of-function) experiments are easily accomplished in poplar, there are no T-DNA insertion mutation (loss-of-function) collections available for poplar trees. Thus, RNA interference (RNAi) techniques are typically used to generate loss-of-function mutants for *Populus*.

The term RNAi was first proposed in 1998 to describe the phenomenon that the introduction of short double-stranded RNA (dsRNA) into *Caenorhabditis elegans* is substantially more effective at silencing gene expression than either sense or antisense RNA (Guo and Kemphues, 1995; Rocheleau et al., 1997; Fire et al., 1998). This powerful mechanism is conserved among various organisms from plants and fungi to animals to defend against viruses and mobile genetic elements and regulate endogenous gene expression. Two types of RNA molecules, small-interfering RNAs (siRNAs) and microRNAs (miRNAs) are involved in post-transcriptional gene silencing (PTGS).

siRNAs are generated from endogenous or exogenous long dsRNA by cleavage carried out by a ribonuclease III type enzyme called Dicer (Zhang et al., 2004). Usually 21-24 nucleotides long, siRNAs are then incorporated into RNA-induced Silencing Complex (RISC) inside which the Argonaute (Ago) family proteins are core components (Vaucheret, 2008). Target mRNAs are degraded based on homology with siRNAs loaded into RISC (Tang, 2005).

The biogenesis, maturation, and incorporation of miRNAs into RISC differs from that for siRNAs. miRNAs are usually transcribed by RNA polymerase II as long precursor transcripts (pre-miRNAs) (Lee et al., 2004). Pre-miRNAs need to be processed to ~22 bp miRNA:miRNA* duplexes before loading to the silencing complex (Bartel, 2004). Mature miRNA (miRNA strand) is the template to guide targeted gene silencing, while miRNA* is degraded (Jones-Rhoades et al., 2006).

For researchers working with ROP GTPases, numerous examples from Arabidopsis transgenic studies showed that direct down regulation or overexpression of native ROP genes were not sufficient to alter phenotypes (Li et al., 1999; Bloch et al., 2005; Brembu et al., 2005). However, ectopic expression of constitutively active (CA) or dominant negative (DN) mutants of ROPs often causes morphological changes and hence provides key information on the function of the ROP of interest (Li et al., 1999; Oda and Fukuda, 2012).

In this chapter, we present our effort on functional characterization of PB15 and PB129 by both loss-of-function and gain-of-function approaches in *Populus*.

3.2 Materials and methods

3.2.1 Plants and growth conditions

Poplar clone 717-1B4 (*Populus tremula* × *Populus alba*) was used as WT for transformation. Young plants were grown in Magenta GA-7 boxes (dimension 3 x 3 x 4") containing propagation medium (1/2-strength Murashige-Skoog, pH 5.8, 0.7% agar) under long-day condition (16 h photoperiod, 8 h dark) and continuous 25°C. New plants were regenerated asexually about every 4 to 6 weeks. Typically, 6-week-old poplar plants were used for making explants for transformation.

3.2.2 Constructs

Vector construction for silencing *PB15* and/or *PB129* by double strand RNAi (dsRNAi)

pHANNIBAL vector was employed for generation of intron-containing `hairpin' RNA (ihpRNA) constructs. Transcript sequences of *PB15* and *PB129* from *Populus trichocarpa* were used as reference for primer designs and silencing target regions selection. However, nucleotide sequences that were used for vector construction were amplified from *Populus tremula* × *Populus alba* clone 717-1B4.

Cloning strategies and pHANNIBAL vectors were described previously (Wesley et al., 2001). In summary, the selected region of the target gene was amplified from 717-1B4 cDNA and cloned into pGEM-T easy vector. The sequenced DNA fragment was then cleaved from pGEM-T easy vector and subcloned into pHANNIBAL vector twice: first, upstream of the intron region with *Xho*I and *Xba*I restriction enzymes; and second, downstream of the intron region with *Xba*I and *Cla*I, respectively.

Completed construct for double strand RNAi (dsRNAi) made in pHANNIBAL vector was then digested with *Not*I and transferred into pART27 binary vector (Gleave, 1992) for *Agrobacterium*-mediated transformation. Primers used during vector construction are listed in Table 3.1. Sequenced DNA fragments used were shown in supplementary data.

Table 3.1 Primers used for dsRNAi contructs

Construct name	Primer sequence (5' to 3')	Primer name
35S::PB15-RNAi	ctcgagCGCAAGCAAAGAACATGTGC	XhoI+15U
	ggtaccTGAACTGATGTACAAAACTC	KpnI+15D
	tctagaCGCAAGCAAAGAACATGTGC	XbaI+15U
	atcgatTGAACTGATGTACAAAACTC	15D+ClaI
35S:PB129-RNAi	ctcgagGGCATGTACTGTATGGCTAT	XhoI+129U
	ggtaccTCATGGAGAAGCATCATAGA	KpnI+129D
	tctagaGGCATGTACTGTATGGCTAT	XbaI+129U
	atcgatTCATGGAGAAGCATCATAGA	129D+ClaI
35S::PB15+PB129-RNAi	cccgggTGAACTGATGTACAAAACTC	15D+XmaI
	cccgggGGCATGTACTGTATGGCTAT	XmaI+129U

Restriction enzyme adapter sequences in the primers are presented by lowercase letters

The DNA fragment used in *35::PB15+PB129-RNAi* construct is a chimeric fusion of DNA fragment used in *35::PB15-RNAi* and *35::PB129-RNAi*. Two additional primers 15D+*Xma*I and *Xma*I+129U were used to facilitate cloning. The two sequences were linked together using *Xma*I

restriction enzymatic sites and put into pGEM-T easy vector. Next, the cloning strategy is the same as aforementioned except for using the chimeric DNA as sense or anti-sense arms for silencing constructs.

LMX5*::*CA-PB15* and *LMX5*::*DN-PB15

PB15 was amplified from previous *PB15* construct (Chapter 2) and cloned into pGEM-T vector using primer set TTAATTAAATGAGTACAGCAAGATTTATC and GAGCTCCTAGAGGAAAGCACATGTTCTTTGCTTGC, restriction enzymes sites added are *Pac*I and *Sac*I for 5 prime end and 3 prime end, respectively.

The 15th amino acid residue of PB15 glycine is substituted by valine (D15V) to create CA-PB15. The 121st amino acid residue of PB15 aspartic acid is substituted by alanine for DN-PB15 (Berken and Wittinghofer, 2008). Site-directed mutagenesis protocol was adopted from previous literature (Bloch et al., 2005).

LMX5 promoter was amplified from 717-1B4 genomic DNA as previously described (Love et al., 2009). *Hind*III and *Pac*I restriction enzymes were used to replace the *35S* promoter with the *LMX5* promoter in the binary vector pBI121. *CA-PB15* and *DN-PB15* were cleaved from corresponding pGEM-T vectors and put downstream of *LMX5* in pBI121.

3.2.3 *Populus* Transformation

The transformation method used for this research was reported by (Meilan and Ma, 2006). Explants (leaf discs or stem and petiole segments) obtained from 6-week-old plants were co-cultivated with transgenic *Agrobacterium* strains containing the desired vector at 150-200 rpm for 1 h. After co-cultivation, explants were washed with sterile ddH_2O and carefully placed on Callus Induction Media (CIM). CIM plates were kept at room temperature in the dark for 2-3 weeks until callus formed. Callus was then transferred onto Shoot Induction Media (SIM) and maintained in tissue culture room for 2-3 weeks until shoots formed. Shoots were excised at 0.5-1 cm down from growing tip and placed in Root Induction Media (RIM) containing appropriate selective antibiotics and 100 mg/L timentin. Usually 9 to 12 shoots were placed in each Magenta box. Magenta boxes were maintained in growth room until roots formed. Plants that survived on rooting media were considered candidate transgenic plants and were subjected to further testing.

3.2.4 Genotyping

Genomic DNA of potential transgenic plantlets was isolated and used as a template for PCR based genotyping. The *35S* forward (CGCACAATCCCACTATCCTT) and transgene-specific reverse primers were combined to differentiate RNAi transgenic lines and endogenous genes.

LMX5 forward (GGAGTATGGGTTAAGTCATCT) and *PB15* reverse primers (CTAGAGGAAAGCACATGTTCT) were used for genotyping of *LMX5::CA-PB15* and *LMX5::DN-PB15* transgenic poplar.

3.2.5 Transcript analysis

PB15 and *PB129* transcript levels were measured by reverse transcription quantitative PCR (RT-qPCR). Total mRNAs were prepared from leaf and stem tissues of 6-week-old transgenic plants using RNeasy Mini Kit (QIAGEN, Venlo, Netherlands). About 2 μg of mRNA was reverse transcribed into cDNA using High Capacity cDNA Reverse Transcription Kit (Life Technologies, Carlsbad, CA). PCR reactions were run on an Applied Biosystems 7500 Real-Time PCR System using *power* SYBR Green PCR Master Mix (ABI, Foster City, CA, USA). Ubiquitin (*UBQ*) gene was used as internal control gene. Three duplicates for each sample were run within a 96-well plate. Relative transcript levels were generated by the applied biosystems 7500 software using $2^{(-\Delta\Delta Ct)}$ analysis (Livak and Schmittgen, 2001) with the transcript level for wild type being set as 1.

Gene specific primers used for *PB15* transcript analysis are TGCAATAAAGGTTGCTTTGC and AATGGACTGTATTCCTTGCT. For *PB129* transcript analysis: CGATGATGTCGTGTTCAATG and AGCAGCTACATACTACACTT.

3.3 Results

3.3.1 Genotyping of *PB15-RNAi* and *PB129-RNAi* lines in *Populus*

Populus ROP gene family members share high sequence identity. Fortunately for this research, the C-terminal portion of ROP transcripts comprise the hypervariable regions (HVR) and have little homology. Therefore the C-terminal HVR of *PB15* transcripts was used for double-strand RNAi silencing of *PB15* to minimize off-target effects.

PB129 has a paralogous gene (*Potri.008G081700*) in *Populus* due to a recent gene duplication event and their transcripts share over 75% sequence similarity (Tuskan et al., 2006). Using double-strand RNAi strategy to silence *PB129* would inevitably silence its paralog. On the other hand, it is also reasonable to believe that *PB129* and its paralog may function redundantly. It might be necessary to silence both genes to achieve a loss-of-function phenotype. Based on this reasoning, *35S::PB129-RNAi* constructs was designed to silence both genes.

Based on genotyping, 14 and 13 independent transformation events were shown to include *35S::PB15-RNAi* (Fig. 3.1) and *35S::PB129-RNAi* (Fig. 3.2) silencing constructs, respectively. In addition, 2 independent transformation events were recovered for *PB15+PB129-RNAi* co-silencing lines (Figure 3.3).

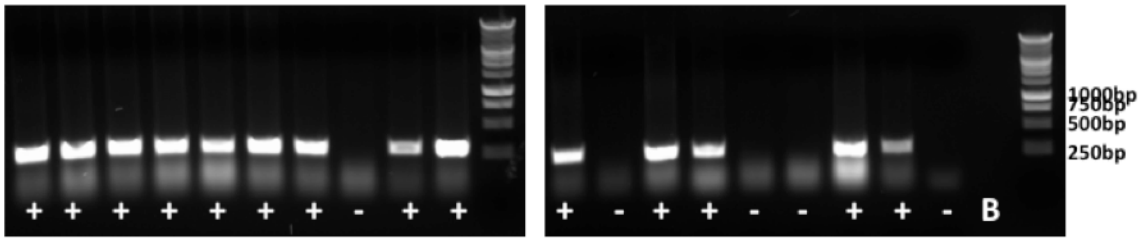

Figure 3.1. PCR based genotyping of potential *PB15-RNAi* lines

+, lines containing the *35S::PB15-RNAi* construct. -, lines that do not contain the *35S::PB15-RNAi* construct. B, blank lane.

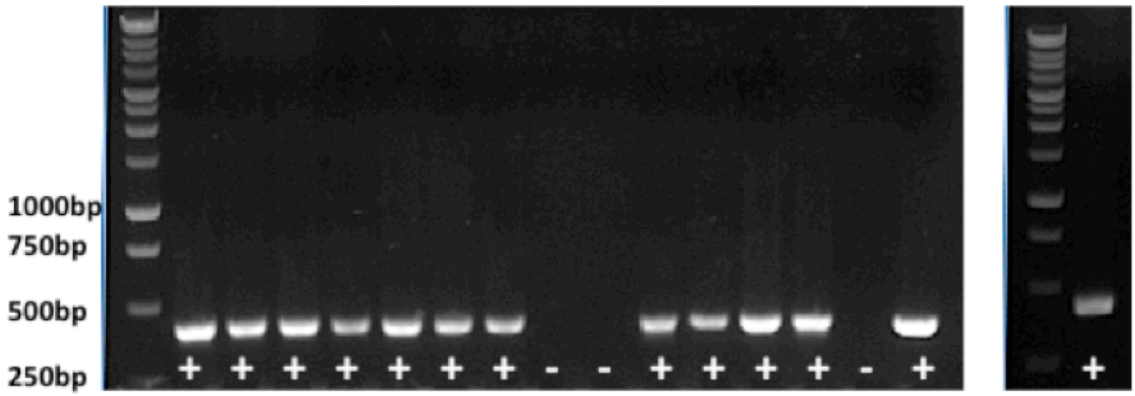

Figure 3.2. PCR based genotyping of putative *PB129-RNAi* lines

+, lines containing the *35S::PB129-RNAi* construct. -, lines that do not contain the *35S::PB129-RNAi* construct.

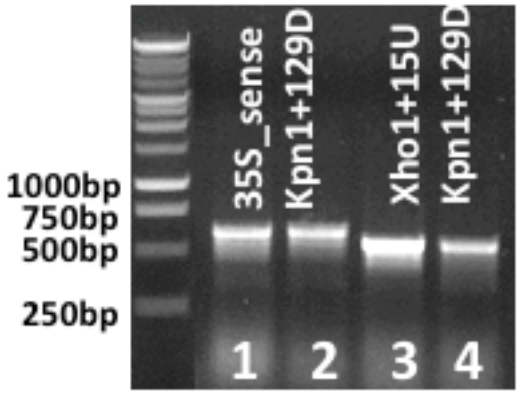

Figure 3.3. PCR based genotyping of putative *PB15+129-RNAi* lines

Lane 1 and 2, primer set 35_sense and *Kpn*I+*129*D used.
Lane 3 and 4, primer set *Xho*I+*15*U and *Kpn*I+*129*D used, templates used were the same as those of Lane 1 and 2, respectively.

3.3.2 Transcripts analysis for *PB15* and *PB129* in corresponding putative silencing lines

Total mRNAs were isolated from stem and leaf tissues of putative transgenic poplars aforementioned and reverse transcribed for real time PCR analysis. 7 *PB15-RNAi* and 6 *PB129-RNAi* transgenic lines show down-regulation for *PB15* and *PB129* transcripts, respectively. Down-regulations of both *PB15* and *PB129* were detected for two *PB15+PB129-RNAi* transgenic lines.

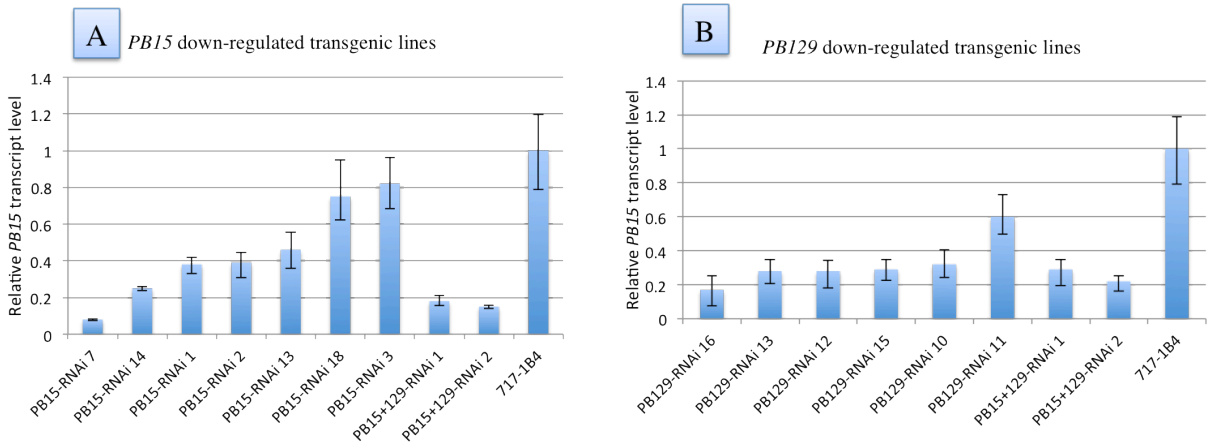

Figure 3.4. Relative transcript levels of *PB15* and *PB129* in transgenic plants

Transcript level in *Populus tremula* × *Populus alba* 717-1B4 was set as 1. (A) *PB15* transcript level in selected *PB15-RNAi* lines relative to wide type. (B) *PB129* transcript level in selected *PB129-RNAi* lines relative to wide type.

3.3.3 Poplar xylem specific expression of *CA-PB15* and *DN-PB15* driven by *LMX5* promoter

The *LMX5* promoter was first tested by Love and colleagues (Love et al., 2009). *GUS* reporter expression patterns of the *LMX5* promoter in *Populus* stem tissues demonstrated that this promoter preferentially directs expression of downstream genes to the cambial meristem and developing wood cells (Figure 3.5). The *LMX5* promoter was used in this research to limit the ectopic expression of *CA-PB15* and *DN-PB15* to vascular tissue, where native *PB15* is normally expressed. Inserted *CA-PB15* or *DN-PB15* T-DNA was detected in at least 10 putative transgenic plants for each construct according to PCR based genotyping.

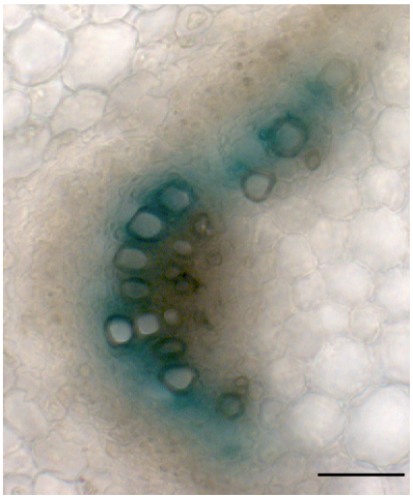

Figure 3.5. *GUS* expression driven by *LMX5* promoter in 717-1B4 stems

LMX5 directs gene expression (represented here by *GUS* activity) in the cambial zone and developing xylem, consistent with the observation reported previously (Love et al., 2009). Bar = 100 mm.

3.4 Future work and discussion

For each of the constructs described above, at least three independent transgenic events per construct will be characterized. A minimum of four replications per transgenic event will be planted in pairs for a field trial and/or studied in controlled environments (greenhouse/growth chamber). Properties of transgenic plants to be further analyzed include wood anatomy, development and morphology, wood density, biomass production, and cell wall chemistry.

The functional analysis in Arabidopsis has shown that the phenotype was only observed for overexpression *PB129* with *PB15*, but not for co-silencing of their Arabidopsis orthologs. The lack of loss-of-function phenotype could be because that Arabidopsis lacks some structural and lifestyle characteristics that are unique to perennial woody crops. Consequently, transgenic polar lines would provide useful tools to study the functions of PB15 and PB129 in poplar.

For most ROP GTPases, it is the active GTP-bound state that interacts with effector proteins to initiate downstream signaling (Berken and Wittinghofer, 2008). Many ROP effector proteins were orginally identified as interacting proteins for native ROPs or constutively active ROPs (Wu et al., 2001; Lavy et al., 2007). High level expression of constutively active PB15 in vascular tissue of poplar stem may faciliate the recruitment of its effectors and transduce the signal to the ultimate target systems with relevance to and possibly enhancing its natural role in xylem. One could speculate that PB129 acts as an effector for PB15 and plays a role in its specific signaling pathway.

The expression of dominant negative PB15 diven by *LMX5* promoter not only competes with native PB15 and silences its function but may also create a feedback loop to suppress other vascular tissue related ROPs expression. The effect is likely to imitate the co-suppression of PB15 and also its family members that function redundantly in vascular tissue. The phenotype caused by *LMX5::DN-PB15* could potentially reflect the roles that PB15 and other similar ROPs play in wood formation.

3.5 References

Bartel DP (2004) MicroRNAs: Genomics, biogenesis, mechanism, and function. Cell **116:** 281-297

Berken A, Wittinghofer A (2008) Structure and function of Rho-type molecular switches in plants. Plant Physiol Biochem **46:** 380-393

Bloch D, Lavy M, Efrat Y, Efroni I, Bracha-Drori K, Abu-Abied M, Sadot E, Yalovsky S (2005) Ectopic expression of an activated RAC in Arabidopsis disrupts membrane cycling. Mol Biol Cell **16:** 1913-1927

Brasileiro AC, Leple JC, Muzzin J, Ounnoughi D, Michel MF, Jouanin L (1991) An alternative approach for gene transfer in trees using wild-type Agrobacterium strains. Plant Mol Biol **17:** 441-452

Brembu T, Winge P, Bones AM (2005) The small GTPase AtRAC2/ROP7 is specifically expressed during late stages of xylem differentiation in Arabidopsis. J Exp Bot **56:** 2465-2476

Fire A, Xu SQ, Montgomery MK, Kostas SA, Driver SE, Mello CC (1998) Potent and specific genetic interference by double-stranded RNA in Caenorhabditis elegans. Nature **391:** 806-811

Gleave AP (1992) A versatile binary vector system with a T-DNA organisational structure conducive to efficient integration of cloned DNA into the plant genome. Plant Mol Biol **20:** 1203-1207

Guo S, Kemphues KJ (1995) Par-1, a Gene Required for Establishing Polarity in C-Elegans Embryos, Encodes a Putative Ser/Thr Kinase That Is Asymmetrically Distributed. Cell **81:** 611-620

Harfouche A, Meilan R, Altman A (2011) Tree genetic engineering and applications to sustainable forestry and biomass production. Trends Biotechnol **29:** 9-17

Jones-Rhoades MW, Bartel DP, Bartel B (2006) MicroRNAs and their regulatory roles in plants. Annual Review of Plant Biology **57:** 19-53

Lavy M, Bloch D, Hazak O, Gutman I, Poraty L, Sorek N, Sternberg H, Yalovsky S (2007) A Novel ROP/RAC effector links cell polarity, root-meristem maintenance, and vesicle trafficking. Curr Biol **17:** 947-952

Lee Y, Kim M, Han JJ, Yeom KH, Lee S, Baek SH, Kim VN (2004) MicroRNA genes are transcribed by RNA polymerase II. Embo Journal **23:** 4051-4060

Leple JC, Dauwe R, Morreel K, Storme V, Lapierre C, Pollet B, Naumann A, Kang KY, Kim H, Ruel K, Lefebvre A, Joseleau JP, Grima-Pettenati J, De Rycke R, Andersson-Gunneras S, Erban A, Fehrle I, Petit-Conil M, Kopka J, Polle A, Messens E, Sundberg B, Mansfield SD, Ralph J, Pilate G, Boerjan W (2007) Downregulation of cinnamoyl-coenzyme A reductase in poplar: multiple-level phenotyping reveals effects on cell wall polymer metabolism and structure. Plant Cell **19:** 3669-3691

Li H, Lin YK, Heath RM, Zhu MX, Yang ZB (1999) Control of pollen tube tip growth by a pop GTPase-dependent pathway that leads to tip-localized calcium influx. Plant Cell **11:** 1731-1742

Livak KJ, Schmittgen TD (2001) Analysis of relative gene expression data using real-time quantitative PCR and the 2(-Delta Delta C(T)) Method. Methods **25:** 402-408

Love J, Bjorklund S, Vahala J, Hertzberg M, Kangasjarvi J, Sundberg B (2009) Ethylene is an endogenous stimulator of cell division in the cambial meristem of Populus. Proc Natl Acad Sci U S A **106:** 5984-5989

Meilan R, Ma C (2006) Poplar (Populus spp.). Methods Mol Biol **344:** 143-151

Merkle SA, Andrade GM, Nairn CJ, Powell WA, Maynard CA (2007) Restoration of threatened species: a noble cause for transgenic trees. Tree Genetics & Genomes **3:** 111-118

Oda Y, Fukuda H (2012) Initiation of cell wall pattern by a Rho- and microtubule-driven symmetry breaking. Science **337:** 1333-1336

Rocheleau CE, Downs WD, Lin RL, Wittmann C, Bei YX, Cha YH, Ali M, Priess JR, Mello CC (1997) Wnt signaling and an APC-related gene specify endoderm in early C-elegans embryos. Cell **90:** 707-716

Sims RE, Mabee W, Saddler JN, Taylor M (2010) An overview of second generation biofuel technologies. Bioresour Technol **101:** 1570-1580

Tang GL (2005) siRNA and miRNA: an insight into RISCs. Trends in Biochemical Sciences **30:** 106-114

Tuskan GA, Difazio S, Jansson S, Bohlmann J, Grigoriev I, Hellsten U, Putnam N, Ralph S, Rombauts S, Salamov A, Schein J, Sterck L, Aerts A, Bhalerao RR, Bhalerao RP, Blaudez D, Boerjan W, Brun A, Brunner A, Busov V, Campbell M, Carlson J, Chalot M, Chapman J, Chen GL, Cooper D, Coutinho PM, Couturier J, Covert S, Cronk Q, Cunningham R, Davis J, Degroeve S, Dejardin A, Depamphilis C, Detter J, Dirks B, Dubchak I, Duplessis S, Ehlting J, Ellis B, Gendler K, Goodstein D, Gribskov M, Grimwood J, Groover A, Gunter L, Hamberger B, Heinze B, Helariutta Y, Henrissat B, Holligan D, Holt R, Huang W, Islam-Faridi N, Jones S, Jones-Rhoades M, Jorgensen R, Joshi C, Kangasjarvi J, Karlsson J, Kelleher C, Kirkpatrick R, Kirst M, Kohler A, Kalluri U, Larimer F, Leebens-Mack J, Leple JC, Locascio P, Lou Y, Lucas S, Martin F, Montanini B, Napoli C, Nelson DR, Nelson C, Nieminen K, Nilsson O, Pereda V, Peter G, Philippe R, Pilate G, Poliakov A, Razumovskaya J, Richardson P, Rinaldi C, Ritland K, Rouze P, Ryaboy D,

Schmutz J, Schrader J, Segerman B, Shin H, Siddiqui A, Sterky F, Terry A, Tsai CJ, Uberbacher E, Unneberg P, Vahala J, Wall K, Wessler S, Yang G, Yin T, Douglas C, Marra M, Sandberg G, Van de Peer Y, Rokhsar D (2006) The genome of black cottonwood, Populus trichocarpa (Torr. & Gray). Science **313:** 1596-1604

van Frankenhuyzen K, Beardmore T (2004) Current status and environmental impact of transgenic forest trees. Canadian Journal of Forest Research-Revue Canadienne De Recherche Forestiere **34:** 1163-1180

Vaucheret H (2008) Plant ARGONAUTES. Trends in Plant Science **13:** 350-358

Wesley SV, Helliwell CA, Smith NA, Wang MB, Rouse DT, Liu Q, Gooding PS, Singh SP, Abbott D, Stoutjesdijk PA, Robinson SP, Gleave AP, Green AG, Waterhouse PM (2001) Construct design for efficient, effective and high-throughput gene silencing in plants. Plant J **27:** 581-590

Wu G, Gu Y, Li S, Yang Z (2001) A genome-wide analysis of Arabidopsis Rop-interactive CRIB motif-containing proteins that act as Rop GTPase targets. Plant Cell **13:** 2841-2856

Zhang HD, Kolb FA, Jaskiewicz L, Westhof E, Filipowicz W (2004) Single processing center models for human dicer and bacterial RNase III. Cell **118:** 57-68

3.6 Supplementary data for Chapter 3

Selected DNA fragments for the following constructs:

35S::PB15-RNAi

CGCAAGCAAAGAACATGTGCTTTCCTCTAGTCCCTTTCAATTTCTTGCCATGAATTTGCTTT
ACTAGATTTTTCAAAGCAAGGAATACAGTCCATTTTTATTGAATTACTTATTTTATAAGCGAG
TTCCCTTTGGAGCTATGTAACATCCACAGGGAGGACTTCGATGCCTAAAGTTGTAATATGA
GTTTTGTACATCAGTTCA

35S::PB129-RNAi

GGCATGTACTGTATGGCTATTTTTGCCAAAAAAGTGGCCTCTTAATGTATTTGGAGGACTC
CCATCTAACACGGGTACAAACTCCAGAAAATGAAACTATCTATTGGGAGACTACTATAGGA
AGTAGTATTGGCGACTATAGAGATGTGGATGGTGTGTTAATTGCTCATCAAGGAAGGTCAA
TTGCTACAGTTTTTCGATTCGAGGAAGTGTCAGTGCAACACAGTAGGACTAGAATGGAAGA
AGTATGGAGGATCGATGATGTCGTGTTCAATGTTCCAGGGCTTTCCATGGATTATTTCATC
CCTCCTGCTGATATCTATGATGCTTCTCCATGA

35S::PB15+PB129-RNAi

CGCAAGCAAAGAACATGTGCTTTCCTCTAGTCCCTTTCAATTTCTTGCCATGAATTTGCTCT
ACTAAATTTTTCAAAGGAATACAGTCCATTTTTATTGAATTACTTATTTTATAAGCGAGTTCC
CTTTGGAGCTATGTAACATCCACAGGGAGGACTTCAATGCCTAAAGTTGTAATATGAGTTTT
GTACATCAGTTCACCCGGGGGCATGTACTGTATGGCTATTTTTGCCAAAAAAGTGGCCTCT
TAATGTATTTGGAGGACTCCCATCTAACACGGGTACAAACTCCAGAAAATGAAACTATCTAT
TGGGAGACTACTATAGGAAGTAGTATTGGCGACTATAGAGATGTGGATGGTGTGTTAATTG
CTCATCAAGGAAGGTCAATTGCTACAGTTTTTCGATTCGAGGAAGTGTCAGTGCAACACAG
TAGGACTAGAATGGAAGAAGTATGGAGGATCGATGATGTCGTGTTCAATGTTCCAGGGCTT
TCCATGGATTATTTTCATCCCCTCCTGCTGATATCTATGATGCTTCTCCATGA

Stop codons for *PB15* and *PB129* are indicated by double underline.

Chapter 4

ROP11 is an interactor and negative regulator of CSN5A in Arabidopsis

4.1 Introduction

The COP9 signalosome (CSN) subunit 5 (CSN5) is one of eight CSN subunits. CSN5 is highly conserved between the plant and animal kingdoms, with protein sequences from *Arabidopsis* and humans sharing greater than 60% amino acid identity (Claret et al., 1996; Kwok et al., 1998; Seeger et al., 1998). The main biochemical function of COP9 is attributed to its ability to remove the ubiquitin-like protein NEDD8 from cullin family proteins of the cullin-RING E3 ligases (CRLs) complexes and thereby contribute to the regulation of the 26S proteasome pathway (Lyapina et al., 2001; Zhou et al., 2001). The deneddylation activity of COP9 depends on the metalloprotease motif within the MPN^+ domain of the CSN5 subunit (Cope et al., 2002; Maytal-Kivity et al., 2002). Mutations of conserved key residues in the MPN motif did not affect the incorporation of CSN5 into COP9 but abolished CSN-dependent cleavage of NEDD8 from cullins (Cope et al., 2002; Gusmaroli et al., 2004).

There are two genes encoding CSN5 subunits in *Arabidopsis*, *AT1G22920* and *AT1G71230*, designated as *CSN5A* and *CSN5B*, respectively. It has been shown that CSN5A and CSN5B are incorporated into distinct COP9 protein complexes, and they play unequal roles in plant development, with CSN5A predominating in both functionality and expression level (Kwok et al., 1998; Gusmaroli et al., 2004). Loss of CSN5A has severe pleiotropic effects on *Arabidopsis* plants (Dohmann et al., 2005). The null mutant *csn5a-1* displayed a typical *cop/det/fus* phenotype characterized by reduced growth, accumulation of anthocyanin, loss of apical dominance, and photomorphogenesis in darkness. A second mutant of *CSN5A*, *csn5a-2*, has a nearly identical but less extreme phenotype compared to *csn5a-1*, due to a low level of splicing-out of its intron-localized T-DNA insertion, which results in severely reduced but detectable expression of full length CSN5A protein (Gusmaroli et al., 2007). However, both lines are viable and fertile (Dohmann et al., 2005). A complete depletion of CSN5, which can be achieved by knocking out both CSN5A and CSN5B, designated as *csn5a-1 csn5b-1*, is lethal. All *csn5a-1 csn5b-1* double null mutants die at the seedling stage without exception. However, *csn5a-2 csn5b-1* double mutants can survive to the mature stage, despite the fact that they are virtually indistinguishable from *csn5a-1 csn5b-1* at the seedling stage and are severely compromised in later development (Gusmaroli et al., 2007).

CSN5 was originally identified and known as Jun activation domain-binding protein 1 (JAB1) in mammalian systems (Claret et al., 1996). Multiple proteins regulating signal transduction and cell proliferation/survival are regulated by CSN5/JAB1 (Bech-Otschir et al., 2001; Tomoda et al., 2002; Wan et al., 2002; Oh et al., 2006). CSN5/JAB1 knockout mice exhibited growth arrest and lethality at embryogenesis correlating with higher levels of the G1 cell cycle regulators p53, p27 and cyclin E, and ultimately induced apoptosis (Tomoda et al., 2004; Tian et al., 2010). Abnormal overexpression of CSN5/JAB1 in many types of human cancers also provides evidence that it is implicated in the tumorigenic process (Sui et al., 2001; Fukumoto et al., 2004; Dong et al., 2005).

Ras superfamily monomeric GTPases (guanosine triphosphatases) are low molecular weight protein switches in eukaryotic signal transduction pathways that regulate a wide variety of cellular and developmental processes, such as cell division, vesicle transport, and control of the cytoskeleton (Wennerberg et al., 2005; Rojas et al., 2012). These small GTPases have two interconvertible forms: GDP-bound inactive and GTP-bound active. The conversion of GTP to GDP is catalyzed by their shared intrinsic GTPase activity, residing on evolutionarily preserved G-domains (Vetter and Wittinghofer, 2001; Berken and Wittinghofer, 2008). This superfamily is comprised of five major families: Ras, Rho, Arf/Sar, Ran, and Rab. Ras subfamily of small GTPases are well studied and frequently mutated oncoproteins in human cancers (Rojas et al., 2012). Viridiplantae (land plants and green algae) apparently lack members of the Ras subfamily but contain a unique subfamily of Rho GTPases, called ROPs (Rho of Plants), which presumably could carry out both functions of Ras and Rho (Vernoud et al., 2003; Berken and Wittinghofer, 2008; Craddock et al., 2012).

By far the best-characterized ROPs are the eleven members of the *Arabidopsis* ROP GTPase family (Berken and Wittinghofer, 2008; Craddock et al., 2012). The functions of these ROPs are linked to cell polarization, cell divisions and cell morphogenesis (Yang, 2008; Craddock et al., 2012). Expression of a constitutively active mutant of ROP1 resulted in non-polarized pollen tube growth (Li et al., 1999). ROP2 and ROP4 are reported to regulate tip growth in root hairs (Jones et al., 2007; Duan et al., 2010; Yoo et al., 2012). ROP2 and ROP6 are both activated by auxin to regulate pavement cells complementary lobe formation and indentation, respectively, but in an antagonizing manner (Xu et al., 2010). Research also showed that ROPs mediate auxin-regulated gene expression and directional auxin transport (Wu et al., 2011). However, due to the functional redundancy and relative lack of loss-of-function phenotypes, our knowledge about this family of molecular switches is still limited.

Several functions have been attributed to ROP11. Neither loss-of-function nor overexpression of native *ROP11* in *Arabidopsis* resulted in visible phenotypes. However, ectopic expression of constitutively active *ROP11* (*CA-ROP11*) induced changes in leaf and root metaxylem cell morphologies (Bloch et al., 2005; Oda and Fukuda, 2012). ROP11 was also a negative regulator of multiple ABA responses in *Arabidopsis*, including induction of ABA-responsive genes, ABA-mediated seed germination, seedling growth, stomatal closure, and plant response to drought stress (Li et al., 2012; Li et al., 2012). More recent work found ROP11 to be locally activated in xylem cells to recruit MIDD1 and induce local disassembly of cortical microtubules yielding the pitted patterning of secondary cell walls (Oda and Fukuda, 2012). Expression of GFP-tagged CA-ROP11 but not native ROP11 in differentiating metaxylem cells disrupted the pit formation and result in smooth-surfaced (pitless) metaxylem cells.

From the high-quality binary protein-protein interactome map generated by *Arabidopsis* Interactome Mapping Consortium, ROP11 was found to interact with CSN5A in the AI-I_{MAIN} network (Arabidopsis Interactome Mapping, 2011). Here we confirm that ROP11 interacts with CSN5A in Y2H. Additionally, we have used available mutants for ROP11 and CSN5A in Arabidopsis to genetically characterize this interaction. Our findings indicate that ROP11 is a negative regulator of CSN5A protein stability or accumulation.

4.2 Materials and methods

4.2.1 Yeast two-hybrids assays

Yeast transformation protocols were adopted from (Walhout and Vidal, 2001). To summarize: harvested yeast cells were suspended in sterile water and then washed using TE/LiAc solution. Mix 50 µl TE/LiAc resuspended cells with 5 µl boiled carrier DNA (salmon sperm DNA, sigma) and about 100 ng vector DNA to be transformed. Add 300 µl TE/LiAc/PEG to the mixture and incubate at 30 °C for 30 min followed by 15 min incubation at 42 °C. Centrifuge to remove all the supernatant and suspend pellet in sterile water to plate transformed cells on corresponding selective plates.

Yeast strains Y8800 and Y8930 with the mating type *MAT*a and *MATα* respectively, were used in this research (Dreze et al., 2010). The genotype of these strains is: *leu2-3, 112 trp1-901 his3Δ200 ura3-52 gal4Δ gal80Δ GAL2::ADE2 GAL1::HIS3@LYS2 GAL7::lacZ@MET2 cyh2*^{R}. Vectors pDEST-AD and pDEST-DB used in this research were also described in (Dreze et al., 2010).

To avoid the auto-activation of yeast cells transformed with DB-CSN5A, CSN5A was cloned into pDEST-AD vector and all ROP GTPases were cloned into pDEST-DB vector individually in this study. pDEST-DB-X and pDEST-AD-Y were transformed into Y8800 and Y8930, respectively, and then two strains were mated to form diploid yeast cells. Diploid cells were then selected on yeast growth media plates lacking leucine and tryptophan for 48 hours. Only cells growing on –Leu –Trp plates would be tested for *GAL1::HIS3* reporter gene with 5 mM 3-AT and *GAL7::lacZ* reporter gene with X-gal (5-bromo-4-chloro-indolyl-β-D-galactopyranoside).

4.2.2 Arabidopsis plants and growth

Ecotype Columbia-0 was used as Arabidopsis wild-type control in this study. Arabidopsis plants were grown under long-day conditions (16 h of light/8 h of dark) in growth chamber at 22 °C unless otherwise specified. Arabidopsis transformation protocol was summaried in Chapter 2.

The *CSN5* mutants *csn5a-1* (SALK_063436), *csn5a-2* (SALK_027705) and *csn5b-1* (SALK_007134) were described previously (Gusmaroli et al., 2007) and kindly provided by the Schwechheimer lab. *ROP11* T-DNA insertion lines *rop11-0* (SALK_039681), *rop11-1* (SALK_013327) and *rop11-3* (GABI_345D05) were obtained from ABRC and NASC, respectively.

4.2.3 Genotyping and transcript analysis

Protocols for PCR based genotyping and transcript analysis were desbribed in Chapter 2. Transcript analysis protocols were described in Chapter 3. *PP2A* gene was used as internal control. Primers used for genotyping of *ROP11* mutants and *CSN5A* relative transcript level measurement are listed in suppplementary Table 4.S1. Genotyping of *CSN5* mutants were described previously (Gusmaroli et al., 2007).

4.2.4 Western blots

Total protein extraction protocol was obtained from the Bako lab (Umeå University).

Approximately 100 mg 8-day-old Arabidopsis seedlings were ground in liquid nitrogen and homogenized in KEB buffer (25 mM Tris-HCl 7.8, 10 mM $MgCl_2$, 5 mM EGTA, 2 mM DTT, 10% glycerol, 75 mM NaCl, 60 mM ß-glycerophosphate, 0.2% NP-40, 0.1 mM Na_3VO_4, 1 mM benzamidine, and 1X EDTA free protease inhibitor). DTT, ß-glycerophosphate, benzamidine and protease inhibitor (Halt Protease Inhibitor Cocktail 100X, Thermo Scientific) were freshly added to KEB buffer prior to use. The homogenates were then centrifuged for 10 min twice full speed at 4°C and the supernatants were saved. Relative protein concentrations were determined by BCA assay (Pierce BCA Protein Assay Kit, Thermo Scientific).

For gel blots assays, estimated equal amount of total proteins were loaded on pre-casted 4-12% gel (NuPAGE Novex 4-12% Bis-Tris Gel, Life Technologies Corporation). Rabbit polyclonal antibodies anti-RPN6 (BML-PW8370, Enzo life science, Farmingdale, New York) and anti-CSN5 (BML-PW8365, Enzo life science) were used as control and to detect CSN5A protein level, respectively, with dilution ratio 1:4000. Goat anti-rabbit Ig AP (SouthernBiotech, Birmingham, USA) was used as secondary antibody with dilution ratio 1:2000. Colorimetric detection method with NBT and BCIP was employed to visualize protein signal.

4.3 Results

4.3.1 CSN5A selectively interacts with ROP GTPases from *Populus* and *Arabidopsis*

Populus trichocarpa gene *Potri.011G061500* (*PtROP7*) (referred as PB15 in Chapters 2 and 3) encodes a ROP GTPase that shares most amino acid identity (87%) with *Arabidopsis* ROP7 (phylogenetic tree shown in supplementary Figure 4. S1) and is highly upregulated in differentiating secondary xylem cells (Rodgers-Melnick et al., 2012). In the context of our ongoing poplar biomass interactome project (http://xylome.vbi.vt.edu/index.html), PtROP7 was screened against a cDNA prey library prepared from poplar xylem tissue. Several putative novel interactors of PtROP7 were identified and later confirmed by cloning full-length ORFs and retesting in Y2H binary assays. One of these proteins confirmed to interact with PtROP7, PtDUF620 (*Potri.010G174200*), also interacted with a ROP GTPase (ROP11) from *Arabidopsis*. From the high-quality binary protein-protein interactome map generated by *Arabidopsis* Interactome Mapping Consortium, ROP11 was found to interact with CSN5A in the AI-I_{MAIN} network (Arabidopsis Interactome Mapping, 2011). As part of our effort to characterize protein-protein interactions associated with wood formation and the influence that may have to poplar biomass accumulation, we took advantage of existing ROP11 (*AT5G62880*) and CSN5A (*AT1G22920*) alleles in *Arabidopsis* to investigate roles that depend on their interaction.

PtROP7 and all 11 members of the *Arabidopsis* ROP GTPase family were cloned to test for interactions with CSN5A by Y2H (Yeast two-hybrid). Auto-activation by *CSN5A* fused to the *Gal4* DNA-binding domain (DB) in Y2H was reported previously (Arabidopsis Interactome Mapping, 2011) and confirmed by our assays (data not shown). However, none of the ROP GTPases are auto-activators (data not shown). Hence, to avoid the interference from auto-activation, *MAT*a yeast cells harboring individual DB-ROP GTPases were mated with *MAT*α type yeast cells containing AD-CSN5A for Y2H assays. Of the 11 ROP GTPases from *Arabidopsis*, only four interacted with CSN5A in yeast (Fig 4.1, A). Diploid yeast cells containing AD-CSN5A and any of DB-ROP7, DB-ROP9, DB-ROP10, DB-ROP11 but not DB-

ROP8 (shown as representative of additional non-interacting ROP1-ROP6) grew on media lacking leucine, tryptophan and histidine supplemented with 5 mM 3-AT (Fig 4.1, A). These four interactions were also shown to activate the Lac Z reporter, again, in contrast to the combination of AD-CSN5A and DB-ROP8, which failed to produce above background levels of β-galactosidase (Fig 4.1, A).

PtROP7 were also tested for interaction with CSN5A from *Arabidopsis* in the Y2H system. Not only PtROP7, but also constitutively active PtROP7 (CA-PtROP7) can interact with CSN5A, however dominant negative PtROP7 failed to activate either reporter (Fig 4.1, B). In the case of PtROP7, only the GTP binding form has the ability to interact with CSN5A in yeast, but not the GDP binding form. However, in the case of ROP11, neither CA-ROP11 nor DN-ROP11 but only native ROP11 interacted with CSN5A in the Y2H system.

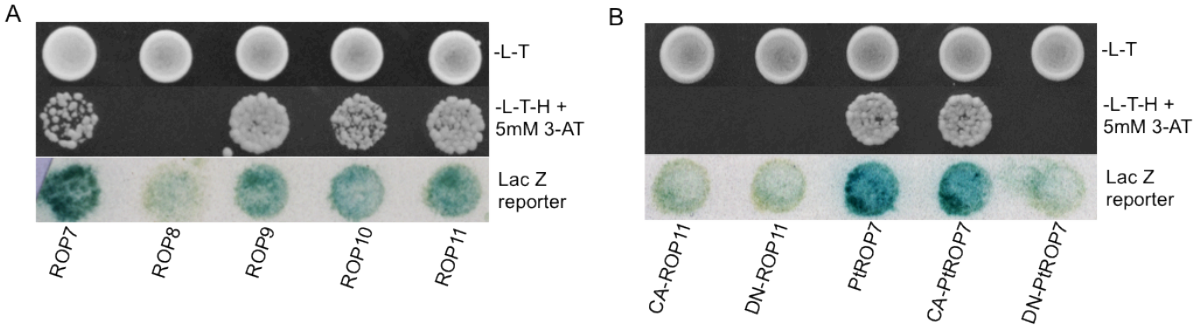

Figure 4.1. CSN5A selectively interacted with ROP GTPases in the Y2H system

(A) Four Arabidopsis ROP GTPases interacted with CSN5A in the Y2H system. All yeast cells shown here contained AD-CSN5A and corresponding DB-ROP GTPase. All 11 Arabidopsis ROP GTPases were tested. ROP1 to ROP6 did not interact with CSN5A and hence are not presented here. -L-T, yeast growth media lacking Leucine and Tryptophan; -L-T-H + 5mM 3-AT, yeast growth media lacking Leucine, Tryptophan and Histidine but supplemented with 5mM 3-AT (3-amino-1,2,4-triazole). Lac Z reporter, yeast cells selected on -L-T supplied with X-gal.

(B) PtROP7 and mutants of ROP11 and PtROP7 were tested for interaction with CSN5A in Y2H system. Experimental set-up was the same as shown in (A). CA-ROP11, constitutively active ROP11, Glycine^{17} was replaced by Valine (G17V); DN-ROP11, dominant negative ROP11, Threonine^{22} was replaced by Asparagine (T22N). CA-PtROP7, Glycine^{15} was replaced by Valine (G15V); DN-PtROP7, Aspartic Acid^{121} was replaced by Alanine (D121A).

4.3.2 Characterization of *ROP11* T-DNA insertional mutants

We reasoned that if the interaction between ROP11 and CSN5A affects CSN5A function, then loss of ROP11 should affect the phenotype of the weak *csn5a-2* allele described above, causing a shift in phenotype either toward wild type or toward the more severe phenotype of null *csn5a-1* line, depending on negative or positive influence, respectively, of ROP11 on CSN5A. To test this hypothesis and study the genetic interactions of *CSN5A* and *ROP11*, we characterized three

independent T-DNA insertion mutants in the *ROP11* locus, designated *rop11-0*, *rop11-1* and *rop11-3*. For *rop11-0* (SALK_039681), the T-DNA was mapped to the 5' untranslated region 46 base pairs upstream of the *ROP11* initiating Met codon (Fig. 4.2, A). Quantitative RT-PCR performed on cDNA from homozygous *rop11-0* and WT plants showed that transcript levels were reduced in *rop11-0* by 47% and 67% using primers located at the N-terminus or C-terminus, respectively (Fig 4.2, B). For *rop11-1* (SALK_013327), the T-DNA is centrally located in the first intron. No intact *ROP11* cDNA could be detected in the *rop11-1* homozygous line using primers set *yROP11F1* and *tROP11R1* (Fig 4.2, C). Quantitative RT-PCR employing a primer set spanning T-DNA insertion region (*yROP11F1* with *ROP11R2*) also failed to detect *ROP11* transcripts (Fig 4.2, B). However, primers located at the C-terminus of *ROP11* (*yROP11F2* and *tROP11R1*) detected relative transcript at about 42% of the WT level. The presence of C-terminal partial *ROP11* transcripts could be caused by a promoter-like sequence in the T-DNA. However, due to premature stop codons or frame shifts, these transcripts are not likely to yield a partial ROP11 protein. Thus, we conclude that the failure to detect full-length *ROP11* transcripts from the *rop11-1* homozygous line indicated it was a null mutant.

The T-DNA insertion site for *rop11-3* line (GABI_345D05) is located precisely in the junction of the third intron and fourth exon of *ROP11*. Although full-length *ROP11* transcripts could not be detected from homozygous *rop11-3* cDNA, two distinct PCR products, approximately 100 bp apart, were discovered using *yROP11F1* and GABI left border primer GR5 (Fig 4.2, C). Sequencing of both products showed that the smaller product was N-terminal cDNA of *ROP11* comprised of the first three exons, while the larger product included the third intron (108 bp) in addition to the first three exons. Chimeric transcripts suggested that *rop11-3* line may produce the N-terminal half of the ROP11 protein, which contains the conserved G1, G2 and G3 domains of ROP GTPases and may fulfill partial function of ROP11. Thus, we view *rop11-3* as a potential reduction-of-function line. Consistent with previous investigations of *ROP11* loss-of-function lines, none of homozygous *rop11* lines is noticeably different from WT plants (Fig. 4.3, C), making these lines especially useful for combining with loss or gain-of-function lines for other genes to test for second-site enhancer/suppressor effects.

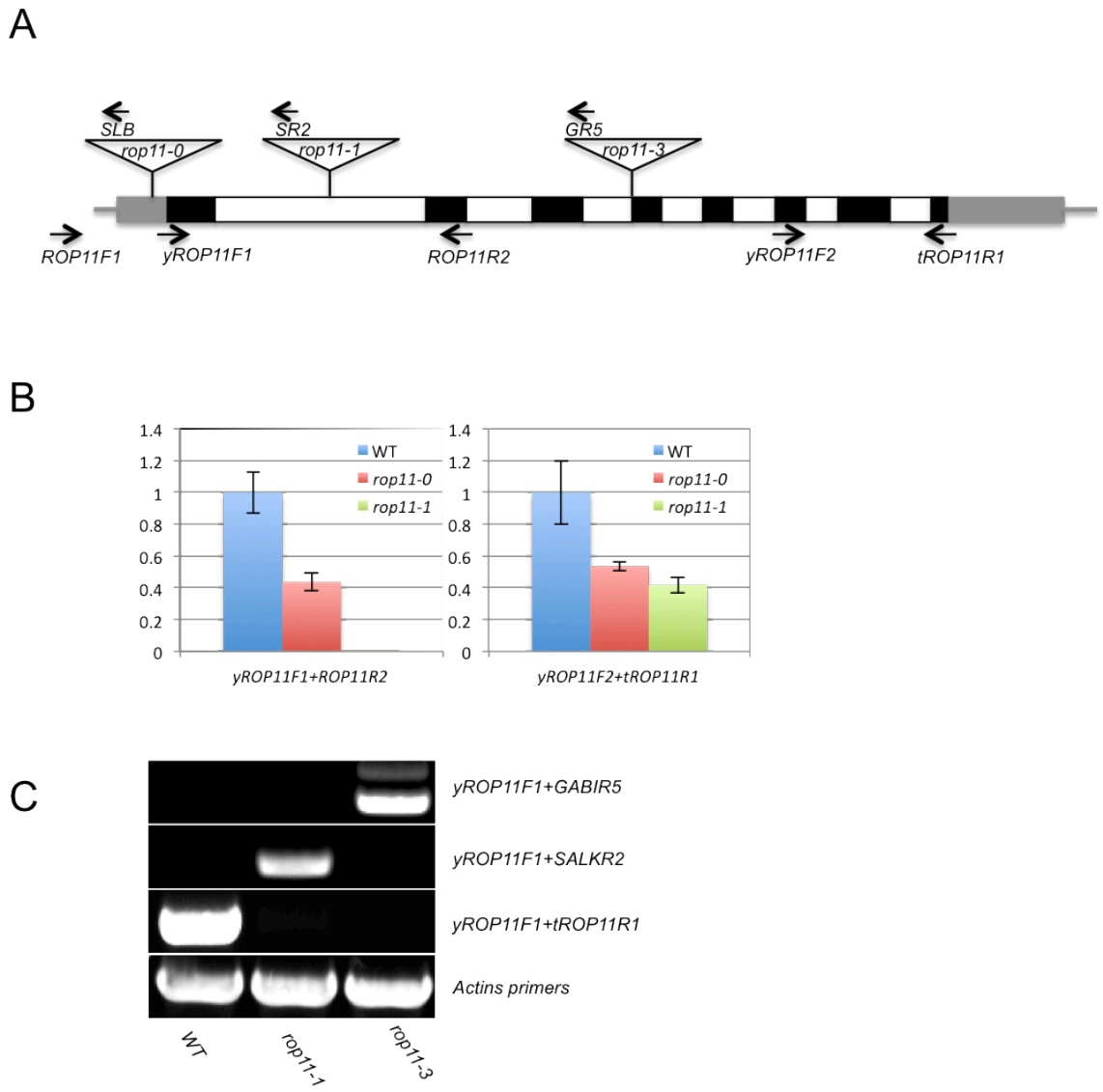

Figure 4.2. Characterization of *ROP11* T-DNA insertion mutants

(A) Schematic illustration of *ROP11* structure and positions of three T-DNA insertions. Untranslated and translated exon regions were represented by gray and black boxes, respectively. White boxes represented introns. Boxes were drawn to scale. Triangles showed the position of T-DNA insertions. Arrows indicated the locations and orientations of primers used.

(B) Relative quantitation of *ROP11* transcripts in *rop11-0* and *rop11-1* homozygous plants. Primer set *yROP11F1+ROP11R2* amplified the cDNA region spanning *rop11-1* T-DNA insertion. *yROP11F2+tROP11R1* amplified the cDNA region close to C-terminus of *ROP11*.

(C) PCR-based transcripts analysis of *rop11-1* and *rop11-3* homozygous mutants. *yROP11F1* and *tROP11R1* were used to amplify full length *ROP11*, which was not detected in cDNA from

either line. Chimeric products were detected using *yROP11F1+SALKR2* and *yROP11F1+GABIR5* from *rop11-1* and *rop11-3* homozygous plants respectively. Actins primers were used as control for cDNAs

4.3.3 The *csn5a-2* phenotype was rescued to different degrees by each of the three independent *ROP11* T-DNA insertion mutants

Loss or reduction-of-functions of *CSN5A* has pleiotropic effects in *Arabidopsis*. Two T-DNA insertion lines for *CSN5A* have been reported, *csn5a-1,* a null mutant, and *csn5a-2*, a reduction-of-function mutant. In the latter line, the T-DNA insert resides in the fourth intron near the C-terminus, resulting in strongly reduced abundance of *CSN5A* transcript and protein. The phenotypes of *csn5a-1* and *csn5a-2* have been described previously (Dohmann et al., 2005; Gusmaroli et al., 2007) and are shown in Figure 4.3. To investigate the effect of *ROP11* loss-of-function on *csn5a-2* mutant, we introduced mutated *ROP11* into the *csn5a-2* background by crossing homozygous *csn5a-2* plants with three *ROP11* T-DNA insertion lines independently.

The double mutant *rop11-1 csn5a-2* was generated and studied first because it is a null for *ROP11*. As mentioned above, the overall morphology of *rop11-1* single mutant has no observable difference relative to WT in all stages of plant development (Fig. 4.3, A), a sharp contrast with the very obvious stunted growth of *csn5a-2* plants. Surprisingly, *rop11-1 csn5a-2* exhibited a strong rescue phenotype, which is almost indistinguishable from WT plants in the mature stage (Fig. 4.3, A) but is characterized by slightly smaller plants evident at earlier stages of development (Fig. 4.3, B). Additionally, *rop11-1 csn5a-2* leaves are more likely to fold downward along the midrib leading to narrower overall leaf morphology when viewed from above. Next we examined the impact of CSN5B loss-of-function on the *rop11-1 csn5a-2* line. *CSN5B* (AT1G71230) encodes an isoform of CSN5A, with which it shares 88% amino acid identity. CSN5A and CSN5B incorporate into distinct COP9 protein complexes in planta, but play unequal roles, with CSN5A being the dominant subunit in terms of both protein abundance and functionality. The null mutant *csn5b-1* has no visible phenotype, however the *csn5a-1 csn5b-1* double mutant that lacks both CSN5A and CSN5B is lethal for *Arabidopsis*. On the other hand, the *csn5a-2 csn5b-1* double mutant is similar to *csn5a-2* and can survive and reproduce despite the fact that overall growth is severely compromised. We prepared the *rop11-1 csn5a-2 csn5b-1* triple mutant and found that the triple mutant no longer displayed the severe pleiotropic phenotype of *csn5a-2 csn5b-1*, although the downward folding of leaves along the midrib appeared more pronounced in *rop11-1 csn5a-2 csn5b-1* triple mutant compared to the *rop11-1 csn5a-2* double mutant (Fig 4.3, B). From this experiment, we can conclude that the overall rescue of the *csn5a-2* phenotype by the loss of *ROP11* does not require the function of *CSN5B*, but that CSN5B does contribute to normal leaf morphology.

To determine whether the rescuing effect of *rop11-1* on *csn5a* required some expression of CSN5A or could also be observed for null CSN5A mutants, the *rop11-1 csn5a-1* double mutant was generated. In contrast to the result with the weak *csn5a-2* allele, the phenotype of *rop11-1 csn5a-1* was indistinguishable from the *csn5a-1* single mutant, indicating that the ability of *ROP11* loss-of-function lines to rescue the *csn5a* phenotype required some CSN5A expression.

To confirm that the rescue of the pleiotropic *csn5a-2* phenotype was due to loss of *ROP11* function, *rop11-0* and *rop11-3* T-DNA insertion lines were also crossed with homozygous *csn5a-2*. As shown in Figure 4.3, C, both *rop11-0 csn5a-2* and *rop11-3 csn5a-2* double homozygous mutants displayed a complemented phenotype but the complementing powers of these two *ROP11* mutants and the *rop11-1* mutant were not equivalent. For 15-day-old plants grown under long-day conditions, the double mutant *rop11-1 csn5a-2* was the most similar to WT except for the slightly smaller plant size and aforementioned leaf curvature, while *rop11-3 csn5a-2* double mutants were more similar to *csn5a-2*, including a small portion of plants in the population exhibiting only very subtle complementation of the *csn5a-2* phenotype. Finally, *rop11-0 csn5a-2* exibited a rescued phenotype intermediate between *rop11-1 csn5a-2* and *rop11-3 csn5a-2*.

These distinctions in phenotypes of double mutants are presumably attributable to the differential effects of T-DNA insertions at the *ROP11* locus. In other words, the rescue powers of *ROP11* T-DNA insertion lines negatively correlated with their remaining function of *ROP11* gene, with null mutant *rop11-1* being the most efficacious, followed by *rop11-0* and *rop11-3* . It's worth mentioning that the highest levels of phenotypical variations were observed within the *rop11-3 csn5a-2* double homozygous plant population, possibly caused by ratio variations of the two transcripts from the *rop11-3* T-DNA insertion.

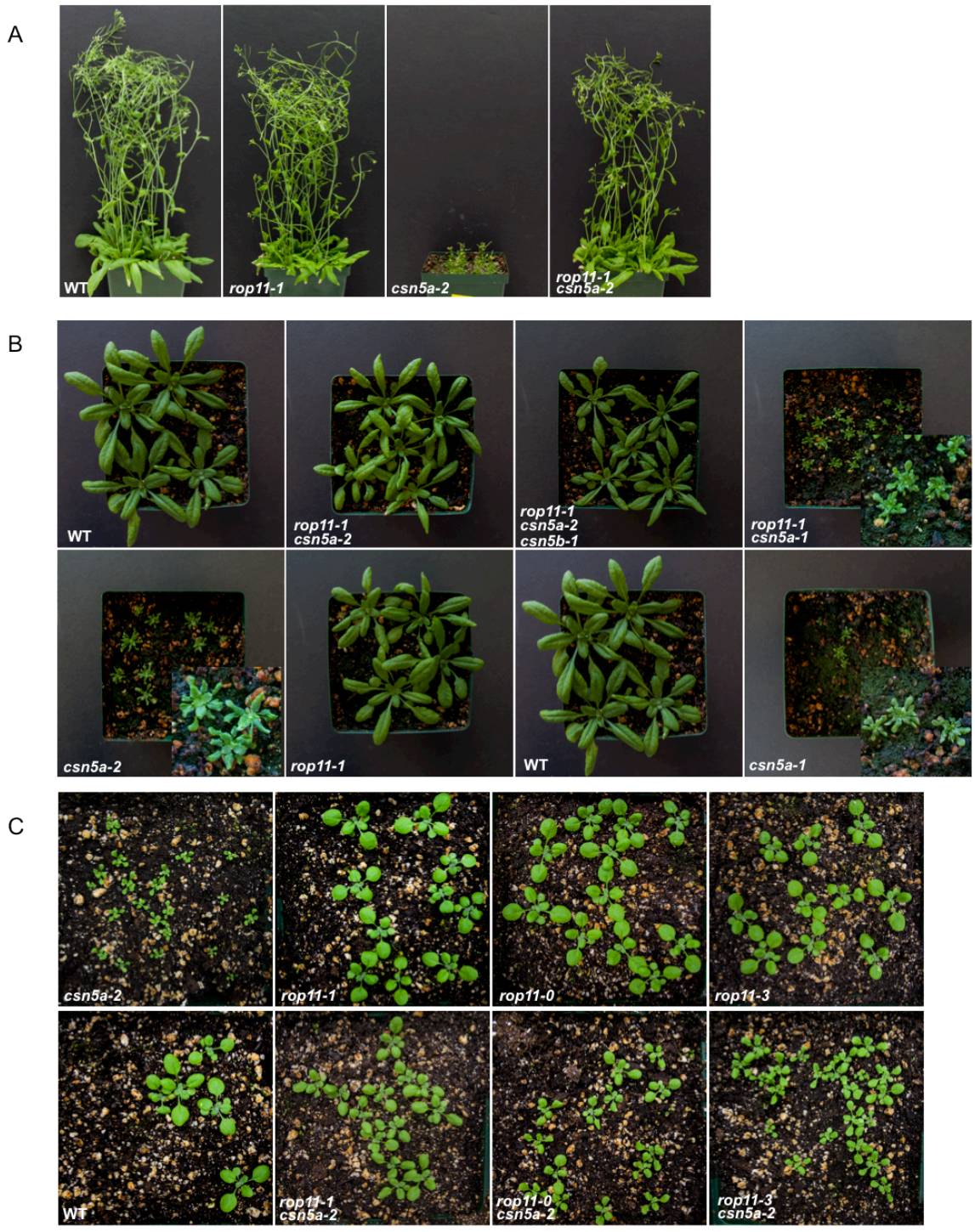

Figure 4.3. The phenotype of *csn5a-2* was rescued by *ROP11* T-DNA insertion mutants

(A) 45-days-old Arabidopsis grown under identical long day environment. *rop11-1* has no obvious phenotype throughout life cycle. *rop11-1 csn5a-2* double mutants showed no visible difference with WT at this stage but is a rescue compared to *csn5a-2* stunted growth morphology.

(B) 23-days-old Arabidopsis grown under identical long day environment. *rop11-1 csn5a-2* double mutants displayed a rescue phenotype compared to *csn5a-2* single mutant, but still showed subtle difference with WT in leaf morphology. Triple mutants *rop11-1 csn5a-2 csn5b-1* had stronger leaf edge curled downward morphology than *rop11-1 csn5a-2* due to *CSN5B* loss-of-function. *rop11-1 csn5a-1* had no visible phenotype difference with *csn5a-1* single mutants.

(C) 15-days-old Arabidopsis grown under identical long day environment. Three *ROP11* mutants *rop11-1*, *rop11-0*, and *rop11-3* did not show visible difference with WT. All three double mutants *rop11-1 csn5a-2*, *rop11-0 csn5a-2* and *rop11-3 csn5a-2* showed improved growth phenotype to different degrees compared to *csn5a-2* single mutant, with *rop11-1 csn5a-2* most similar to WT, *rop11-3 csn5a-2* most similar to *csn5a-2*, and *rop11-0 csn5a-2* intermediate.

4.3.4 Ectopic expression of *DN-ROP11* also rescues *csn5a-2* phenotype

ROP GTPases are molecular switches that catalyze the hydrolysis of GTP to GDP. The GTP-binding form is the active state for ROP G proteins. Previous reports have shown that mutations in the key residues within G-box-motifs can affect the affinity of ROP GTPases for nucleotides (Berken and Wittinghofer, 2008). Based on previous work, it is believed that substitution of the threonine[22] residue with asparagine in ROP11 will increase its affinity for GDP and reduce affinity for GEF (Guanine Exchange Factor), thereby "locking" ROP11 in the inactive state. Ectopic expression of this inactive mutant allele of ROP11 (T22N) is thought to compete with native ROP11, resulting in a dominant negative effect (Bloch et al., 2005).

We showed that the dominant negative ROP11 lost the ability to interact with CSN5A in the Y2H system (Fig. 4.1). To determine whether dominant negative ROP11 can phenocopy the rescue of *csn5a-2* observed for *ROP11* loss-of-function lines, *DN-ROP11* was transformed into *csn5a-2* homozygous plants. Three T2 *Arabidopsis* lines ectopically expressing *DN-ROP11* were selected and evaluated for phenotypic rescue. As expected for overexpression experiments, we observed variation in the degree of rescue among these transgenic lines. Importantly, however, each line produced numerous plants showing substantial rescue of the csn5a-2 phenotype (Fig. 4.4).

Figure 4.4. Ectopic expression of *DN-ROP11* also rescued *csn5a-2* phenotype

Plants shown in Figure 4.4 were 25-days-old Arabidopsis grown in long day condition. *csn5a-2 + DN-ROP11* L1, *csn5a-2 + DN-ROP11* L2, and *csn5a-2 + DN-ROP11* L3 were 3 independent

lines T2 transgenic plants that ectopically expressed *DN-ROP11* (T22N) in *csn5a-2* single mutants background. They all showed rescued phenotype but with variations.

4.3.5 CSN5A protein levels increase in all rescue lines without significant transcript levels change

The fact that *rop11-1 csn5a-2* double mutants were nearly identical to WT in growth and appearance while *rop11-1 csn5a-1* plants were not different from the *csn5a-1* null mutant suggested that some level of *CSN5A* expression was required for the rescue of the *csn5a* mutant phenotype by reduction of *ROP11* expression. We hypothesized that a reduction in *ROP11* expression may have resulted in an increase of CSN5A protein via either increased production of *CSN5A* mRNA or inhibition of CSN5A protein turnover. To test the above hypothesis, we measured mRNA levels for *CSN5A* in *csn5a-2*, *rop11-0 csn5a-2*, *rop11-1 csn5a-2*, *rop11-3 csn5a-2*, *csn5a-2 DN-ROP11* and WT plants. Quantitative real time PCR showed that *csn5a-2* and all double mutant lines produced approximately 80% less mRNA relative to WT (Fig. 4.5). The observed reduction in *CSN5A* transcript in *csn5a-2* is consistent with previous observations (Gusmaroli et al., 2007). The transcript analysis results ruled out the possibility that introduction of loss-of-function *rop11* alleles resulted in substantially increased expression of *CSN5A* in *csn5a-2*, indicating that a posttranscriptional mechanism was responsible for the apparent increase in CSN5A function in rescued lines.

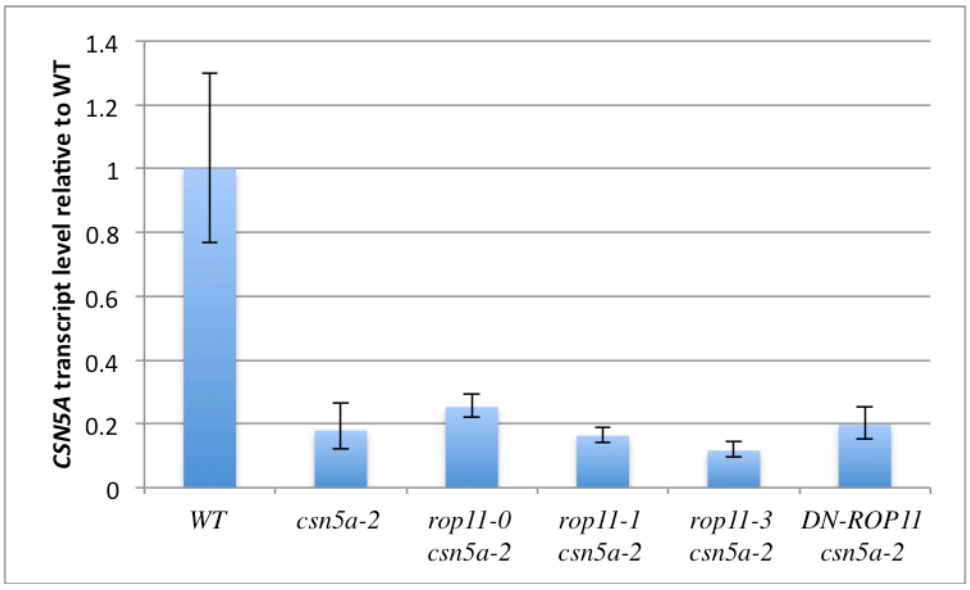

Figure 4.5. Transcript analysis of WT, *csn5a-2* and rescuing lines

RT-qPCR was performed to measure the *CSN5A* transcript relative level in 8-day-old *csn5a-2*, *rop11-0 csn5a-2*, *rop11-1 csn5a-2*, *rop11-3 csn5a-2*, *csn5a-2 DN-ROP11* and WT plants. The transcript level of WT was set to 1.

Protein extracts were obtained from all the relevant genotypes and analyzed on western blot. Equal amount of total protein were loaded as shown by RPN6 protein control (Fig 4.6, A). As expected, no CSN5A protein could be detected in the null *csn5a-1* homozygous line and only a

very weak signal was detected by anti-CSN5A in extracts from the weak allele *csn5a-2*. However, CSN5A protein accumulation increased in the *rop11-1 csn5a-2* double and *rop11-1 csn5a-2 csn5b-1* triple mutants compared to *csn5a-2*. CSN5A protein level was also higher in *rop11-1* single mutants compared to WT.

The western blots clearly showed that ROP11 loss-of-function resulted in stabilization of CSN5A. Notably, CSN5A protein level in the *rop11-1 csn5a-2* double mutant was still less than WT, which means that the rescue by *ROP11* knockout is not a full rescue with regard to CSN5A protein, consistent with the observation that the phenotype of *rop11 csn5a*-2 double mutants were not identical to WT.

Further analysis demonstrates that CSN5A stability is negatively regulated by *ROP11* mutants in all *csn5a-2* complementing lines (Fig 4.6, B). CSN5A protein accumulation also increased in extracts from *csn5a-2 rop11-0*, *csn5a-2 rop11-3* and *csn5a-2 DN-ROP11* lines relative to those from *csn5a-2* single mutants (Fig 4.6, B).The CSN5A protein level appears to correlates with the phenotype of corresponding double mutants i.e., the rescuing power of each *rop11* mutant. In conclusion, the role of ROP11 in the ROP11-CSN5A interaction is to facilitate the degradation (or destabilization or inactivation) of CSN5A protein, and removal of ROP11 leads to CSN5A accumulation in the *csn5a-2* background.

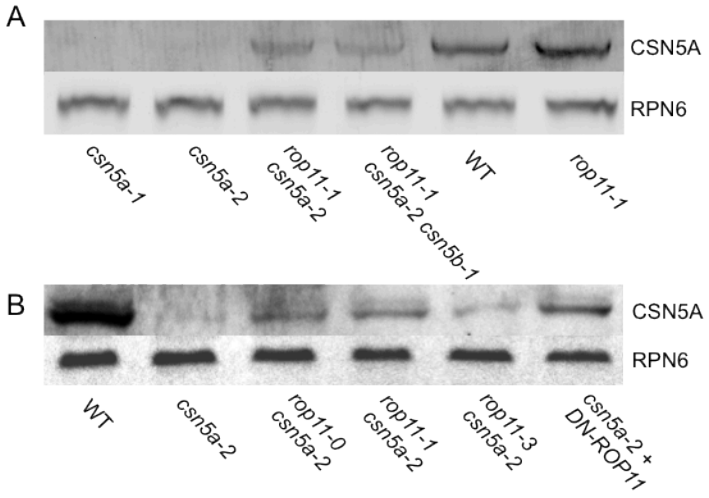

Figure 4.6. *ROP11* loss-of-function stabilized CSN5A protein

(A) Equal amounts of total proteins were loaded in each lane. Anti-RPN6 was used to detect and visualize RPN6 protein to show equal loading. Polyclonal antibody anti-CSN5A was used to detect CSN5A protein. No protein could be detected from *csn5a-1* plant extract. Only a very faint band was revealed in the *csn5a-2* extract lane. Significantly more CSN5A protein was detected in extracts from both double and triple mutants relative to the *csn5a-2* single mutants, but the quantity was lower compared to WT. More CSN5A protein was present in the *rop11-1* mutant than WT.

(B) Western blot to show CSN5A abundance in WT, *csn5a-2*, *rop11-1 csn5a-2*, *rop11-0 csn5a-2*, *rop11-3 csn5a-2* and *csn5a-2 +DN-ROP11* plant extracts. Equal amount of total proteins were loaded in each lane as shown by RPN6 protein control. CSN5A protein was barely detectable in extracts from the *csn5a-2* line. All rescue lines accumulated more CSN5A protein than the *csn5a-2* single mutant yet less than WT, with various abundances, correlating to their phenotypes (degree of rescue).

4.4 Discussion

4.4.1 Protein-protein interactions as a tool to distinguish protein function from its redundant family members

Many single gene loss-of-function or gain-of-function plants do not exhibit phenotypes relative to wild type plants due to genetic redundancy or lacking adequate interacting partners necessary for connections to downstream pathway components. If members of a multi-gene family have both gene-specific and redundant functions, simultaneous manipulation of multiple related genes may compromise the interpretation of individual gene function. To resolve this dilemma in reverse genetics, we employed the Y2H system to identify novel protein-protein interactions and then manipulate these interacting partners simultaneously to study discrete gene function (within multigene families) and test for epistasis of interacting proteins. Here we report one of our successful examples of uncovering gene functions by applying the above functional interactomics approach.

ROP11 is one the of 11 members of the *Arabidopsis* ROP GTPases family. It has been shown in previous research and also shown in this work that the *ROP11* knockout does not yield a visible phenotype relative to WT plants. Simultaneous silencing of both *ROP11* and *ROP10* did not display morphological difference relative to WT without treatment, very likely because other ROPs in the family partly complement their functions (Li et al., 2012). Overexpression of ROP11 in *Arabidopsis* has been tested as well but morphological changes could only be achieved by ectopic expression of the constitutively active version of ROP11 but not native ROP11 (Bloch et al., 2005; Oda and Fukuda, 2012).

As an extension to our current poplar biomass interactome project, we tested and showed here that CSN5A is an interacting protein of ROP11 (Figure 4.1, A). *csn5a-2 rop11-1* double mutants were generated to study epistasis of CSN5A and ROP11. To our surprise, the severe growth defects phenotype of *csn5a-2* was rescued by loss- or reduction-of-function of *ROP11*. Later we found that for the rescue to take place, the presence of CSN5A protein was required, because silencing of *ROP11* failed to complement the null mutant *csn5a-1*. Both CSN5A transcripts and protein abundances were analyzed in the rescued plants. It was discovered that, whereas transcript level remained unchanged, protein level increased compared to the *csn5a-2* single mutants. These findings strongly suggest that the interaction between ROP11 and CSN5A plays an important role in the regulation of CSN5A protein level and as a consequence affects plant growth and development. The crosstalk between these two proteins would have been be difficult to unveil without knowledge of their physical protein-protein interactions and further interrogation of the functional relevance of this interaction, because they belong to two rather poorly connected pathways.

4.4.2 The interaction of CSN5 with Ras GTPases

Direct interaction and regulation between a ROP GTPase and CSN5 has not been reported previously though connections were made between Ras-mediated tumorgenesis and CSN5/Jab1 or other CSN subunits. Knockout of CSN5 in p53-null Ras-transformed mice cells prevents formation of tumors by inducing premature senescence (Tsujimoto et al., 2012). Inhibition of the isopeptidase activity of CSN5 also abolished the transformation of human breast cancer induced by MYC or Ras *in vivo* (Adler et al., 2008). Genome-wide RNAi screen in colorectal cancer cells line DLD-1 found that silencing of CSN3 or CSN4 could selectively kill cells carrying activating KRAS G13D point mutation but not KRAS WT control (Luo et al., 2009).

There are no close homologs of RAS subfamily GTPases in plants. It's tempting to speculate that some members of the plant-specific ROP GTPases conserved partial functions of RAS GTPases. Functions of ROP GTPases have been often linked to cell division and proliferation. *Arabidopsis csn* mutant cells were shown delayed in G2 phase progression, which may be the underlining cause of *csn* mutant growth arrest at the seedling stage (Dohmann et al., 2008). The interaction and connections between ROP11 and CSN5 we presented in this paper provide new perspectives into both research fields, particularly their regulatory role involving growth and morphology.

4.4.3 Knockout of CUL3A or CUL3B also complement *csn5a-2* phenotype

The phenomena of *csn5a-2* pleiotropic phenotype being rescued by the loss-of-function of other genes has been previously reported. In 2007 the Deng lab published that loss of CUL3A or CUL3B resulted in the suppression of the pleiotropic defects of the *csn5a-2* mutant at all developmental stages (Gusmaroli et al., 2007). Western blots analyses of *cul3a csn5a-2* and *cul3b csn5a-2* indicated that total amount of CSN5 protein was significantly increased relative to *csn5a-2* mutant, which improved deneddylation efficiency of CUL1, CUL3 and CUL4. Interestingly, the authors could not detect *CSN5A* transcripts change but only protein level difference, which is remarkably similar to the rescuing effects by ROP11 silencing.

Based on our results as well as previously published work, we propose two contradicting but not mutually exclusive hypotheses. The first and most likely one is that ROP11 works with CUL3A and CUL3B to negatively regulate CSN5A protein turnover, presumably through the 26S proteasome pathway. In addition to the evidence that loss of ROP11 or either isoform of CUL3 results in higher CSN5A protein accumulation in complementing lines, Rho GTPases, which are not found in plants but are evolutionarily related to the ROPs, bind with cullin 3 in mammalian systems. Specifically, a 3-member subset of the Rho GTPases called RhoBTB proteins possess not only the highly conserved GTPase domain, but also contain the unique features of a proline-rich region and a tandem of 2 BTB (broad-complexes, tramtrack, bric à brac) domains. Interestingly, all three RhoBTB in human have been experimentally verified to interact with cullin 3 possibly as components of cullin3-dependent E3 ligases complexes and the GTPase domains of these RhoBTBs are able to interact with the BTB domain regions (Berthold et al., 2008). Several Arabidopsis BTB domain proteins were also shown to interact with CUL3A/B (Figueroa et al., 2005; Gingerich et al., 2005). Considered together, it is tempting to speculate that in plants ROP11 may act as the free GTPase domain of RhoBTB hence participating in the cullin3-BTB E3 ubiquitin ligase complexes that target proteins (in this case CSN5A) for degradation via the proteasome pathway.

The second hypothesis appears unlikely, but it also can not be completely ruled out at present. All of the rescuing events (including loss of *CUL3*) of the *csn5a* pleiotropic phenotype were carried out on a *csn5a-2* mutant line. The absence of a second *csn5a* line that express reduced CSN5A protein imposes a weakness on the current conclusion, because epigenetic suppression of T-DNA insertion in *csn5a-2* line could potentially explain the observed CSN5A protein level increase. Very recently, Gao and Zhao demonstrated that *trans*-interaction between T-DNA insertions could trigger T-DNA insertion suppression (Gao and Zhao, 2013). However, our evidence strongly disagrees with the epignenetic suppression theory for the following reasons. First, we crossed three independent *ROP11* T-DNA insertion lines with *csn5a-2* and phenotypes of double mutants correlated with the degrees of *ROP11* silencing and contradicted with the suppression by trans-interaction mechanism. For *rop11-3 csn5a-2* double mutant, the binary vector used to generate *rop11-3* (GABI-KAT) was distinct from the vector used for *csn5a-2* (SALK). Second, ectopic expression of *DN-ROP11* in *csn5a-2* single mutants background rescue the severely impaired growth phenotype, showing that the rescue is dependent on ROP11 functionality. Third, we compared *CSN5A* transcript levels in rescued lines with those in *csn5a-2* and WT by quantitative RCR. The results demonstrated that *CSN5A* transcript abundance remained significantly lower in complemented lines than WT and relatively unchanged compared to *csn5a-2*. The behavior of *CSN5A* transcript is not in line with the *AGAMOUS* shown by Gao and Zhao, when intronic T-DNA mutant *ag-TD* was epigenetically suppressed by *yuc1-1* and converted to *ag-TD**, clearly more *AGAMOUS* mRNA were detected by *in situ* hybridization (Gao and Zhao, 2013).

4.4.4 A Working model

Our research implies that ROP11 negatively affects the accumulation of CSN5A protein in plant cells. Based on reported evidence, a mechanism is proposed to show how CSN5A is regulated by ROP11. In mamalian systems, Rho-BTB domain proteins unify the BTB domain and GTPase domain covalently to take part in the cullin 3 E3 ligase complexes (Figure 4.7, A). However, though conserved GTPases and BTB domain proteins exist in plant, Rho-BTB proteins are not found. We hypotheze that plant BTB proteins are working together with GTPases to compensate the functions of Rho-BTB proteins in *planta* (Figure 4.7, B).

CSN5A has been reported to be a ubiquitylation target in an advanced proteomic analyses (Kim et al., 2013). In our model, CSN5A is a substrate of CUL3 E3 ligase complexes, which explains the observation that CSN5A protein level is increased when one isoform of CUL3 is lost (Gusmaroli et al., 2007). In the model proposed here, ROP11 functions to faciliate the recognition of CSN5A by CUL3 E3 ligase complexes, potentially acting as a adapter between BTB domain proteins and CSN5A. If the interaction between CSN5A and ROP11 is abolished due to either loss of ROP11 or ROP11 mutation, ubiquitination of CSN5A would be inhibited, hence resulting in protein level increase. This model is also consistent with the report that CSN5 colocalizes with 26S proteasome component proteins in auxin induced nuclear protien bodies (NPB), and 26S proteasome-dependent Aux/IAA degradation in the NPB is negatively affected by ROP GTPases (Tao et al., 2005).

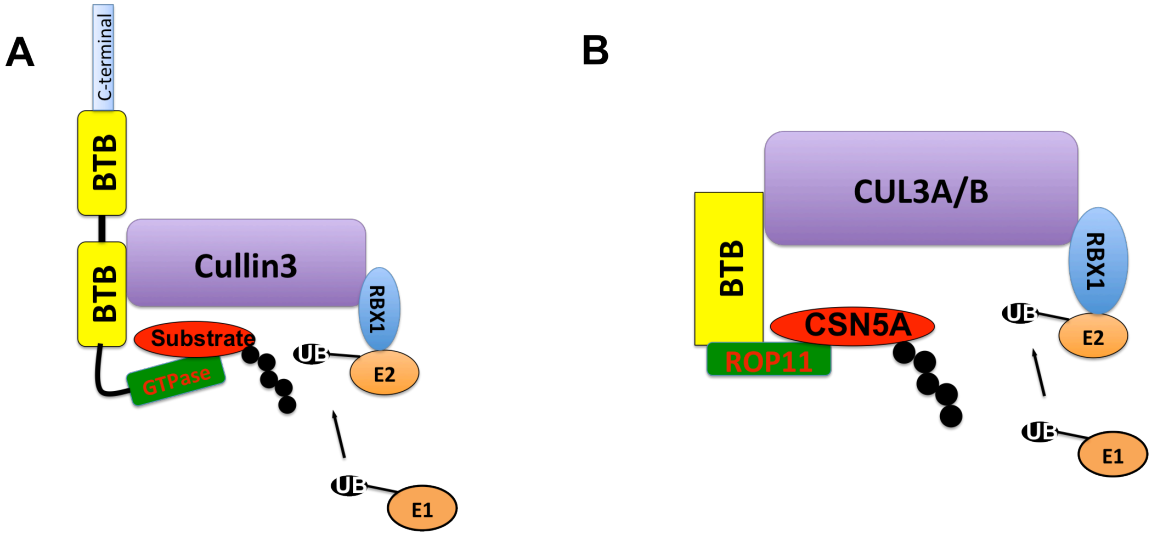

Figure 4.7. Models for Cullin3 E3 ligase complexes in human and in Arabidopsis

(A) Cullin3 E3 ligase complexes involving Rho-BTB domain proteins in human

(B) Proposed mechanism for CSN5A turnover and negative regulation by ROP11 in Arabidopsis

4.5 References

Adler AS, Littlepage LE, Lin M, Kawahara TL, Wong DJ, Werb Z, Chang HY (2008) CSN5 isopeptidase activity links COP9 signalosome activation to breast cancer progression. Cancer Res **68:** 506-515

Arabidopsis Interactome Mapping C (2011) Evidence for network evolution in an Arabidopsis interactome map. Science **333:** 601-607

Bech-Otschir D, Kraft R, Huang X, Henklein P, Kapelari B, Pollmann C, Dubiel W (2001) COP9 signalosome-specific phosphorylation targets p53 to degradation by the ubiquitin system. EMBO J **20:** 1630-1639

Berken A, Wittinghofer A (2008) Structure and function of Rho-type molecular switches in plants. Plant Physiol Biochem **46:** 380-393

Berthold J, Schenkova K, Ramos S, Miura Y, Furukawa M, Aspenstrom P, Rivero F (2008) Characterization of RhoBTB-dependent Cul3 ubiquitin ligase complexes--evidence for an autoregulatory mechanism. Exp Cell Res **314:** 3453-3465

Bloch D, Lavy M, Efrat Y, Efroni I, Bracha-Drori K, Abu-Abied M, Sadot E, Yalovsky S (2005) Ectopic expression of an activated RAC in Arabidopsis disrupts membrane cycling. Mol Biol Cell **16:** 1913-1927

Claret FX, Hibi M, Dhut S, Toda T, Karin M (1996) A new group of conserved coactivators that increase the specificity of AP-1 transcription factors. Nature **383:** 453-457

Cope GA, Suh GS, Aravind L, Schwarz SE, Zipursky SL, Koonin EV, Deshaies RJ (2002) Role of predicted metalloprotease motif of Jab1/Csn5 in cleavage of Nedd8 from Cul1. Science **298:** 608-611

Craddock C, Lavagi I, Yang Z (2012) New insights into Rho signaling from plant ROP/Rac GTPases. Trends Cell Biol **22:** 492-501

Dohmann EM, Kuhnle C, Schwechheimer C (2005) Loss of the CONSTITUTIVE PHOTOMORPHOGENIC9 signalosome subunit 5 is sufficient to cause the cop/det/fus mutant phenotype in Arabidopsis. Plant Cell **17:** 1967-1978

Dohmann EM, Levesque MP, De Veylder L, Reichardt I, Jurgens G, Schmid M, Schwechheimer C (2008) The Arabidopsis COP9 signalosome is essential for G2 phase progression and genomic stability. Development **135:** 2013-2022

Dong Y, Sui L, Watanabe Y, Yamaguchi F, Hatano N, Tokuda M (2005) Prognostic significance of Jab1 expression in laryngeal squamous cell carcinomas. Clin Cancer Res **11:** 259-266

Dreze M, Monachello D, Lurin C, Cusick ME, Hill DE, Vidal M, Braun P (2010) High-quality binary interactome mapping. Methods Enzymol **470:** 281-315

Duan Q, Kita D, Li C, Cheung AY, Wu HM (2010) FERONIA receptor-like kinase regulates RHO GTPase signaling of root hair development. Proc Natl Acad Sci U S A **107:** 17821-17826

Edgar RC (2004) MUSCLE: multiple sequence alignment with high accuracy and high throughput. Nucleic Acids Res **32:** 1792-1797

Figueroa P, Gusmaroli G, Serino G, Habashi J, Ma L, Shen Y, Feng S, Bostick M, Callis J, Hellmann H, Deng XW (2005) Arabidopsis has two redundant Cullin3 proteins that are essential for embryo development and that interact with RBX1 and BTB proteins to form multisubunit E3 ubiquitin ligase complexes in vivo. Plant Cell **17:** 1180-1195

Fukumoto A, Ikeda N, Sho M, Tomoda K, Kanehiro H, Hisanaga M, Tsurui Y, Tsutsumi M, Kato JY, Nakajima Y (2004) Prognostic significance of localized p27Kip1 and potential role of Jab1/CSN5 in pancreatic cancer. Oncol Rep **11:** 277-284

Gao Y, Zhao Y (2013) Epigenetic suppression of T-DNA insertion mutants in Arabidopsis. Mol Plant **6:** 539-545

Gingerich DJ, Gagne JM, Salter DW, Hellmann H, Estelle M, Ma L, Vierstra RD (2005) Cullins 3a and 3b assemble with members of the broad complex/tramtrack/bric-a-brac (BTB) protein family to form essential ubiquitin-protein ligases (E3s) in Arabidopsis. J Biol Chem **280:** 18810-18821

Gusmaroli G, Feng S, Deng XW (2004) The Arabidopsis CSN5A and CSN5B subunits are present in distinct COP9 signalosome complexes, and mutations in their JAMM domains exhibit differential dominant negative effects on development. Plant Cell **16:** 2984-3001

Gusmaroli G, Figueroa P, Serino G, Deng XW (2007) Role of the MPN subunits in COP9 signalosome assembly and activity, and their regulatory interaction with Arabidopsis Cullin3-based E3 ligases. Plant Cell **19:** 564-581

Jones MA, Raymond MJ, Yang Z, Smirnoff N (2007) NADPH oxidase-dependent reactive oxygen species formation required for root hair growth depends on ROP GTPase. J Exp Bot **58:** 1261-1270

Kim DY, Scalf M, Smith LM, Vierstra RD (2013) Advanced proteomic analyses yield a deep catalog of ubiquitylation targets in Arabidopsis. Plant Cell **25:** 1523-1540

Kwok SF, Solano R, Tsuge T, Chamovitz DA, Ecker JR, Matsui M, Deng XW (1998) Arabidopsis homologs of a c-Jun coactivator are present both in monomeric form and in the COP9 complex, and their abundance is differentially affected by the pleiotropic cop/det/fus mutations. Plant Cell **10:** 1779-1790

Li H, Lin Y, Heath RM, Zhu MX, Yang Z (1999) Control of pollen tube tip growth by a Rop GTPase-dependent pathway that leads to tip-localized calcium influx. Plant Cell **11:** 1731-1742

Li Z, Kang J, Sui N, Liu D (2012) ROP11 GTPase is a negative regulator of multiple ABA responses in Arabidopsis. J Integr Plant Biol **54:** 169-179

Li Z, Li Z, Gao X, Chinnusamy V, Bressan R, Wang ZX, Zhu JK, Wu JW, Liu D (2012) ROP11 GTPase negatively regulates ABA signaling by protecting ABI1 phosphatase activity from inhibition by the ABA receptor RCAR1/PYL9 in Arabidopsis. J Integr Plant Biol **54:** 180-188

Luo J, Emanuele MJ, Li D, Creighton CJ, Schlabach MR, Westbrook TF, Wong KK, Elledge SJ (2009) A genome-wide RNAi screen identifies multiple synthetic lethal interactions with the Ras oncogene. Cell **137:** 835-848

Lyapina S, Cope G, Shevchenko A, Serino G, Tsuge T, Zhou C, Wolf DA, Wei N, Shevchenko A, Deshaies RJ (2001) Promotion of NEDD-CUL1 conjugate cleavage by COP9 signalosome. Science **292:** 1382-1385

Maytal-Kivity V, Reis N, Hofmann K, Glickman MH (2002) MPN+, a putative catalytic motif found in a subset of MPN domain proteins from eukaryotes and prokaryotes, is critical for Rpn11 function. BMC Biochem **3:** 28

Oda Y, Fukuda H (2012) Initiation of cell wall pattern by a Rho- and microtubule-driven symmetry breaking. Science **337:** 1333-1336

Oh W, Lee EW, Sung YH, Yang MR, Ghim J, Lee HW, Song J (2006) Jab1 induces the cytoplasmic localization and degradation of p53 in coordination with Hdm2. J Biol Chem **281:** 17457-17465

Rodgers-Melnick E, Mane SP, Dharmawardhana P, Slavov GT, Crasta OR, Strauss SH, Brunner AM, Difazio SP (2012) Contrasting patterns of evolution following whole genome versus tandem duplication events in Populus. Genome Res **22:** 95-105

Rojas AM, Fuentes G, Rausell A, Valencia A (2012) The Ras protein superfamily: evolutionary tree and role of conserved amino acids. J Cell Biol **196:** 189-201

Seeger M, Kraft R, Ferrell K, Bech-Otschir D, Dumdey R, Schade R, Gordon C, Naumann M, Dubiel W (1998) A novel protein complex involved in signal transduction possessing similarities to 26S proteasome subunits. FASEB J **12:** 469-478

Sui L, Dong Y, Ohno M, Watanabe Y, Sugimoto K, Tai Y, Tokuda M (2001) Jab1 expression is associated with inverse expression of p27(kip1) and poor prognosis in epithelial ovarian tumors. Clin Cancer Res **7:** 4130-4135

Tamura K, Peterson D, Peterson N, Stecher G, Nei M, Kumar S (2011) MEGA5: molecular evolutionary genetics analysis using maximum likelihood, evolutionary distance, and maximum parsimony methods. Mol Biol Evol **28:** 2731-2739

Tao LZ, Cheung AY, Nibau C, Wu HM (2005) RAC GTPases in tobacco and Arabidopsis mediate auxin-induced formation of proteolytically active nuclear protein bodies that contain AUX/IAA proteins. Plant Cell **17:** 2369-2383

Tian L, Peng G, Parant JM, Leventaki V, Drakos E, Zhang Q, Parker-Thornburg J, Shackleford TJ, Dai H, Lin SY, Lozano G, Rassidakis GZ, Claret FX (2010) Essential roles of Jab1 in cell survival, spontaneous DNA damage and DNA repair. Oncogene **29:** 6125-6137

Tomoda K, Kubota Y, Arata Y, Mori S, Maeda M, Tanaka T, Yoshida M, Yoneda-Kato N, Kato JY (2002) The cytoplasmic shuttling and subsequent degradation of p27Kip1

mediated by Jab1/CSN5 and the COP9 signalosome complex. J Biol Chem **277:** 2302-2310

Tomoda K, Yoneda-Kato N, Fukumoto A, Yamanaka S, Kato JY (2004) Multiple functions of Jab1 are required for early embryonic development and growth potential in mice. J Biol Chem **279:** 43013-43018

Tsujimoto I, Yoshida A, Yoneda-Kato N, Kato JY (2012) Depletion of CSN5 inhibits Ras-mediated tumorigenesis by inducing premature senescence in p53-null cells. FEBS Lett **586:** 4326-4331

Vernoud V, Horton AC, Yang Z, Nielsen E (2003) Analysis of the small GTPase gene superfamily of Arabidopsis. Plant Physiol **131:** 1191-1208

Vetter IR, Wittinghofer A (2001) The guanine nucleotide-binding switch in three dimensions. Science **294:** 1299-1304

Walhout AJ, Vidal M (2001) High-throughput yeast two-hybrid assays for large-scale protein interaction mapping. Methods **24:** 297-306

Wan M, Cao X, Wu Y, Bai S, Wu L, Shi X, Wang N, Cao X (2002) Jab1 antagonizes TGF-beta signaling by inducing Smad4 degradation. EMBO Rep **3:** 171-176

Wennerberg K, Rossman KL, Der CJ (2005) The Ras superfamily at a glance. J Cell Sci **118:** 843-846

Wu HM, Hazak O, Cheung AY, Yalovsky S (2011) RAC/ROP GTPases and auxin signaling. Plant Cell **23:** 1208-1218

Xu T, Wen M, Nagawa S, Fu Y, Chen JG, Wu MJ, Perrot-Rechenmann C, Friml J, Jones AM, Yang Z (2010) Cell surface- and rho GTPase-based auxin signaling controls cellular interdigitation in Arabidopsis. Cell **143:** 99-110

Yang Z (2008) Cell polarity signaling in Arabidopsis. Annu Rev Cell Dev Biol **24:** 551-575

Yoo CM, Quan L, Cannon AE, Wen J, Blancaflor EB (2012) AGD1, a class 1 ARF-GAP, acts in common signaling pathways with phosphoinositide metabolism and the actin cytoskeleton in controlling Arabidopsis root hair polarity. Plant J **69:** 1064-1076

Zhou C, Seibert V, Geyer R, Rhee E, Lyapina S, Cope G, Deshaies RJ, Wolf DA (2001) The fission yeast COP9/signalosome is involved in cullin modification by ubiquitin-related Ned8p. BMC Biochem **2:** 7

Table 4.S1. Primers used for *ROP11* mutants genotyping and transcript analysis

Primer Name	Sequence	Purpose
ROP11F1	TCGATTCGTAACGCCATACT	Genotyping for *rop11-0*
yROP11F1	CACCATGGCTTCAAGTGCTTCAAAG	Genotyping for *rop11-1* and *rop11-3*, RT-qPCR for N-terminal *ROP11*
yROP11F2	CACCGAAGTGATCAAACCTCTGG	RT-qPCR for C-terminal *ROP11*
ROP11R2	TTGACAGTGGTGCCTTCAAC	Genotyping for *rop11-0* and *rop11-1*, RT-qPCR for N-terminal *ROP11*
tROP11R1	CCCGGGTCAATGCCGAGTCACTATCC	Genotyping for *rop11-3* and RT-qPCR for C-terminal *ROP11*
GABIR5/GR5	AACGCTGCGGACATCTACAT	Genotyping for *rop11-3*
SALKR2/SR2	AGAAAAACCACCCCAGTACA	Genotyping for *rop11-1*
SALKLB/SLB	CAGCGTGGACCGCTTGCTGCAACTCTCTCA	Genotyping for *rop11-0*
rtCSN5AF1	AGCCTCAACTCGCGAAGATA	RT-qPCR for *CSN5A*
rtCSN5AR3	CAGATCCAGAGCCCATGATT	RT-qPCR for *CSN5A*

Figure 4.S1. ROP family phylogenic tree

All ROP protein sequences were obtained from Phytozyme. Sequences alignment was done with MUSCLE (Edgar, 2004) and tree was created using the neighboring-joining method in MEGA5.1 (Tamura et al., 2011).

ROP members that interact with CSN5A are highlighted in yellow.

A

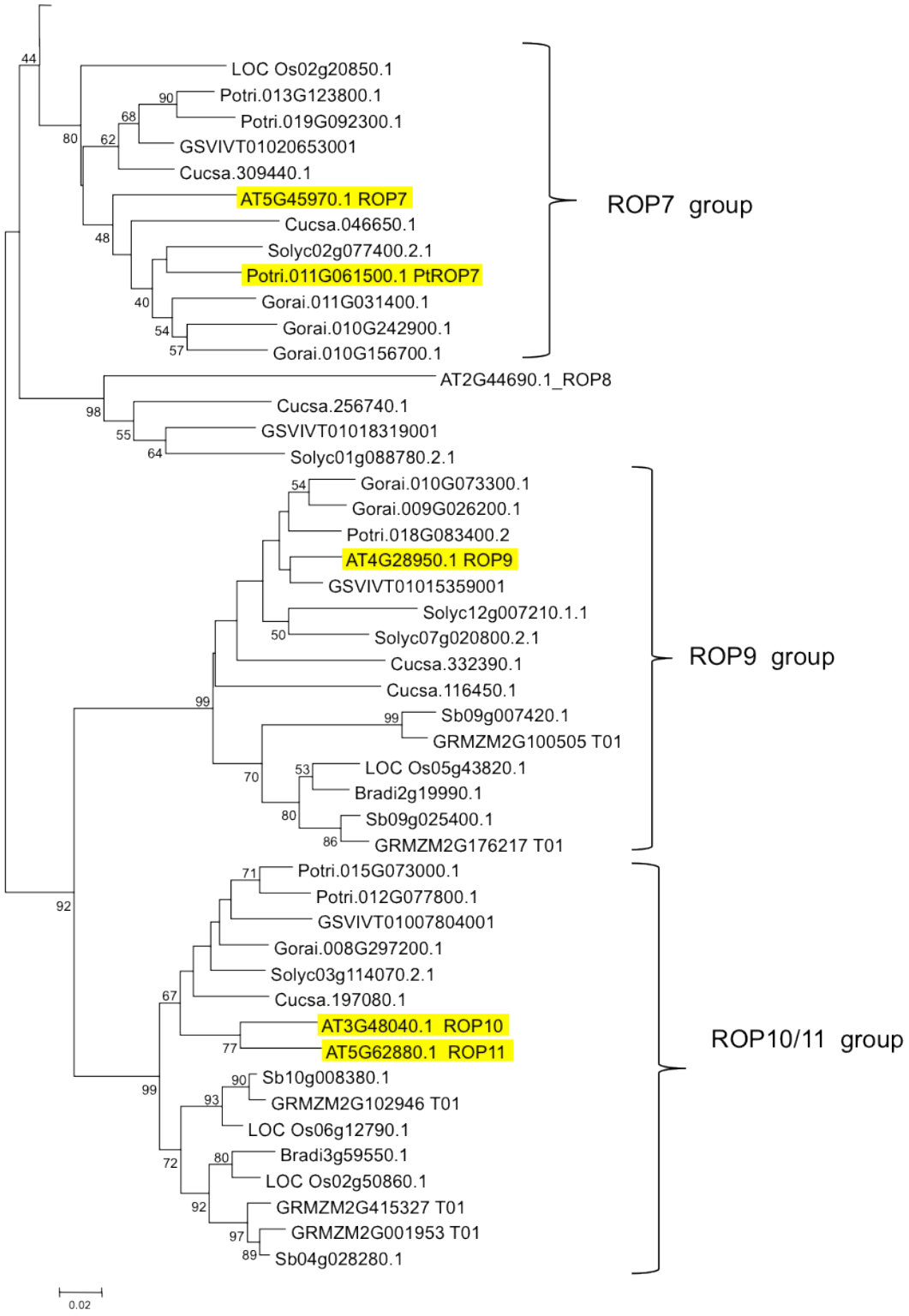
LOC Os02g20850.1
Potri.013G123800.1
Potri.019G092300.1
GSVIVT01020653001
Cucsa.309440.1
AT5G45970.1 ROP7
Cucsa.046650.1
Solyc02g077400.2.1
Potri.011G061500.1 PtROP7
Gorai.011G031400.1
Gorai.010G242900.1
Gorai.010G156700.1
ROP7 group
AT2G44690.1_ROP8
Cucsa.256740.1
GSVIVT01018319001
Solyc01g088780.2.1
Gorai.010G073300.1
Gorai.009G026200.1
Potri.018G083400.2
AT4G28950.1 ROP9
GSVIVT01015359001
Solyc12g007210.1.1
Solyc07g020800.2.1
Cucsa.332390.1
Cucsa.116450.1
Sb09g007420.1
GRMZM2G100505 T01
LOC Os05g43820.1
Bradi2g19990.1
Sb09g025400.1
GRMZM2G176217 T01
ROP9 group
Potri.015G073000.1
Potri.012G077800.1
GSVIVT01007804001
Gorai.008G297200.1
Solyc03g114070.2.1
Cucsa.197080.1
AT3G48040.1 ROP10
AT5G62880.1 ROP11
Sb10g008380.1
GRMZM2G102946 T01
LOC Os06g12790.1
Bradi3g59550.1
LOC Os02g50860.1
GRMZM2G415327 T01
GRMZM2G001953 T01
Sb04g028280.1
ROP10/11 group
0.02

Appendix A

Functional characterization of *Populus* NAC154 subfamily

A.1 Introduction

NAC (NAM, ATAF1,2, CUC2) domain transcription factors (NACs) are plant-specific transcriptional regulators that regulate a wide variety of plant developmental processes and responses, including shoot apical meristem formation (Aida et al., 1997), auxin related lateral root initiation (Xie et al., 2000), and biotic and abiotic stress responses (Hegedus et al., 2003). The N-terminal portion of NACs contains the highly conserved NAC DNA-binding domain, while the C-terminal region is highly variable (Ooka et al., 2003). However, our lab has demonstrated that the C-terminus of XND1 (Zhong et al., 2008) and XND1-like NACs contain a conserved domain for binding the RETINOBLASTOMA-RELATED protein (C. Zhao et al, unpublished).

A subgroup of closely-related NACs have been characterized as master regulators of secondary wall formation (Zhong et al., 2010). Overexpression of *VND6* (*VASCULAR-RELATED NAC-DOMAIN 6)* and *VND7* in various types of cells induces ectopic deposition of secondary walls and cell transdifferentiation into vessel elements (Kubo et al., 2005). Simultaneous loss of SND1 (SECONDARY WALL ASSOCIATED NAC DOMAIN PROTEIN 1) and NST1 (NAC SECONDARY WALL THICKENING PROMOTING FACTOR 1) leads to absence of secondary walls in fibers (Mitsuda et al., 2007). In addition, overexpression of SND2 and SND3 induces expression of secondary wall biosynthetic genes and secondary wall thickening in fiber cells (Zhong et al., 2008). In contrast to the positive influence exherted by members of the VND/NST/SND subgroup on xylem differentiation, two other NACs, VNI2 and XND1, are able to inhibit xylem differentiation when overexpressed (Zhao et al., 2008; Yamaguchi et al., 2010).

Phylogenetic analysis indicated a subgroup of 4 poplar NAC domain proteins (PtNAC105 *Potri.011G058400*, PtNAC154 *Potri.017G016700*, PtNAC156 *Potri.007G135300* and PtNAC157 *Potri.004G049300*) to be most closely related to SND2 and SND3 (Grant et al., 2010). These four genes are most highly expressed in *Populus* xylem tissue among all the tissues tested (Grant et al., 2010). Transgenic 717-1B4 lines that overexpress *PtNAC154* driven by the *35S* promoter are significantly shorter compared to WT trees after 116 days in soil under greenhouse conditions. Additionally, the relative proportion of xylem versus bark was reduced for transgenic trees (Grant et al., 2010).

As mentioned in Chapter 3, in contrast to Arabidopsis, there is no collection of *Popolus* T-DNA insertional mutants that covers all genes for loss-of-function studies (Alonso et al., 2003). Traditionally, tree geneticists have been using antisense, co-suppression or RNA interference (RNAi) for targeted silencing of poplar genes (Baucher et al., 1996; Pilate et al., 2002; Meyer et al., 2004; Leple et al., 2007; Li et al., 2008). Ideally these techniques would only silence transcripts that contain perfectly complementary regions with designed probes, but in practice, imperfectly complementary messenger RNA could also be affected (Jackson et al., 2003; Xu et al., 2006), a phenomena called off-target effect.

To increase the specificity of RNAi, several groups developed and used the artificial microRNAs (amiRNA) to down-regulate gene expression in Arabidopsis (Alvarez et al., 2006; Niu et al., 2006; Schwab et al., 2006). Artificial microRNAs use the backbone of naturally existing microRNAs but replace the region that specifies target genes to be degraded with custom made sequences, thereby silencing any gene of interest by design. The Chiang lab adopted the principles of artificial microRNAi and tested a new amiRNA expression system specifically for gene functional analysis in *Populus trichocarpa* (Shi et al., 2010). The authors were able to verify by qRT-PCR and 5'RACE-PCR that expression of precisely designed amiRNA constructs in *Populus trichocarpa* could selectively silence *PAL* gene family subset A (*PAL2*, *PAL4* and *PAL5*) without significantly down-regulating subset B (*PAL1* and *PAL3*) and vice versa (Shi et al., 2010).

Here we report updated progress on *PtNAC154* overexpression transgenic trees and our efforts to further study PtNAC154 subgroup functions using amiRNA silencing mutants.

A.2 Materials and methods

A.2.1 Plant growth and transformation

Poplar materials, growth conditions and transformation methods were the same as described previously in Chapter 3.

A.2.2 Artificial microRNAs construction

Cloning strategies for all three amiRNAs were the same except for primers design. The microRNA backbone for all amiRNAs in this research is from a native *Populus trichocarpa* gene encoding for miRNA408 (Lu et al., 2005). The protocol for microRNAi cloning was described previously (Shi et al., 2010). *35S* primer CCCACTATCCTTCGCAAGACC and *Nos* primer TTTATTGCCAAATGTTTGAACGATC were used during amplifications.

amiRNA-NAC154 is designed to silence *PtNAC154* and *PtNAC156* in *P. tremula* × *P. alba* clone 717-1B4

Primers used:
NAC154I miR-s ccTCCAAAGTTAACATTCTCTCCTTGTGGCTCTTCCTTTTC
NAC154II miR-a aaGGAGAGAATGTTAACTTTGGAGGGTAGAGCCAAAACAAG
NAC154III miR*s aaGGCGAGAATGTTATCTTTGGTGGATGGAGCTACTAACAG
NAC154IV miR*a ccACCAAAGATAACATTCTCGCCTTCATCTGTCTCTGCTCC

amiRNA-NAC156 is designed to silence *PtNAC154*, *PtNAC156*, *PtNAC157* and *PtNAC105* in *P. tremula* × *P. alba* clone 717-1B4

Primers used:
NAC156I miR-s ccTCAAACTTCACTCCGGCTGGCTTGTGGCTCTTCCTTTTC
NAC156II miR-a aaGCCAGCCGGAGTGAAGTTTGAGGGTAGAGCCAAAACAAG
NAC156III miR*s aaGCAAGCCGGAGTGTAGTTTGTGGATGGAGCTACTAACAG

NAC156IV miR*a ccACAAACTACACTCCGGCTTGCTTCATCTGTCTCTGCTCC

amiRNA-NAC157 is designed to silence *PtNAC157* and *PtNAC105* in *P. tremula* × *P. alba* clone 717-1B4

Primers used:
NAC157I miR-s ccTTCTGCTCTACCAAATGCTCATTGTGGCTCTTCCTTTTC
NAC157II miR-a aaTGAGCATTTGGTAGAGCAGAAGGGTAGAGCCAAAACAAG
NAC157III miR*s aaTGCGCATTTGGTACAGCAGATGGATGGAGCTACTAACAG
NAC157IV miR*a ccATCTGCTGTACCAAATGCGCATTCATCTGTCTCTGCTCC

PCR products were first ligated into pGEM-T vector (Promega Corp. Madison, WI) for further reproductive amplification in bacteria. Isolated pGEM-T vector harboring amiRNAs were digested by *Bam*HI and *Sac*I and subcloned into pBI121 binary vector.

A.2.3 Transcript analysis

Total RNA isolation and RT-qPCR protocols were described previously in Chapter 3. The approaches used for relative transcript level measurement of *PtNAC154*, *PtNAC156* and *PtNAC157* were the same as those for *PB15* and *PB129* except gene specific primers. Gene specific primers for *PtNAC154*, *PtNAC156* and *PtNAC157* were listed in Table A.1.

Table A.1 Primers used in RT-qPCR

Primer Name	Primer Sequence	Purpose
UBQ_For	TGTACTCTTTTGAAGTTGGTGT	RT-qPCR control
UBQ_Rev	TCCAATGGAACGGCCATTAA	RT-qPCR control
PtNAC154_For	TCTTGCTGAGTACTATCACCCTTCTTC	RT-qPCR
PtNAC154_Rev	GCTACATGAGCCACCATATCATG	RT-qPCR
PtNAC156_For	GTACCACTCCTGTCGACTACTATAATCC	RT-qPCR
PtNAC156_Rev	TCACCAAGGCTCAATGATTGC	RT-qPCR
PtNAC157_For	CGAGTGCATGGTTGTTGCTTC	RT-qPCR
PtNAC157_Rev	ACGGCAAAGCTTCCAAAGAAC	RT-qPCR

A.2.4 Field-grown tree growth measurements

Six independent events of transgenic poplar trees overexpressing *PtNAC154* were transferred to Reynolds Homestead Forest Resources Research Center (FRRC) in Critz, Virginia for field trial. Transgenic trees were planted in May 2009, plant stem heights (from ground to meristem) and stem basal diameters were measured at fall of 2012. Stem heights and basal diameters of 717-1B4 and all *PtNAC154* overexpressors lines were shown in supplementary Table A.S1. Statistical analysis was performed in JMP®10 (SAS Institute Inc., Cary, NC) with Dunnett's multiple comparison procedure and 717-1B4 set as control.

A.2.5 Field-grown tree leaf angle measurements

Full-angle-view photographs were taken during the spring of 2011 and 2012 for each field-grown tree for leaf angle measurements. ImageJ software developed by NIH (National Institutes of Health) was employed for image processing. With manual curation, angle tools of ImageJ generated two sets of angles. They are leaf petiole angles (the angle between leaf petiole and main stem) and blade angles (leaf blade angle relative to petiole).

For accurate angle measurements, appropriate photograph was selected for each angle to ensure the angle is at the same plane as image itself. Leaf petiole angle was added with leaf blade angle to generate a leaf angle composite score for each leaf. More than 3 leaf angle composite scores were collected from each tree for statistical analysis.

A.3 Results

A.3.1 Over-expression of *PtNAC154* in 717-1B4 inhibits growth

For trees grown on the same one-acre plot, mean growth rates of all *PtNAC154* overexpressor lines were less (based on stem height and stem basal diameter measurements) compared to those of control trees (Table A.2). In the most extreme example of stunting, *PtNAC154* OE-9C was less than half the size of the control non-transgenic *P. tremula* × *P. alba* clone 717-1B4. Statistical analysis showed that stem heights of four *PtNAC154* OE lines (OE-30D, OE-14C, OE-15D and OE-9C) were significantly less than those of 717-1B4 control trees, while *PtNAC154* OE-31A and *PtNAC154* OE-16C were not significantly shorter than 717-1B4. Stem basal diameters of three *PtNAC154* OE lines (OE-14C, OE-15D and OE-9C) were significantly less than those of 717-1B4 control trees, while *PtNAC154* OE-31A, *PtNAC154* OE-16C and *PtNAC154* OE-30D were not significantly thinner than 717-1B4.

Table A.2 Statistical analysis for stem heights and basal diameters of 717-1B4 and *PtNAC154* overexpressor lines

Genotype	Stem height mean value (cm)	Stem height *P* value	Stem basal diameter mean value (mm)	Stem basal diameter *P* value
717-1B4	312	1	35.65	1
PtNAC154 OE-31A	184	0.9197	23	0.9823
PtNAC154 OE-16C	152	0.3676	18.9333	0.6633
PtNAC154 OE-30D	257.667*	0.0026	28.3333	0.1292
PtNAC154 OE-14C	187.75*	0.0019	18.725*	0.0468
PtNAC154 OE-15D	283*	0.0005	31.85*	0.027
PtNAC154 OE-9C	150.75*	0.0002	17.275*	0.0154

Mean values of transgenic lines that are significantly (*P* value <0.05) different with mean value of 717-1B4 are indicated by *.

A.3.2 Over-expression of *PtNAC154* in 717-1B4 alters leaf petiole and blade angles

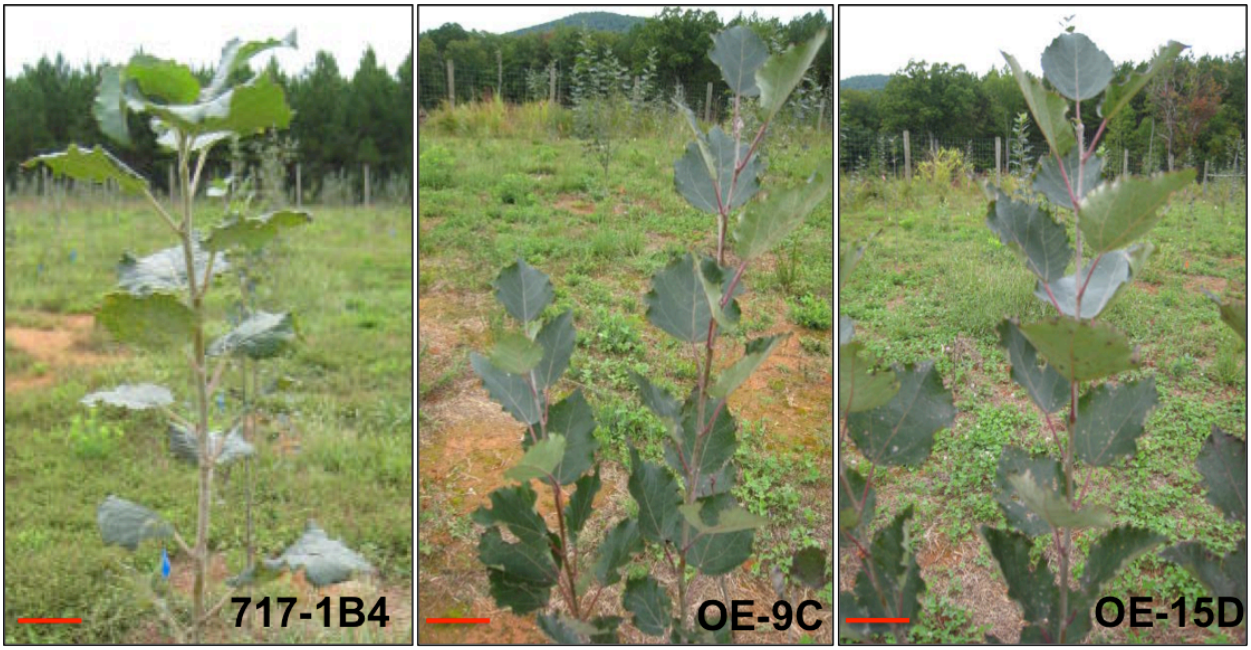

Figure A.1. Field-grown wild type and *PtNAC154* overexpression transgenic trees
Scale bars represent approximately 5 cm.

In addition to the aforementioned stunting, angles between the main stem and leaves were decreased in *PtNAC154* OE lines, i.e., leaves were more upright, producing a more narrow overall habit of growth (Figs. A.1, 2). *PtNAC154* overexpression also appeared to be associated with darker red petioles and veins in leaves, possibly due to increased anthocyanin accumulation in OE lines compared to controls. Metabolite analysis of overexpressors compared to WT is currently being conducted by R. Helm lab at Virginia Tech. Notably, the transgenic lines (OE-9C and OE-15D) with the greatest changes in leaf angle also display the greatest reduction in growth (Table A.2 and Figs A.1,2).

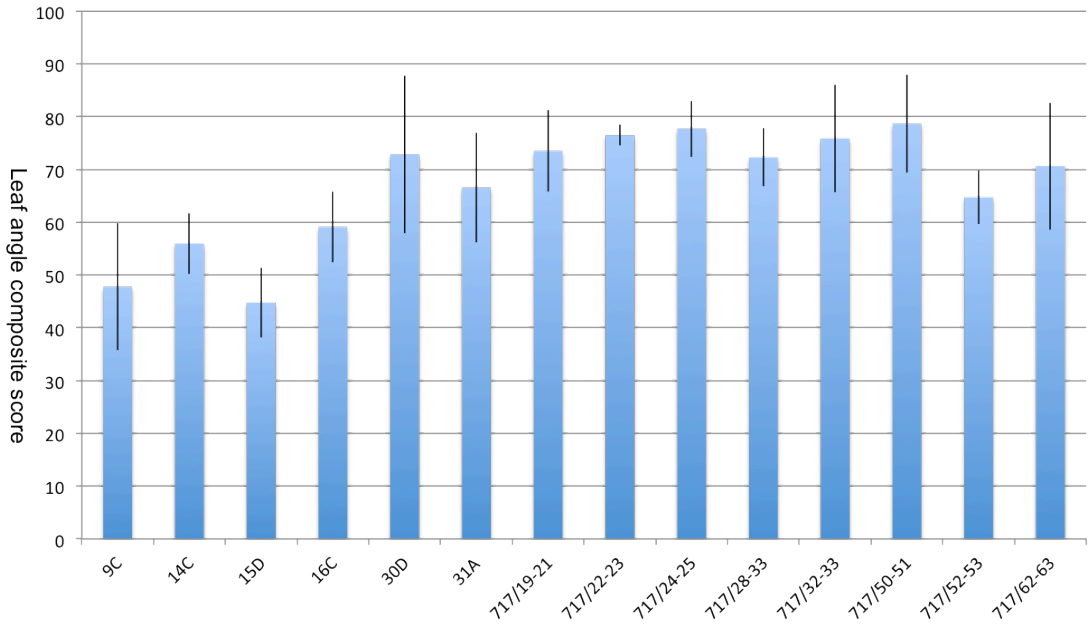

Figure A.2. Multiple independent *PtNAC154* overexpression transgenic events show reduced leaf angles.

Mean values ± SD (standard deviation) of leaf angle composite score (leaf petiole angle relative to main stem plus leaf blade angle relative to petiole) from year 2012 are shown.

A.3.3. Loss-of-function transgenic lines for *PtNAC154* clade were generated by artificial microRNAi

As a complementary approach to understand the functions of PtNAC154 subfamily in *Populus*, artificial microRNAi was employed to selectively silence two or four genes of this clade in *P. tremula* × *P. alba* clone 717-1B4. Among the four PtNAC154 subfamily proteins, PtNAC154 and PtNAC156 are a paralogous pair, and PtNAC157 and PtNAC105 constitute another paralogous pair.

Proteins within paralogous pairs shares 96.64% (PtNAC154 and PtNAC156) and 86.58% (PtNAC157 and PtNAC105) amino acid identities. Paralogous proteins are likely to be functionally redundant with each other, and thus, their genes were silenced in pairs in order to see phenotypes for loss-of-function analysis.

amiRNA-NAC156 is designed to silence all four members of PtNAC154 subfamily in *P. tremula* × *P. alba* clone 717-1B4. *amiRNA-NAC154* and *amiRNA-NAC157* were designed to down-regulate their paralogous pairs respectively.

After *Agrobacterium*-mediated transformation, about 40 putative *amiRNA-NAC154* transgenic plants were recovered from kanamycin selection growth media. 30 for *amiRNA-NAC156* and 30

for *amiRNA-NAC157*, respectively. All the survived plants were genotyped by PCR with *35S* and *Nos* primers to confirm the existence of T-DNA insertion.

To determine if endogenous target genes were downregulated in the transgenic plants, RT-qPCR was performed. Ten lines of *amiRNA-NAC154* transgenic plants showed down-regulation of both the *PtNAC154* and *PtNAC156* genes (Fig. A.3). Down-regulation of *PtNAC157* is detected in 6 lines of *amiRNA-NAC156* transgenics and 6 lines of *amiRNA-NAC157* transgenics, respectively (Fig. A.4).

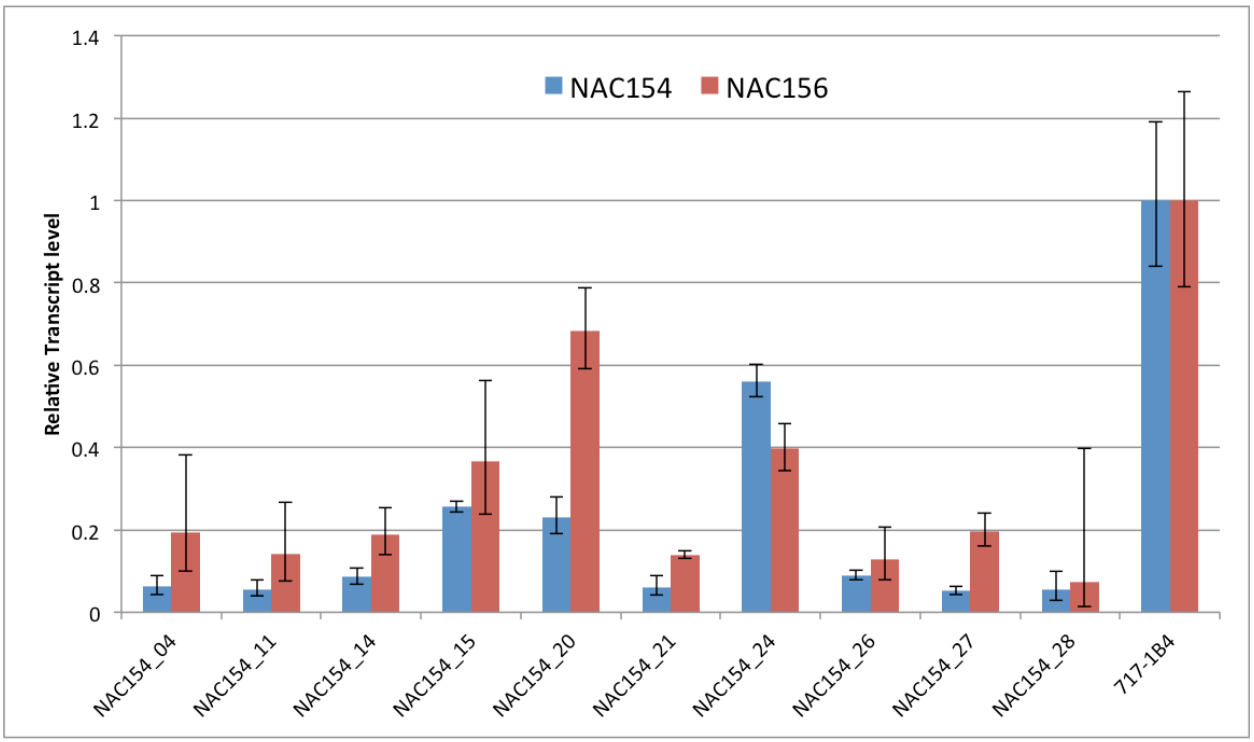

Figure A.3. *NAC154* and *NAC156* relative transcript levels in *amiRNA-NAC154* transgenics

Blue bars, *NAC154* transcript levels in *amiRNA-NAC154* transgenics relative to 717-1B4. Red bars, *NAC156* transcript levels in *amiRNA-NAC154* transgenics relative to 717-1B4. Target genes transcript levels in 717-1B4 are set to 1.

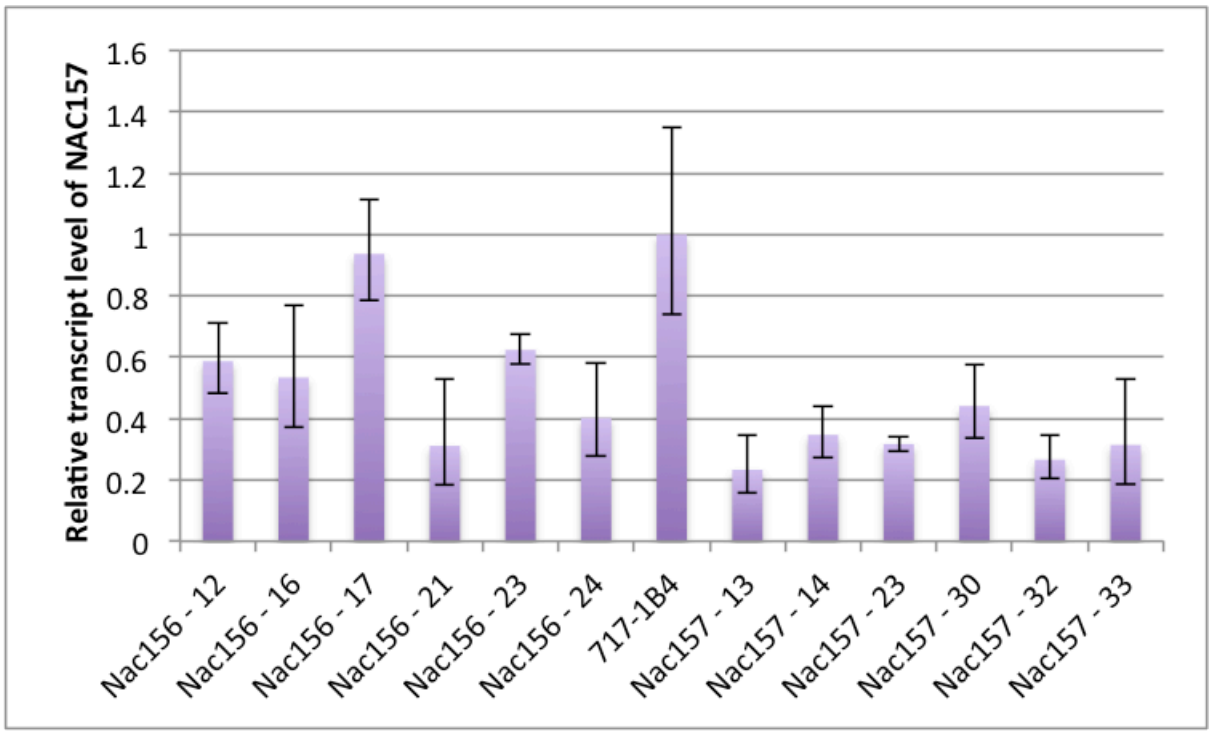

Figure A.4. *PtNAC157* transcript level in *amiRNA-NAC156* and *amiRNA-NAC157* transgenic plants

NAC157 Transcript level in 717-1B4 is set to 1.

A.4 Discussion

A.4.1 Field trials reveal novel phenotypes for transgenic trees overexpressing *PtNAC154*

Over the course of three years (two full growth seasons) in a field trial, *PtNAC154* OE trees exhibited significantly reduced growth rate relative to non-transgenic 717-1B4 controls, which is consistent with early observation in greenhouse trials (Grant et al., 2010). Surprisingly, in contrast to prior observations for greenhouse-grown *PtNAC154* OE trees, no evidence for increased growth of phloem versus xylem was detected for field-grown *PtNAC154* OE trees (data not shown). Moreover, two additional characteristics (more upright leaf orientation and possible changes in metabolites reflected in changes in leaf color) that were not apparent or were only weakly evident in greenhouse-grown *PtNAC154* OE trees were clearly discernable in field-grown *PtNAC154* OE trees, demonstrating the value and importance of field trials for more complete characterization of transgenic poplar.

It is likely that the field-grown *PtNAC154* OE lines described here are different from greenhouse-grown transgenic plants shown in (Grant et al., 2010) for two major reasons: 1, field-grown trees were 2 years older than those under greenhouse conditions and, as such, had more time to accumulate secondary tissues and experience the influences of intra-annual cycling on growth and development, and 2, field-grown trees are exposed to more complex environmental conditions that are almost impossible to entirely imitate in the greenhouse, for example,

coordinated changes in day-length and temperature, and exposure to abiotic and biotic stresses, all of which contribute to the phenotypes of plants.

Previous field trials on lignin modified poplar trees have also demonstrated the importance of field studies (Voelker et al., 2010; Voelker et al., 2011). Research on *4CL* down-regulated poplar trees showed that greenhouse-grown staked trees were taller and thinner than field-grown self-standing trees (Voelker et al., 2011). The altered leaf angle phenotype of *PtNAC154* OE lines is likely to be the result of genotype × environment interaction rather than solely a genetic effect.

A.4.2 Trait of reduced leaf angles is potentially beneficial for biomass production

The erect leaves phenotype in rice cultivars was associated with higher grain yields and enhanced biomass production under conditions of dense planting (Sakamoto et al., 2006; Yang and Hwa, 2008). The ultimate driving force for wood production is solar energy, which is perceived and captured by photosynthesis machinery within tree leaves. The canopy structure of a tree determines the area it occupies and is greatly affected by angles between leaf blade and vertical stem. Forest trees with more erect leaves potentially increase stand yield because more trees could be planted per acre. However, for any decrease in leaf angle to be beneficial, it should not be linked with an overall decrease in biomass accumulation, such as observed for the *PtNAC154* overexpression lines described here.

The underlying molecular and biochemical principles controlling poplar tree leaf angle are unknown. Currently, we do not know how overexpression of *PtNAC154* in *Populus* alters leaf angle. A reasonable explanation for leaf angle alteration in *PtNAC154* overexpression transgenic trees is that the mechanic properties of petioles is strengthened, therefore making leaves to be less affected by gravity. Careful examination and comparison of petiole anatomy for WT and transgenic trees may also improve our understanding. Additionally, global metabolic profiling of field-grown trees is ongoing in our collaborating lab and forthcoming results may provide some clues as to the mechanism driving the change in leaf angle.

A.4.3 Future field trials for PtNAC154 subfamily silencing transgenic mutants

Selected representatives of PtNAC154 subfamily-silencing lines are being propagated in the lab and are expected to be transplanted for field trials in November 2013. Multipe remets of approximately 9 lines of *amiRNA-NAC154* transgenic plants, 6 lines for *amiRNA-NAC156* and 6 lines for *amiRNA-NAC157* will be planted. Properties of transgenic plants to be further analyzed may include wood anatomy, development and morphology, wood density, biomass production, and cell wall components and chemistry.

A.5 References

Aida M, Ishida T, Fukaki H, Fujisawa H, Tasaka M (1997) Genes involved in organ separation in Arabidopsis: an analysis of the cup-shaped cotyledon mutant. Plant Cell **9:** 841-857

Alonso JM, Stepanova AN, Leisse TJ, Kim CJ, Chen H, Shinn P, Stevenson DK, Zimmerman J, Barajas P, Cheuk R, Gadrinab C, Heller C, Jeske A, Koesema E, Meyers CC, Parker H, Prednis L, Ansari Y, Choy N, Deen H, Geralt M, Hazari N,

Hom E, Karnes M, Mulholland C, Ndubaku R, Schmidt I, Guzman P, Aguilar-Henonin L, Schmid M, Weigel D, Carter DE, Marchand T, Risseeuw E, Brogden D, Zeko A, Crosby WL, Berry CC, Ecker JR (2003) Genome-wide insertional mutagenesis of Arabidopsis thaliana. Science **301:** 653-657

Alvarez JP, Pekker I, Goldshmidt A, Blum E, Amsellem Z, Eshed Y (2006) Endogenous and synthetic microRNAs stimulate simultaneous, efficient, and localized regulation of multiple targets in diverse species. Plant Cell **18:** 1134-1151

Baucher M, Chabbert B, Pilate G, Van Doorsselaere J, Tollier MT, Petit-Conil M, Cornu D, Monties B, Van Montagu M, Inze D, Jouanin L, Boerjan W (1996) Red Xylem and Higher Lignin Extractability by Down-Regulating a Cinnamyl Alcohol Dehydrogenase in Poplar. Plant Physiol **112:** 1479-1490

Grant EH, Fujino T, Beers EP, Brunner AM (2010) Characterization of NAC domain transcription factors implicated in control of vascular cell differentiation in Arabidopsis and Populus. Planta **232:** 337-352

Hegedus D, Yu M, Baldwin D, Gruber M, Sharpe A, Parkin I, Whitwill S, Lydiate D (2003) Molecular characterization of Brassica napus NAC domain transcriptional activators induced in response to biotic and abiotic stress. Plant Mol Biol **53:** 383-397

Jackson AL, Bartz SR, Schelter J, Kobayashi SV, Burchard J, Mao M, Li B, Cavet G, Linsley PS (2003) Expression profiling reveals off-target gene regulation by RNAi. Nat Biotechnol **21:** 635-637

Kubo M, Udagawa M, Nishikubo N, Horiguchi G, Yamaguchi M, Ito J, Mimura T, Fukuda H, Demura T (2005) Transcription switches for protoxylem and metaxylem vessel formation. Genes Dev **19:** 1855-1860

Leple JC, Dauwe R, Morreel K, Storme V, Lapierre C, Pollet B, Naumann A, Kang KY, Kim H, Ruel K, Lefebvre A, Joseleau JP, Grima-Pettenati J, De Rycke R, Andersson-Gunneras S, Erban A, Fehrle I, Petit-Conil M, Kopka J, Polle A, Messens E, Sundberg B, Mansfield SD, Ralph J, Pilate G, Boerjan W (2007) Downregulation of cinnamoyl-coenzyme A reductase in poplar: multiple-level phenotyping reveals effects on cell wall polymer metabolism and structure. Plant Cell **19:** 3669-3691

Li J, Brunner AM, Shevchenko O, Meilan R, Ma C, Skinner JS, Strauss SH (2008) Efficient and stable transgene suppression via RNAi in field-grown poplars. Transgenic Res **17:** 679-694

Lu S, Sun YH, Shi R, Clark C, Li L, Chiang VL (2005) Novel and mechanical stress-responsive MicroRNAs in Populus trichocarpa that are absent from Arabidopsis. Plant Cell **17:** 2186-2203

Meyer S, Nowak K, Sharma VK, Schulze J, Mendel RR, Hansch R (2004) Vectors for RNAi technology in poplar. Plant Biol (Stuttg) **6:** 100-103

Mitsuda N, Iwase A, Yamamoto H, Yoshida M, Seki M, Shinozaki K, Ohme-Takagi M (2007) NAC transcription factors, NST1 and NST3, are key regulators of the formation of secondary walls in woody tissues of Arabidopsis. Plant Cell **19:** 270-280

Niu QW, Lin SS, Reyes JL, Chen KC, Wu HW, Yeh SD, Chua NH (2006) Expression of artificial microRNAs in transgenic Arabidopsis thaliana confers virus resistance. Nat Biotechnol **24:** 1420-1428

Ooka H, Satoh K, Doi K, Nagata T, Otomo Y, Murakami K, Matsubara K, Osato N, Kawai J, Carninci P, Hayashizaki Y, Suzuki K, Kojima K, Takahara Y, Yamamoto K,

Kikuchi S (2003) Comprehensive analysis of NAC family genes in Oryza sativa and Arabidopsis thaliana. DNA Res **10:** 239-247

Pilate G, Guiney E, Holt K, Petit-Conil M, Lapierre C, Leple JC, Pollet B, Mila I, Webster EA, Marstorp HG, Hopkins DW, Jouanin L, Boerjan W, Schuch W, Cornu D, Halpin C (2002) Field and pulping performances of transgenic trees with altered lignification. Nat Biotechnol **20:** 607-612

Sakamoto T, Morinaka Y, Ohnishi T, Sunohara H, Fujioka S, Ueguchi-Tanaka M, Mizutani M, Sakata K, Takatsuto S, Yoshida S, Tanaka H, Kitano H, Matsuoka M (2006) Erect leaves caused by brassinosteroid deficiency increase biomass production and grain yield in rice. Nat Biotechnol **24:** 105-109

Schwab R, Ossowski S, Riester M, Warthmann N, Weigel D (2006) Highly specific gene silencing by artificial microRNAs in Arabidopsis. Plant Cell **18:** 1121-1133

Shi R, Yang C, Lu S, Sederoff R, Chiang VL (2010) Specific down-regulation of PAL genes by artificial microRNAs in Populus trichocarpa. Planta **232:** 1281-1288

Voelker SL, Lachenbruch B, Meinzer FC, Jourdes M, Ki C, Patten AM, Davin LB, Lewis NG, Tuskan GA, Gunter L, Decker SR, Selig MJ, Sykes R, Himmel ME, Kitin P, Shevchenko O, Strauss SH (2010) Antisense down-regulation of 4CL expression alters lignification, tree growth, and saccharification potential of field-grown poplar. Plant Physiol **154:** 874-886

Voelker SL, Lachenbruch B, Meinzer FC, Strauss SH (2011) Reduced wood stiffness and strength, and altered stem form, in young antisense 4CL transgenic poplars with reduced lignin contents. New Phytol **189:** 1096-1109

Xie Q, Frugis G, Colgan D, Chua NH (2000) Arabidopsis NAC1 transduces auxin signal downstream of TIR1 to promote lateral root development. Genes Dev **14:** 3024-3036

Xu P, Zhang Y, Kang L, Roossinck MJ, Mysore KS (2006) Computational estimation and experimental verification of off-target silencing during posttranscriptional gene silencing in plants. Plant Physiol **142:** 429-440

Yamaguchi M, Ohtani M, Mitsuda N, Kubo M, Ohme-Takagi M, Fukuda H, Demura T (2010) VND-INTERACTING2, a NAC domain transcription factor, negatively regulates xylem vessel formation in Arabidopsis. Plant Cell **22:** 1249-1263

Yang XC, Hwa CM (2008) Genetic modification of plant architecture and variety improvement in rice. Heredity (Edinb) **101:** 396-404

Zhao C, Avci U, Grant EH, Haigler CH, Beers EP (2008) XND1, a member of the NAC domain family in Arabidopsis thaliana, negatively regulates lignocellulose synthesis and programmed cell death in xylem. Plant J **53:** 425-436

Zhong R, Lee C, Ye ZH (2010) Evolutionary conservation of the transcriptional network regulating secondary cell wall biosynthesis. Trends Plant Sci **15:** 625-632

Zhong R, Lee C, Zhou J, McCarthy RL, Ye ZH (2008) A battery of transcription factors involved in the regulation of secondary cell wall biosynthesis in Arabidopsis. Plant Cell **20:** 2763-2782

Table A.S1 Stem heights and basal diameters of field-grown trees

Genotype	Stem height (cm)	Stem basal diameter (mm)
717-1B4	317	35.1
717-1B4	287	27.4
717-1B4	285	29.7
717-1B4	359	50.4
PtNAC154 OE-14C	181	23.2
PtNAC154 OE-14C	182	26.6
PtNAC154 OE-14C	188	24.8
PtNAC154 OE-14C	185	17.4
PtNAC154 OE-15D	123	16.5
PtNAC154 OE-15D	130	14.9
PtNAC154 OE-15D	203	25.4
PtNAC154 OE-16C	291	30.7
PtNAC154 OE-16C	236	29.6
PtNAC154 OE-16C	246	24.7
PtNAC154 OE-30D	218	21.2
PtNAC154 OE-30D	220	26.9
PtNAC154 OE-30D	100	9.4
PtNAC154 OE-30D	213	17.4
PtNAC154 OE-9C	157	16.6
PtNAC154 OE-9C	144	14.5
PtNAC154 OE-9C	168	24.4
PtNAC154 OE-9C	134	13.6
PtNAC154 OE-31A	219	20
PtNAC154 OE-31A	347	43.7

Appendix B

Characterization of CesA interacting protein PB504 and PB504 interaction network

B.1 Introduction

There are two major types of cell walls in plants: primary and secondary. Primary cell walls are mainly comprised of cellulose, hemicellulose, pectins and structural proteins (Cosgrove, 1997). Secondary cell walls exist mainly in fibers and treachery elements. Components of secondary cell walls, including cellulose, hemicellulose and lignins, are deposited inside of primary cell walls after cessation of cell expansion (Oda and Fukuda, 2012).

The biosynthesis of cellulose is catalyzed by plasma membrane localized hexameric rosette-like structures of cellulose synthase (CesA) complexes (CSCs) (Kimura et al., 1999). There are 10 CesA proteins (CesA 1-10) in *Arabidopsis thaliana*, and 18 genes identified encoding CesAs in the *Populus trichocarpa* genome (Pear et al., 1996; Djerbi et al., 2005). Three CesA genes in Arabidopsis, *CesA4*, *CesA7* and *CesA8*, corresponding to irregular xylem mutants *irx5*, *irx3* and *irx1,* were required for secondary cell wall cellulose synthesis (Turner and Somerville, 1997). In contrast, quantitative RT-PCR showed that five CesA genes, including *PtCesA4*, *PtCesA7-A*, *PtCesA7-B*, *PtCesA8-A* and *PtCesA8-B*, were expressed in xylem and likely responsible for cellulose synthesis in wood-forming tissue of *Populus* (Suzuki et al., 2006).

A typical CesA protein is comprised of a N-terminal RING-type zinc finger domain, eight transmembrane (TM) domains and a highly conserved large central domain in which the glycosyltransferase activity resides (Somerville, 2006). The eight TM domains are not clustered together in CesAs. The two TM domains near the amino terminus and the other six near the carboxy terminus are separated by approximately 530 amino acids comprising the cytoplasmic region (Delmer, 1999). The zinc finger-containing N-terminus of cotton CesA1 was shown to interact with itself and cotton CesA2. Therefore zinc finger domains were hypothesized to be responsible for interactions between CesA proteins (Kurek et al., 2002). However, this zinc finger-based dimerization does not exclude the existence of additional points of interaction between the subunits to form the CesA complexes (Somerville, 2006).

For a long time, CesA proteins were the only verified components of CSCs. Recently, however, non-CesA proteins were found to interact or co-precipitate with CSCs (Gu et al., 2010; Song et al., 2010). CESA interacting protein 1 (CSI1) was initially identified from a Y2H screen using the cytoplasmic region of AtCesA6 as bait and it was later shown to be associated with primary cell wall CSCs (Gu et al., 2010). The function of CSI1 was speculated to direct CesA complexes along the microtubules during cellulose synthesis (Gu and Somerville, 2010; Endler and Persson, 2011). Co-immunoprecipitation of *Populus* CSCs followed by LC-MS/MS analysis revealed several putative xylem CSCs interacting proteins, such as KOR protein, sucrose synthase (SuSy), COBRA-like proteins, cytoskeleton and vesicle trafficking related proteins and other proteins (Song et al., 2010). However, further verification by independent approaches and characterization of these putative xylem CSCs interacting proteins are needed. The Y2H studies presented here would advance current research on CesA interacting proteins in *Populus*.

Cell growth and expansion also require the harmonious coordination of protein-mediated cell wall loosening and deposition of other wall polymers. Currently, expansins, endoglucanases and xyloglucan endotransglycosylases are principal proteins implicated in wall loosening and hemicellulose synthesis (Nicol et al., 1998; Cosgrove, 1999; Maris et al., 2009). Pectins are major components of cell walls. They may be involved in limiting cell growth and reducing cell wall biodegradability by forming covalent cross-links with cellulose fibrils and hemicellulose. In secondary cell walls, lignin biosynthesis is another intensively studied aspect of wall polymerization (Boerjan et al., 2003; Weng and Chapple, 2010). Several enzymes in our poplar biomass (PB) protein set are predicted to be involved in the aforementioned polymerization and depolymerization of non-cellulosic cell wall components. We attempted to identify proteins that interact with carbohydrate-active cell wall enzymes and enzymes in the lignification pathway through Y2H library screens. Unfortunately, of the several putative interactions discovered in this screen, only one, that of PB504 with CesA (PB144), could be confirmed.

For example, PB376 (*Potri.003G131700*) has 10-fold higher expression in developing secondary xylem versus phloem-cambiam (Rodgers-Melnick et al., 2011). Phylogenic study indicates that PB376 belong to the glycoside hydrolase family 28 (pectinase). A putative alpha-L-arabinofuranosidase (*Potri.016G025500*) was found to interact with PB376 from our poplar xylem cDNA prey library. We designated this putative arabinofuranosidase PB508. A full-length clone of PB508 was retested for interaction with PB376, but failed to activate any of the three Y2H reporters. Thus, it was a false positive from the Y2H library screen.

In this chapter, we report on the current state of our ongoing efforts to further characterize the interaction between PB144 and PB504.

B.2 Materials and methods

B.2.1 Yeast two-hybrid system

Protocols for Y2H experiments were described previously in Chapter 4.

B.3 Results

B.3.1 Poplar cellulose synthase PB144 interacts with PB504 in the Y2H system

PB144 (*Potri.011G069600*) is a poplar cellulose synthase that exhibited an 18-fold higher expression in differentiating secondary xylem relative to phloem-cambiam (Rodgers-Melnick et al., 2011). Phylogenic analysis indicated that this CesA is most homologous (86% amino acid sequence identity) to Arabidopsis CesA8 or IRX1 (IRREGULAR XYLEM 1, *AT4G18780*). Quantitative RT-PCR-based transcript analysis also demonstrated that this gene (referred as *PtCesA8*) is most highly expressed in xylem tissue of *Populus trichocarpa* (Suzuki et al., 2006). For consistency with Arabidopsis CesAs family structure, a new nomenclature system was proposed for *Populus CesA* genes in (Kumar et al., 2009). From this point, PB144 will be referred as PtCesA8-A based on this new nomenclature.

DB-PtCesA8-A was used as bait protein to screen against a *Populus trichocarpa* xylem AD prey library. Three prey peptides were found to interact with PtCesA8-A as a result of library screening. All three full-length proteins were cloned and tested against PtCesA8-A via Y2H binary assays, but only one (*Potri.015G099100*) was confirmed as interactor of PtCesA8-A. We designated this poplar-specific protein PB504 (Fig B.1).

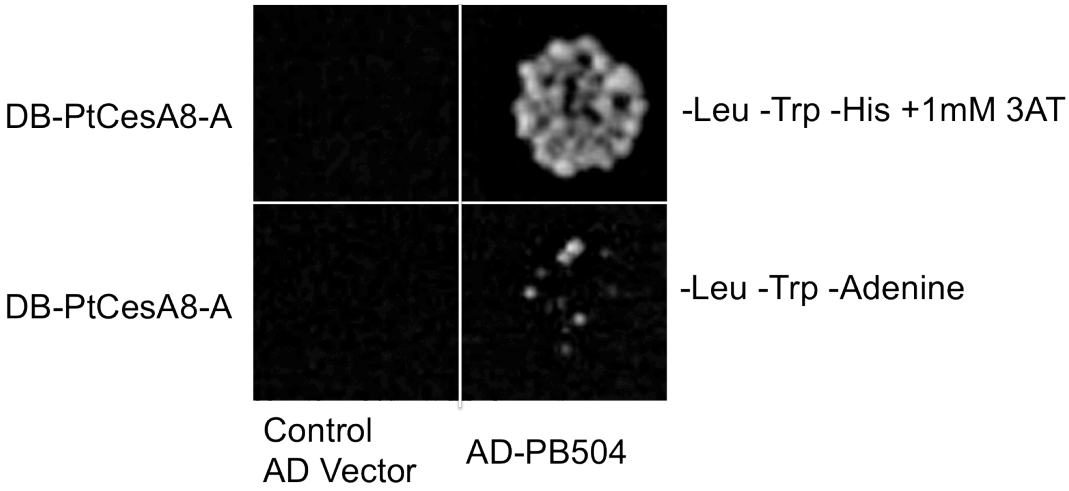

Figure B.1. Confirmation of interaction between PtCesA8-A and PB504 by Y2H binary assay

To further characterize the interaction between PtCesA8-A and PB504, truncated versions of PtCesA8-A were cloned for testing against PB504 in Y2H. PB505 and PB506 represented PtCesA8-A lacking the N-terminal zinc finger or the C-terminal six transmembrane domains, respectively. The interaction was preserved for PB505 with PB504 but abolished for PB506 with PB504 (data not shown), which suggested that the six TM domains near carboxy terminus of PtCesA8-A are necessary for interacting with PB504, while the zinc finger motif is not required.

B.3.2 Subcellular localizations of PB504 and PtCesA8-A

PB504 is a small protein (216 amino acid) that shares no homology with any known Arabidopsis protein. PB504 is predicted to contain a transmembrane domain near its C-terminus and to localize to the plasma membrane (http://psort.hgc.jp/form.html). To study its subcellular localization, PB504 was fused with YFP and transiently expressed in *Nicotiana benthamiana*. Initial studies indicated that PB504 localized to components of the endomembrane system, and possibly the plasma membrane. In some cells, YFP-PB504 was also seen in the nucleus. To further evaluate the possibility of endomembrane localization, YFP-PB504 and endoplasmic reticulum (ER) marker mCherry were co-expressed transiently for 48 hours in leaves of tobacco and observed under Zeiss LSM 510 confocal laser scanning microscope (Fig. B.2)**.**

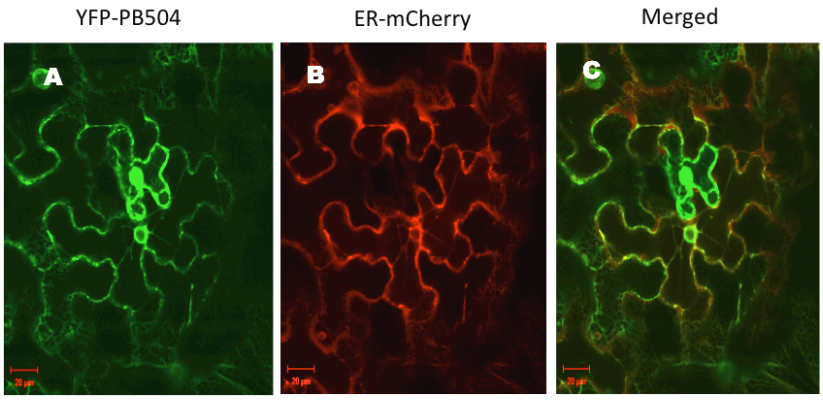

Figure B.2. Transient co-localization studies of PB504 with ER-mCherry in *Nicotiana benthamiana*

(A) Confocal image of YFP-tagged PB504 in epidermal cells of tobacco. (B) Confocal image of ER-targeted mCherry forming an interconnected network continuous with the outer nuclear and plasma membranes in epidermal cells of tobacco. (C) Merged image shows some sites of co-localized forYFP-PB504 and ER-mCherry. Scale bars from A-C: 20µm.

Merger of the YFP and RFP channels revealed some points of possible co-localization for YFP-PB504 and mCherry, but did not support the conclusion that PB504 is exclusively an ER-localized protein. However, the results suggest that PB504 traffics in vesicles rather than localizing in the soluble cytosolic compartments. Importantly, transient co-expression studies in tobacco also showed that YFP-PB504 and RFP-PtCesA8-A show a high degree of co-localization in plant cells, consistent with possible *in vivo* interaction between these proteins (Fig. B.3).

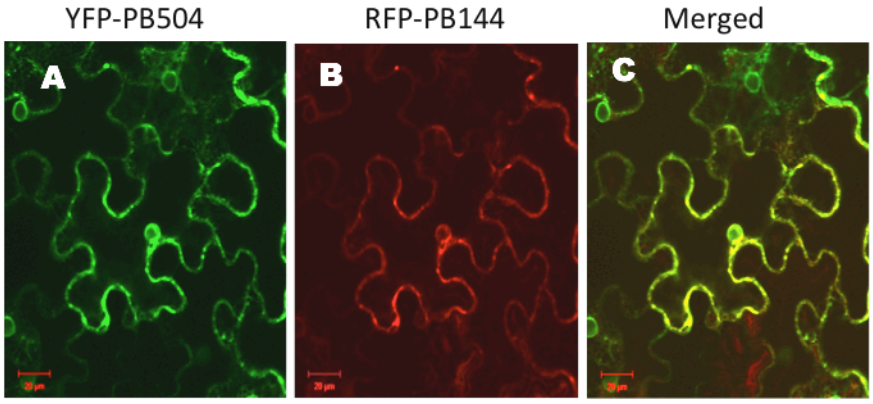

Figure B.3. Transient co-localization studies of PB504 and PtCesA8-A in *Nicotiana benthamiana*

(A) Confocal image of YFP-PB504 in epidermal cells of tobacco (B) Confocal image of RFP-PtCesA8-A in epidermal cells of tobacco (C) Merged image shows many sites of co-localized for YFP-PB504 and RFP-PtCesA8-A. Scale bars from A-C: 20µm.

B.3.3 Interaction network involving PB504

PB504 is a protein of unknown function. To gain some insight regarding its function and the significance of the PB504-PtCesA8-A interaction, we performed an interactome walk using DB-PB504 as bait to screen the xylem cDNA prey library. The current interaction network for PB504 is shown in Figure B.4.

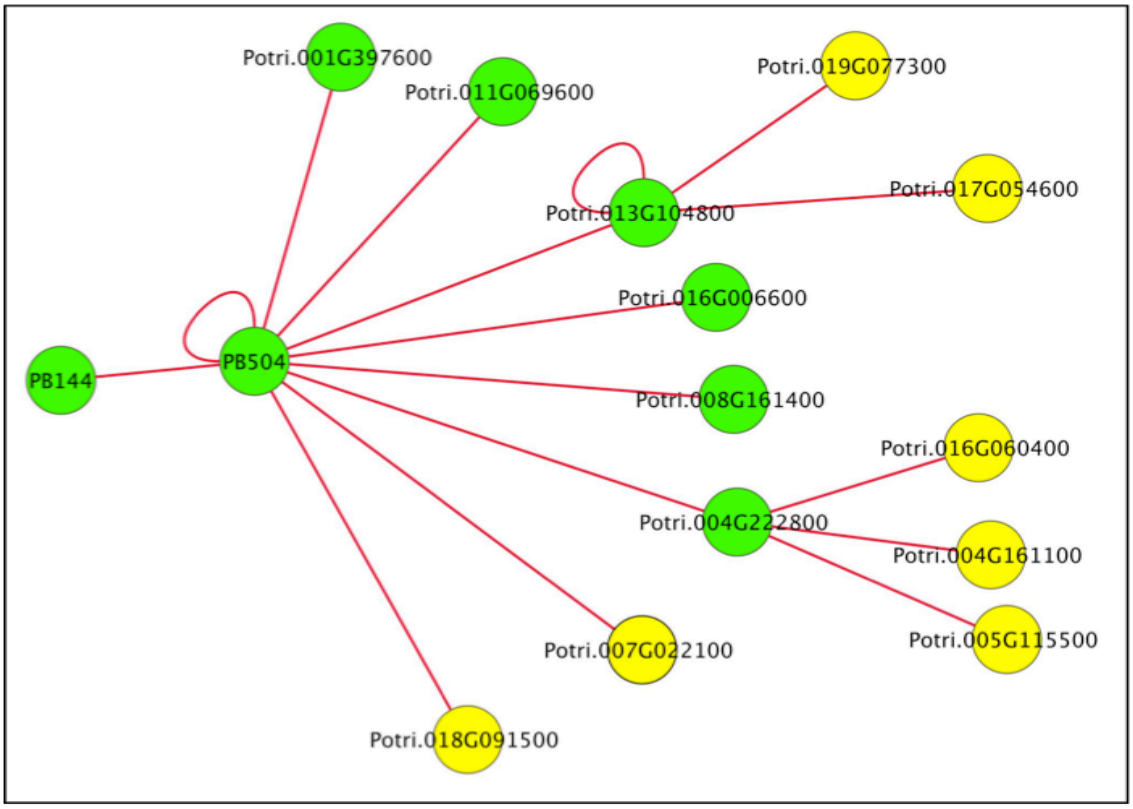

Figure B.4. The interaction network for PB504.

Each node (circle) depicts an interacting protein labeled with their respective gene IDs. Green and yellow circles are interacting proteins identified by the Y2H binary assay or library screens, respectively. Predicted functions for these proteins are listed in Table B.1

Table B.1. Predicted functions for proteins (nodes) shown in Figure B.4

Populus trichocarpa ID	PB index	Predicted function
Potri.001G397600	PB518	encodes Ser/Thr protein kinase
Potri.011G069600	PB144	cellulose synthase PtCesA8-A
Potri.013G104800	PB512	small GTPase
Potri.016G006600	PB517	Cu/Zn binding protein
Potri.008G161400	PB519	Mg transporters
Potri.004G222800	PB425	Unknown protein
Potri.007G022100	N/A	Fibronectin
Potri.018G091500	N/A	Actin Bundling
Potri.019G077300	N/A	Avirulence responsive protein (small GTPase)
Potri.017G054600	N/A	Ribosomal protein
Potri.016G060400	N/A	Kinesin Heavy Chain protein
Potri.004G161100	N/A	Kinectin Related protein
Potri.005G115500	N/A	Kinesin Heavy Chain protein

Selected putative interacting proteins for PB504 were cloned in full-length and tested for interaction with PB504 in Y2H binary assays. Four proteins (PB517, PB518, PB519 and PtCesA8-A) were confirmed to be authentic interactors of PB504.

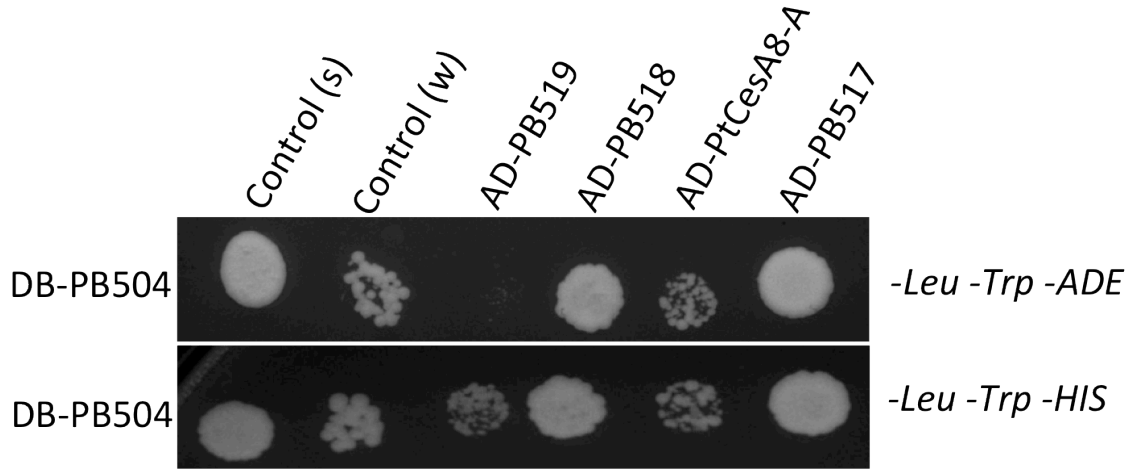

Figure B.5. Y2H binary tests of PB504 with its interacting proteins

Control (s) and (w) are two positive controls showing strong and weak interactions for this experiment, respectively.

B.4 Discussion

B.4.1 Novel poplar-specific interacting protein for PtCesA8-A

In Arabidopsis, the CesA complexes comprised of AtCesA4, 7 and 8 were shown to be responsible for secondary cell wall cellulose synthesis (Turner and Somerville, 1997). Song and

colleagues, however, suggested there might be two different CesA complexes in differentiating secondary xylem of *populus*. They also detected a shared set of proteins that are associated with both types of CSCs (Song et al., 2010). These findings indicate cellulose biosynthesis in *Populus* xylem may have new features that are not present in Arabidopsis.

Both phylogenic and transcript analysis implicate PtCesA8-A with cellulose synthesis of the secondary rather than the primary cell wall (Suzuki et al., 2006; Kumar et al., 2009). The discovery of PB504 as a novel interactor for PtCesA8-A may lead to unveiling of a new regulatory pathway of CesA complexes during cellulose synthesis. Transient expression demonstrated PB504 to be localized within the endomembrane network in plant cells. PB504 could be involved with directing trafficking and final localization for PtCesA8-A in that way sharing some similarity of function with CSI1 directing primary CesA complexes along microtubules (Gu et al., 2010). It is also noteworthy that the overall PB504 interaction network (Fig. B.4; Table B.1) includes membrane, signaling and cytoskeletal proteins, potentially placing PB504 at a nexus of the cell wall-cytoskeletal continuum involving CesA.

B.4.2 Ongoing and Future work of PB504

Arabidopsis transgenic plants ectopically expressing *PB504* and trangenic poplar expressing *LMX5*-driven *amiRNAi-PB504* are under characterization by Brunner lab members, with the latter scheduled for greenhouse trails beginning fall 2013. Among the newly identified interactors for PB504, a small GTPase (*Potri.013G104800,* PB512), a Cu/Zn-binding protein (*Potri.016G006600,* PB517) and a Ser/Thr protein kinase *(Potri.001G397600,* PB518) are particularly interesting, because a ROP GTPase protein is responsible for cell wall patterning in cooperation with a plant specific microtubule-binding protein (Oda and Fukuda, 2012), CesA contains a zinc-binding domain, and CesA requires phosphorylation for both the activity and motility of the cellulose synthase complex (Lei et al., 2012). Site-directed mutagenesis of the PB512 and PB517 for production of transgenic poplar expressing constitutively active and dominant negative versions of both of these PB504 interactors is underway.

B.5 References

Boerjan W, Ralph J, Baucher M (2003) Lignin biosynthesis. Annu Rev Plant Biol **54:** 519-546

Cosgrove DJ (1997) Assembly and enlargement of the primary cell wall in plants. Annu Rev Cell Dev Biol **13:** 171-201

Cosgrove DJ (1999) Enzymes and other agents that enhance cell wall extensibility. Annu Rev Plant Physiol Plant Mol Biol **50:** 391-417

Delmer DP (1999) CELLULOSE BIOSYNTHESIS: Exciting Times for A Difficult Field of Study. Annu Rev Plant Physiol Plant Mol Biol **50:** 245-276

Djerbi S, Lindskog M, Arvestad L, Sterky F, Teeri TT (2005) The genome sequence of black cottonwood (Populus trichocarpa) reveals 18 conserved cellulose synthase (CesA) genes. Planta **221:** 739-746

Endler A, Persson S (2011) Cellulose synthases and synthesis in Arabidopsis. Mol Plant **4:** 199-211

Gu Y, Kaplinsky N, Bringmann M, Cobb A, Carroll A, Sampathkumar A, Baskin TI, Persson S, Somerville CR (2010) Identification of a cellulose synthase-associated protein required for cellulose biosynthesis. Proc Natl Acad Sci U S A **107:** 12866-12871

Gu Y, Somerville C (2010) Cellulose synthase interacting protein: a new factor in cellulose synthesis. Plant Signal Behav **5:** 1571-1574

Kimura S, Laosinchai W, Itoh T, Cui X, Linder CR, Brown RM, Jr. (1999) Immunogold labeling of rosette terminal cellulose-synthesizing complexes in the vascular plant vigna angularis. Plant Cell **11:** 2075-2086

Kumar M, Thammannagowda S, Bulone V, Chiang V, Han KH, Joshi CP, Mansfield SD, Mellerowicz E, Sundberg B, Teeri T, Ellis BE (2009) An update on the nomenclature for the cellulose synthase genes in Populus. Trends Plant Sci **14:** 248-254

Kurek I, Kawagoe Y, Jacob-Wilk D, Doblin M, Delmer D (2002) Dimerization of cotton fiber cellulose synthase catalytic subunits occurs via oxidation of the zinc-binding domains. Proc Natl Acad Sci U S A **99:** 11109-11114

Lei L, Li S, Gu Y (2012) Cellulose synthase complexes: composition and regulation. Front Plant Sci **3:** 75

Maris A, Suslov D, Fry SC, Verbelen JP, Vissenberg K (2009) Enzymic characterization of two recombinant xyloglucan endotransglucosylase/hydrolase (XTH) proteins of Arabidopsis and their effect on root growth and cell wall extension. J Exp Bot **60:** 3959-3972

Nicol F, His I, Jauneau A, Vernhettes S, Canut H, Hofte H (1998) A plasma membrane-bound putative endo-1,4-beta-D-glucanase is required for normal wall assembly and cell elongation in Arabidopsis. EMBO J **17:** 5563-5576

Oda Y, Fukuda H (2012) Initiation of cell wall pattern by a Rho- and microtubule-driven symmetry breaking. Science **337:** 1333-1336

Oda Y, Fukuda H (2012) Secondary cell wall patterning during xylem differentiation. Curr Opin Plant Biol **15:** 38-44

Pear JR, Kawagoe Y, Schreckengost WE, Delmer DP, Stalker DM (1996) Higher plants contain homologs of the bacterial celA genes encoding the catalytic subunit of cellulose synthase. Proc Natl Acad Sci U S A **93:** 12637-12642

Rodgers-Melnick E, Mane SP, Dharmawardhana P, Slavov GT, Crasta OR, Strauss SH, Brunner AM, Difazio S (2011) Contrasting patterns of evolution following whole genome versus tandem duplication events in Populus. Genome Res

Somerville C (2006) Cellulose synthesis in higher plants. Annu Rev Cell Dev Biol **22:** 53-78

Song D, Shen J, Li L (2010) Characterization of cellulose synthase complexes in Populus xylem differentiation. New Phytol **187:** 777-790

Suzuki S, Li L, Sun YH, Chiang VL (2006) The cellulose synthase gene superfamily and biochemical functions of xylem-specific cellulose synthase-like genes in Populus trichocarpa. Plant Physiol **142:** 1233-1245

Turner SR, Somerville CR (1997) Collapsed xylem phenotype of Arabidopsis identifies mutants deficient in cellulose deposition in the secondary cell wall. Plant Cell **9:** 689-701

Weng JK, Chapple C (2010) The origin and evolution of lignin biosynthesis. New Phytol **187:** 273-285